2min4

Department of AERONAUTICS and ASTRONAUTICS
STANFORD UNIVERSITY

JAMES I. LERNER

UNSTEADY VISCOUS EFFECTS IN THE FLOW OVER AN OSCILLATING SURFACE

(NASA-CR-136581) UNSTEADY VISCOUS EFFECTS IN THE FLOW OVER AN OSCILLATING SURFACE (Stanford Univ.) 207 p HC $12.50 CSCL 20D

N74-14976

Unclas
G3/12 27224

The investigation described in this report was supported by the Air Force Office of Scientific Research under Contract No. F44620-68-C-0036 and by the National Aeronautics and Space Administration under Grant No. 05-020-102

DECEMBER 1972

SUDAAR NO. 453

Department of Aeronautics and Astronautics
Stanford University
Stanford, California

UNSTEADY VISCOUS EFFECTS IN THE FLOW OVER AN OSCILLATING SURFACE

by

James I. Lerner

SUDAAR NO. 453

December 1972

The investigation described in this report was supported by the Air Force Office of Scientific Research under Contract No. F44620-68-C-0036 and by the National Aeronautics and Space Administration under Grant No. 05-020-102

PRECEDING PAGE BLANK NOT FILMED

ABSTRACT

A theoretical model for the interaction of a turbulent boundary layer with an oscillating wavy surface over which a fluid is flowing is developed, with an application to wind-driven water waves and to panel flutter in low supersonic flow. A systematic methodology is developed to obtain the surface pressure distribution by considering separately the effects on the perturbed flow of a mean shear velocity profile, viscous stresses, the turbulent Reynolds stresses, compressibility, and three-dimensionality.

The problem is formulated initially for an inviscid incompressible two-dimensional shear layer of constant thickness, and the analysis is restricted to small-amplitude wavy surfaces and to thin boundary layers. The resulting linearized equations are reduced to ordinary differential equations in the transverse space coordinate by assuming simple harmonic time dependence and taking the Fourier transform with respect to the streamwise space variable. An expression for the pressure is obtained by integrating the resulting equations and inverting the Fourier transforms analytically. The effects of including viscosity in the perturbed flow are shown to be negligible for sufficient flow unsteadiness and for sufficiently large Reynolds number by means of a singular perturbation treatment in which it is shown that the unsteady viscous effects are confined to a thin region of nonuniformity near the wavy surface. Employing an eddy viscosity assumption for the turbulent Reynolds stresses in the perturbed flow and applying this to the singular perturbation procedure, an order of magnitude estimate is obtained for the effects of turbulence which indicates that the Reynolds stresses, though small, are not negligible. The inviscid shear flow theory is extended to include compressibility, and an expression is obtained for the first-order unsteady boundary layer effect on the pressure for subsonic, transonic, and supersonic freestream Mach number.

The inviscid theory is applied to the wind-water wave problem by specializing to traveling-wave disturbances, and the pressure magnitude and phase shift as a function of the wave phase speed are computed for a logarithmic mean velocity profile and compared with inviscid theory and experiment. These comparisons indicate that the inviscid theory is inadequate for this problem and suggest that the interaction between the air and the water is not properly accounted for. The application of the inviscid theory with a power law mean velocity profile to the calculation of aerodynamic generalized forces on an oscillating panel yields results which are substantially in agreement with an exact inviscid theory. The major difference arises for the case of boundary layer thickness to panel chord ratio equal to ten percent in which the exact numerical theory predicts no negative aerodynamic damping in the first mode contrary to the present theory. A one-mode Galerkin analysis for the panel flutter problem yields reasonable agreement for flutter dynamic pressure as a function of boundary layer thickness in comparison with other theoretical results based on the exact inviscid theory and on a first-order theory. These results agree with experimental evidence for the stabilization of the panel motion due to the influence of the unsteady boundary layer.

ACKNOWLEDGMENT

I wish to express my gratitude to Professor Krishnamurty Karamcheti for suggesting this problem as a suitable topic for a dissertation, for his guidance during the initial part of this investigation, for his encouragement and moral support, for providing financial assistance, and most of all, for imparting to me his high ideals and his philosophy of education. I am equally grateful to Professor Holt Ashley for providing encouragement and financial support, for imparting to me an appreciation for the practical applications of my work, for teaching me how to be effective and productive by his example, and for introducing me to Professor Marten Landahl.

I owe special thanks to Professor Landahl who provided the inspiration and guidance for the eventual technical solution of my problem. His willingness and eagerness to discuss the formulation and solution of the problem and his manner of assisting a student by providing just the right amount of advice will always be remembered and appreciated.

I also wish to thank Professor Sam McIntosh for his many helpful discussions with regard to the application of my theory to the problem of panel flutter and for his encouragement and gentle insistance on the importance of obtaining results in a study of this nature. With regard to results, I am indebted to my good friend, Dennis Allison, whose expertise in computer science enabled me to obtain numerical results and to overcome my feelings of awe with regard to the use of the computer.

I want to express my thanks to my fellow colleagues in Professor Karamcheti's group, especially to my good friends Robert Kadlec and Chung-nan Chang for their friendship and willingness to share their time and their ideas.

I owe special thanks to Mary Weisshaar and Andrea Dinsmore for their expert typing of the manuscript.

Finally, I want to thank my parents, especially my father, for instilling within me the determination to complete this task when at times the outcome was uncertain or the frustrations exasperating.

My research activity was supported by the National Aeronautics and Space Administration under NASA Grant 05-020-102 and by the Air Force Office of Scientific Research under Contract F44620-68-C-0036.

TABLE OF CONTENTS

LIST OF ILLUSTRATIONS

Figure		Page

NOMENCLATURE

a	Wave amplitude, integral $= \int_0^1 \rho dz^*$
B	Constant $= (M_\infty^2 - 1)^{1/2}$
b	Integral $= \int_0^1 \rho U dz^*$, panel span
C	Dimensional wave phase speed
C_f	Skin friction coefficient
C_p	Pressure coefficient $(= p/q)$
c	Nondimensional wave phase speed $(= C/u_\infty)$ or integral $= \int_0^1 \rho U^2 dz^*$
c_p, c_v	Specific heats
D	Plate stiffness, also derivative operator $(= ik + U\, \partial/\partial x)$
E	Modulus of elasticity, nondimensional eddy viscosity $(= \epsilon/D)$
$\tilde{F}$	Integral Fourier transform $= \int_0^1 (k + \alpha U)^{-2} dz^*$
G_{mn}	Integral over modal functions
g	Acceleration due to gravity
H_{mn}	Mechanical admittance
h	Plate thickness
K	Nondimensional frequency $[= k(\lambda/\mu)^{1/2}]$, also kernel function for pressure
K_1, H_1	Integrals for traveling wave theory

k	Reduced frequency $(= \omega L/u_\infty)$
L	Characteristic length (wavelength, panel chord)
M_∞	Mach number of freestream
p	Pressure
Q_{mn}	Generalized aerodynamic force
q	Dynamic pressure $(= 1/2\rho_\infty U_\infty^2)$
R	Reynolds number $(= Re\delta_0^2)$
Re	Reynolds number $(= u_\infty L/\nu)$
$\tilde{r}_{ij}$	Reynolds stress perturbations
T	Temperature
t	Time
U	Nondimensional mean shear velocity profile
U_1	Nondimensional reference speed $(= u_1/u_\infty)$
u, v, w	Fluid velocity components
u_τ	Shearing velocity $[=(\tau w/\rho)^{1/2}]$
u_∞	Air velocity of freestream
u_1	Reference speed
w	Dimensional plate deflection
x, y, z	Spatial variables
z^*	Nondimensional transverse space variable $(= z/\delta_{b.1.})$
z_s	Nondimensional surface deflection
z_0	Effective roughness height

α	Fourier transform variable, also nondimensional wave number
β	Fourier transform variable, also wave growth parameter, also constant $[=(1-M_\infty^2)^{1/2}]$, also unsteady viscous flow parameter $(= kR^{1/3})$
γ	Ratio of specific heats
γ_1	Constant $[= -kM_\infty/(M_\infty-1)]$
γ_2	Constant $[= -kM_\infty/(M_\infty+1)]$
δ	Streamline deviation
$\delta_{b.1.}$	Boundary layer thickness
δ_0	Nondimensional boundary layer thickness $(= \delta_{b.1.}/L)$
Δ^*	Unsteady displacement thickness
δ^*	Mass displacement thickness
δ_1	Density defect thickness
ϵ	Nondimensional wave amplitude $(= a/L)$, eddy viscosity
θ	Wave phase shift, also momentum thickness
κ	von Kármán turbulence constant
λ	Nondimensional dynamic pressure $(= 2qL^3/D)$, exponent in subsonic solution
μ	Mass ratio $[= \rho_\infty L/(\rho_m h)]$, exponent in subsonic solution
ν	Kinematic viscosity
π	Traveling wave pressure amplitide
ρ	Density
σ	Exponent in supersonic solution
τ	Shear stress, exponent in supersonic solution

φ	Velocity potential
ψ	Stream function
ψ_m	Mode shape function
Ω	Wind-profile parameter $(= gz_0/u_1^2)$
ω	Circular frequency

<u>Subscripts</u>

0	Inviscid
BL	Boundary layer
c	Critical layer
EV	Eddy viscous
f	Flutter
V	Viscous
∞	Free stream

<u>Superscripts</u>

$\hat{}$	Perturbation
$\sim$	Fourier transform

I. INTRODUCTION

1.1 MOTIVATION

This study is primarily concerned with the role of the unsteady boundary layer in modifying the pressure on an oscillating surface over which a fluid flows. One of the factors that motivates this study is the lack of agreement between theoretical and experimental studies of panel flutter at low supersonic Mach numbers. Panel flutter is a dynamic aeroelastic instability which occurs for surface skin panels that have one side exposed to a supersonic airstream and the other side to still air. The flutter amplitudes tend to be limited by structural nonlinearities associated with the lateral deformation of the panel so that the mode of structural failure is one of fatigue rather than explosive fracture of the skin surface. For this reason the present study is of great practical interest.

Another factor which motivates the present study is an interest in understanding the mechanisms by which wind flowing over water waves acts to energize the waves. Several experiments and theoretical analyses have been performed in an attempt to understand the structure of the turbulent air motion above the waves and the transfer of energy from the air to the waves. The current understanding of this air-sea problem is incomplete. More detailed experiments and improved theories are required to enhance understanding of the physical processes involved.

In both of these problems we are concerned with the turbulent flow of air over an oscillating surface. In the case of panel flutter the surface oscillations are predominantly standing waves, while for the air-sea problem the ocean surface admits traveling waves. In both cases we are interested in knowing the pressure on the waving surface. As a designer of flight vehicles the aeroelastician needs to know the pressure as an input to the equations of motion of the panel in order to predict the panel response subject to variations in the Mach number, panel dimensions, and material constants. The oceanographer is concerned with the oscillating pressure field, since it governs the energy transfer between the wind and water waves. This provides the basis for predicting the growth of waves.

For these reasons we choose the pressure as the quantity to be determined in this study.

1.2 SURVEY OF PREVIOUS RESEARCH

In this section we outline briefly some of the theoretical and experimental studies of boundary-layer effects on panel flutter and on the growth of ocean waves. As background to these topics we mention briefly two survey references on the subject of unsteady boundary layers which provide a historical as well as a technical framework from which to conduct research on this problem. The chapter, "Non-steady boundary layers," in the book by Schlichting (1968) presents a comprehensive summary of the calculation of non-steady boundary layers. The sections dealing with periodic boundary layer flows and unsteady compressible boundary layers are of particular interest in our study. He presents a comprehensive list of 69 references covering the past four decades of research in this subject. The work of Lighthill (1954) concerning the case of an external steady stream with small harmonic perturbations is a classic paper in the literature of unsteady boundary layer theory and should be consulted if one is uncertain about whether unsteady effects must be included in the treatment of the boundary layer. Regarding the influence of the unsteady boundary layer in aeroelastic calculations we refer to the article by Landahl and Ashley (1968) which contains qualitative estimates of the effect of an attached boundary layer on the unsteady flow, a discussion of the response of a viscous boundary layer to wavy wall deformations, and a comprehensive list of 24 references.

Some of the earlier analytical studies of panel flutter have been based on the potential flow model. The results of a flutter analysis based on this model disagree sharply with measurements at low supersonic Mach numbers. One of the first attempts to include the effect of the actual velocity profile was proposed by Fung (1963). In his very simplified model the boundary layer is replaced by a region of constant thickness in which the flow is a potential flow of constant velocity. Miles (1959a) has attempted to include the effect of the velocity profile in the boundary layer while at the same time idealizing the panel as an infinite traveling wave surface. A variation on this theme was proposed by Zeydel (1967) in which the boundary layer is divided into many sublayers of constant velocity. He shows that it is possible to treat the finite-chord case by use of the Fourier integral.

By considering the boundary layer as a parallel shear flow McClure (1962) has presented a more refined analysis in which the perturbations due to surface traveling waves are treated by methods analogous to those developed in the theory of boundary layer instability. His analysis includes the effects of viscosity on the perturbation flow quantities. McClure measured velocity profiles and pressures on a rigid wavy wall at supersonic Mach number and compared these results with his theory. He was able to show that a "linear" theory in which the mean flow is taken to be the flow over an unperturbed flat surface gives improved agreement with experimentally measured pressure on a wavy wall over potential flow theory predictions of pressure. Finally McClure applied his theory in an approximate analysis of the flutter of a finite-chord panel. For the pressure he took the result for an infinite standing wave obtained by superimposing two waves traveling with equal speed in opposite directions. His flutter analysis gives improved agreement with experiment over what can be obtained using potential-flow theory pressures.

Recently Dowell (1970, 1971) has undertaken an analysis of the flutter of a finite-chord rectangular panel by treating the boundary layer as an inviscid shear layer of constant thickness. Neglecting viscosity in the perturbed flow, he treats the problem by linearizing the inviscid equations. He uses a computer program to calculate the required aerodynamic forces and employs them in a nonlinear flutter analysis. He compares his theoretical flutter results with the experimental data of Muhlstein, Gaspers, and Riddle (1968). These experiments and the succeeding work of Gaspers, Muhlstein, and Petroff (1970) are the most definitive measurements yet obtained on the influence of the turbulent boundary layer on panel flutter. Dowell's results show better agreement with these experiments for the larger values of boundary layer thickness than for the smaller ones. In the experiments the boundary layer thickness was varied by using a splitter plate to remove a portion of the wall boundary layer. It is not clear why the agreement between theory and experiment turned out to be better for the thicker boundary layers.

Research on the nature of the generation of water waves by wind has proceeded along three different avenues. We find in addition to theoretical investigations both laboratory and field measurements of the generation of gravity waves by turbulent winds. Perhaps the most notable theoretical effort is the work of Miles (1957, 1959b, 1960, 1962, 1967) spanning a decade. He originally proposed an idealized inviscid model including a parallel shear flow of prescribed velocity profile over a two-dimensional surface wave. This theory neglects non-linear effects and first-order perturbations in the turbulent Reynolds stresses in the calculation of the pressure distribution at the interface between the air and the progressive water waves. The theories of Miles (1957) and Benjamin (1959) predict a phase shift between the pressure distribution and the wavy boundary which can be used to explain the energy transfer between air and water. Laboratory measurements conducted by Shemdin and Hsu (1967) and others at the Stanford 115-foot wind, water-wave tunnel compare favorably with the theoretical predictions of Miles (1959b). Recently Davis (1972) presents two methods of predicting the fluctuating turbulent stresses in the flow over a wave and uses them to compare with the surface pressure measurements of Dobson (1969) and Kendall (1970).

Recently there have been several laboratory investigations of wind-driven waves. An experimental study in which the water waves are simulated by mechanically driven deformations in a smooth neoprene rubber sheet was conducted by Kendall (1970). Kendall's pressure measurements compare favorably with the Miles theory; however, evidence of non-linear effects and modulation of the turbulent structure by the waves strongly suggests phenomena which cannot be explained by a linear inviscid theory. Stewart (1970) has measured the wave-induced perturbation-velocity field using a wind-water tunnel. These measurements have been compared with the numerical calculations of Davis (1970) for a model similar to Miles' formulation except for the inclusion of viscous terms and a second model including the turbulent Reynolds stresses. Neither of these theories predicts the velocity field well although they do exhibit the correct qualitative nature of the velocity field. Saeger and Reynolds (1971) have measured the perturbation pressures in a two-dimensional channel flow with one mechanically articulated waving wall. These pressures are compared with theoretical models — an inviscid model, a laminar viscous model, and a turbulent model in which the oscillations of the turbulent Reynolds stresses are modeled using an eddy viscosity assumption. None of the models are entirely satisfactory and the suggestion is made that a more accurate representation of the wave-induced distortions of the turbulent Reynolds stresses is required.

With regard to field measurements Miles (1967) reports that agreement with the laminar viscous model is not as good as with the laboratory measurements. He suggests that the discrepancy between field and laboratory measurements, vis-a-vis the laminar model, is due to the relative importance of the wave-induced Reynolds stresses with scale. He postulates an appropriate scale parameter in which the time scale for the turbulence is larger for the ocean than for the laboratory data. He generalizes the laminar model to include the perturbations in the turbulent Reynolds stresses but indicates that further theoretical progress demands some ad hoc hypothesis for the specification of these stresses. He concludes that more detailed experimental data is required to guide the choice of such hypotheses. The recent field measurements of Kondo et al. (1972) throw some light on the future course of the study of the turbulent transfer mechanism over the sea. Commenting on the discrepancies between their observations and the inviscid theory these authors emphasize the role of turbulent diffusion, the three-dimensional pattern of the sea surface, and the interaction between different frequency components. They cite the high intensity of atmospheric turbulence as a cause for the discrepancy between field and laboratory measurements.

1.3 SCOPE OF THIS STUDY

This study is concerned with flow over an unbounded surface that is characterized by small deviations from a plane. The plane is parallel to the undisturbed freestream and the surface deviations may be unbounded or they may be confined to a region of finite length. The former case characterizes the air-sea problem while the latter is appropriate to the flutter of a finite-chord panel. The unbounded nature of the unperturbed surface permits the characterization of the unperturbed boundary layer as a parallel shear flow. We consider both laminar and turbulent boundary layers, yet our interest is with turbulent flow owing to the applications discussed previously. The Mach number is taken to include the range from zero to low supersonic, and the Reynolds number is taken to be large or infinite.

Generally there are two distinct approaches that can be taken in a theoretical analysis of the boundary layer. One approach employs the differential equations of motion as a starting point while the other employs integral equations which are obtained by integrating the differential equations across the boundary layer. Both methods are considered in this study. An integral scheme is considered in Chapter 2. The effect of the unsteady boundary layer is represented by an unsteady displacement thickness which is determined from the momentum integral equation. Questions regarding the best way to obtain closure for the set of governing equations and the inability to consider separately the effects of the shear profile and the effects of finite Reynolds number lead us to abandon this approach in favor of a scheme based on the differential equations.

We propose an inviscid perturbation of a two-dimensional parallel shear flow in Chapter 3. We assume that the amplitude of the surface deformations is small compared to the boundary layer thickness implying that the mean shear flow is unaffected by the surface motion. The assumption that the boundary-layer thickness is constant along the deformed surface will be satisfactory for thicker boundary layers, yet we restrict the analysis to small values of a nondimensionalized boundary-layer thickness parameter, δ_o, for the purpose of obtaining a first-order effect of the boundary layer. This analysis results in an expression for the perturbation pressure at the surface which gives primarily the effect of the mean shear velocity profile. The effect of including viscosity in the perturbed flow is considered in Chapter 4. The two-dimensional incompressible flow is posed as a singular perturbation problem in which the basic outer flow is the inviscid problem treated in Chapter 3. We determine the effect on the surface pressure of including the viscous stress in the perturbed flow problem. We find that for large finite Reynolds number and sufficient flow unsteadiness the effect of viscosity on the pressure is negligible.

The role of turbulence is known to be rather important, especially in the mechanism of wind-driven water waves. We consider the effect of including the oscillations of the turbulent Reynolds stress in Chapter 5. We formulate the two-dimensional incompressible problem following the framework suggested by Hussain and Reynolds (1970). In seeking mathematical closure of the problem we explore the possibility of making an ad hoc assumption about the behavior of the perturbation Reynolds stress. We demonstrate that the effect of turbulence is considerably more important than the effect of viscosity in the perturbation flow; however, we note that the effect of the turbulent stresses on the pressure is minor compared to the effect of the mean shear profile for sufficiently large Reynolds number.

With the goal of obtaining an expression for the surface pressure suitable for application to the problem of panel flutter we consider the effects of compressibility and three-dimensionality in Chapters 6 and 7. Having determined that the roles of viscosity and turbulent Reynolds stresses are of secondary importance insofar as the pressure is concerned, we extend the analysis developed in Chapter 3 by including separately compressibility and three-dimensionality. We obtain an expression for pressure that is applicable both for subsonic and supersonic flow. For the purposes of performing a flutter analysis we obtain an expression for the generalized aerodynamic forces which employs the Fourier transform of the surface pressure rather than the pressure itself. This simplifies the task considerably owing to the complexity of inverting the double Fourier transform for the case of flutter of a rectangular panel.

The remainder of the study concerns the application of the results to the problems of interest. By specializing the theory to the case of a traveling-wave disturbance we can compare the theory to both the Miles theory for wind-driven water waves and to some of the experimental measurements discussed briefly in the previous section. With the intent of comparison with Dowell's (1970) theory and the experiments of Muhlstein et al. (1968) we consider the flutter of a two-dimensional panel of infinite span, a plate-column. We calculate the generalized aerodynamic forces and use them in an approximate flutter analysis. We indicate the need for a continuation of this study in the application of the theory to the flutter of a rectangular panel. In the concluding discussion we summarize the essential contributions of this research and suggest opportunities for further study based on the experience gained in the present undertaking.

II. AN INTEGRAL METHOD FOR THE ANALYSIS OF THE UNSTEADY BOUNDARY LAYER OVER AN OSCILLATING SURFACE

2.1 INTRODUCTION

As in most research efforts there is a great deal of time and energy spent exploring various approaches to a particular problem. Some of the attempts to treat a particular problem prove to be "blind alleys" through which no further progress can be made, while other approaches prove more fruitful. Usually a great deal is learned in the unsuccessful attempts at solving the problem, and this process must be experienced before the real contribution to a given research can be made. Unfortunately all too often only the details of the finished product are presented in a way that would indicate that the polished result is a complete description of the total work that was performed in the course of the research. This leads to a false impression of the total content of the research and in some cases results in an incomplete reporting of information that could be vitally useful to someone pursuing a related problem in the same field. In the spirit of reporting as much as possible about this research we discuss here some of the details of an approach to the present problem that was later abandoned in favor of the methodology described in the remaining chapters. We highlight here the basic details of this approach and attempt to show the difficulties associated with applying the methodology to the present problem.

2.2 EVOLUTION OF THE IDEA

The problem of determining the surface pressure on an oscillating surface with an unsteady turbulent boundary-layer flow suggests a situation of rather great complexity. In constructing an appropriate theoretical model it is necessary to account for the effect of friction and turbulence in the boundary layer as well as the conditions imposed by the moving boundary. One technique which has been used with some success in the treatment of steady turbulent boundary layers is a method involving integral equations of motion. In this approach the boundary-layer momentum equation is integrated across the boundary layer to obtain the momentum integral equation. The chief advantage of this approach is the implicit manner in which the effects of turbulence and viscosity can be incorporated in the formulation. A disadvantage is the difficulty of extension to a wider class of flows. There is an excellent description of differential and integral methods for treatment of steady turbulent boundary-layer flows in an article by Reynolds (1968).

The obvious idea is to extend the integral approach to the present unsteady problem. There have been several attempts to date to treat unsteady laminar boundary layers by means of an integral method. In the recent work of Teipel (1969, 1970) a procedure similar to that of the Kármán-Pohlhausen method has been used to study the oscillating boundary-layer flow along a flat plate. The method is sufficiently general so as to allow extension to problems involving flutter. Another approach has been taken by Yates (1969) in his treatment of the flutter problem. He suggests that the boundary layer may be assumed to behave in a quasi-steady manner in response to external disturbances. This allows the extension of the integral treatment of the flow over a rigid wavy wall to the flow over an oscillating surface. The quasi-steady assumption is warranted if the surface oscillations are sufficiently slow so as to allow the boundary layer to adjust to the changing conditions imposed by the moving boundary. Comparing the characteristic time for diffusion of disturbances in the boundary layer, $\delta^2_{b.l.}/\nu$, with the period of a surface oscillation we find that the quasi-steady assumption is justified whenever the diffusion time is much smaller than the oscillation period. This condition for a turbulent boundary layer requires that the reduced frequency, k, be so small as to render the quasi-steady assumption outside the realm of most physically meaningful applications. For example, $k \sim 0(1)$ for the problem of panel flutter and for the air-sea interaction problem. In light of this we do not pursue the quasi-steady approach. We concentrate on the unsteady integral approach based on the unsteady momentum-integral equation.

2.3 AN EQUIVALENT INVISCID FLOW OVER THE DISPLACEMENT SURFACE

Consider the two-dimensional incompressible flow over an oscillating surface (Fig. 2.1). The flow field consists of a turbulent boundary layer adjacent to the surface and an inviscid flow outside the boundary layer. We assume that the boundary layer thickness is constant and large compared to the amplitude of the surface oscillations. The latter assumption is justified in the analysis of the stability of infinitesimal panel oscillations. Furthermore, we assume that the amplitude of the oscillations is small compared to their characteristic wavelength. We note that the given flow is equivalent to a fictitious inviscid flow over a displacement surface such that the transverse velocity at some surface $z = h$ (outside the boundary layer) is equivalent for the two flows. We assume that the pressure distribution on the displacement surface in the fictitious inviscid flow is the same as the pressure on the actual surface in the real turbulent boundary-layer flow. In order to determine the pressure we require an expression for the displacement surface.

Moore and Ostrach (1957) have derived a differential equation for such a surface for a compressible, three-dimensional unsteady boundary layer. We assume that the displacement surface may be described as the sum of the actual surface and a displacement thickness as follows:

$$z_D = z_s(x,t) + \Delta^*(x,t) \tag{2.1}$$

Without presenting their derivation here we specialize Moore and Ostrach's result for two-dimensional flow:

$$\partial/\partial x(u_e\Delta^*) + \partial\Delta^*/\partial t = \partial/\partial x(u_e\delta^*) + \partial\delta_1/\partial t \tag{2.2}$$

where

$$\delta^* = \int_0^\infty (1 - \rho u/\rho_e u_e)dz$$

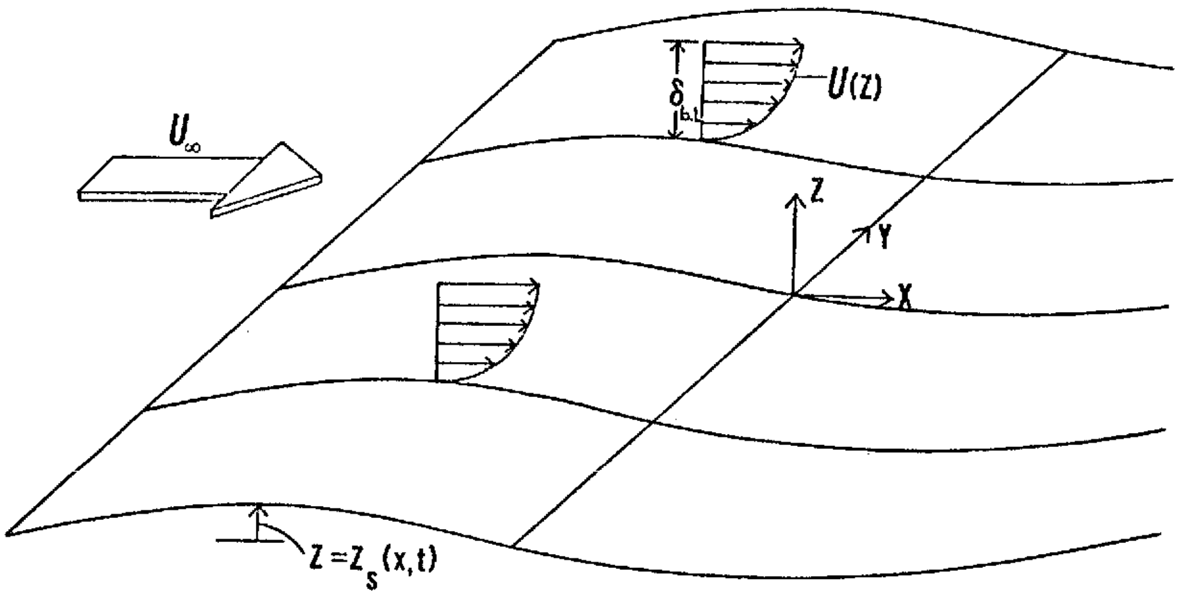

FIGURE 2.1
TWO DIMENSIONAL FLOW OVER AN OSCILLATING WAVY SURFACE

$$\delta_1 = \int_0^\infty (1 - \rho/\rho_e) dz$$

The two quantities δ^* and δ_1 are the displacement thickness and the density defect thickness, respectively. The latter quantity is zero for incompressible flow. The velocity at the edge of the boundary layer is given by u_e. Note that in the case of steady flow we have that

$$\Delta^* = \delta^*, \tag{2.3}$$

so that the displacement surface thickness is given by the mass displacement thickness. For steady flow we use the two interchangeably, but for unsteady flow this is definitely not the case.

Let us assume that the problem of interest may be considered as a small perturbation about the incompressible steady flow boundary layer over a flat plate. We represent the quantities of interest (nondimensionally) as follows:

$$\begin{aligned} \Delta^* &= \Delta_o^* + \epsilon \hat{\Delta}_1^*(x) e^{ikt} \\ \delta^* &= \delta_o^* + \epsilon \hat{\delta}_1^*(x) e^{ikt} \\ u_e &= u_\infty + \epsilon \hat{u}_1(x) e^{ikt} \end{aligned} \tag{2.4}$$

when the actual surface is executing simple harmonic motion about the mean flat plate surface $(z = 0)$ of the form

$$z_s = \epsilon \hat{z}_s(x) e^{ikt} \tag{2.5}$$

where ϵ is a nondimensional amplitude parameter defined in the nomenclature. From (2.3) we have for the mean flow

$$\Delta_o^* = \delta_o^* \tag{2.6}$$

Substituting (2.4) and (2.6) in (2.2) and neglecting the terms of $0(\epsilon^2)$ we obtain the following equation for the perturbation term of $0(\epsilon)$:

$$\hat{\Delta}_1^{*\prime}(x) + ik\hat{\Delta}_1^* = \hat{\delta}_1^{*\prime}(x) \tag{2.7}$$

The solution to (2.7) subject to the boundary condition

$$\hat{\Delta}_1^*(x) = 0, \quad x < 0 \tag{2.8}$$

is

$$\hat{\Delta}_1^* = \int_0^x \hat{\delta}_1^{*\prime}(x_1) e^{-ik(x-x_1)} dx_1 \tag{2.9}$$

The remaining task is to determine the pressure for the inviscid flow over the displacement surface

$$z_D = \Delta_o^* + \epsilon(\hat{z}_s(x) + \hat{\Delta}_1(x))e^{ikt} \tag{2.10}$$

Since the boundary-layer thickness is assumed constant we can assume that the mean part of z_D is constant. We are really interested in the flow over the perturbation part of z_D, which is the actual surface augmented by the variable portion of the displacement surface. In the linearized potential flow theory the surface pressure is given by the superposition

$$p_s = \epsilon(\hat{p}_o + \hat{p}_{BL})e^{ikt} \tag{2.11}$$

where $\hat{p}_o$ is the pressure due to $\hat{z}_s$ and $\hat{p}_{BL}$ is the pressure due to $\hat{\Delta}_1^*$. In order to proceed further we must specify $\hat{z}_s$ and $\hat{\Delta}_1^*$. We assume that $\hat{z}_s$ is given and we find $\hat{\Delta}_1^*$ from (2.9). This requires that we determine the mass displacement thickness, δ^*. We proceed by considering the momentum-integral equation for unsteady flow.

2.4 THE UNSTEADY MOMENTUM-INTEGRAL EQUATION

The unsteady boundary layer may be described by the continuity and momentum equations

$$u_x + w_z = 0 \tag{2.12}$$

$$u_t + uu_x + wu_z = -\frac{1}{\rho}p_{e_x} + \frac{1}{\rho}\tau_x \tag{2.13}$$

We assume that the no-slip conditions apply at the surface. The linearized form of these conditions is

$$w(x, 0, t) = z_{s_t}(x, t) \tag{2.14a}$$

$$u(x, 0, t) = -u_z(x, 0, t) z_s(x, t) \tag{2.14b}$$

The integral statement of the problem is obtained by integrating (2.13) across the boundary layer. See Appendix A for a derivation which parallels that given by Teipel (1970). The result innondimensional variables is the unsteady momentum-integral equation

$$\theta_x + (\delta^* + 2\theta) u_{e_x} + (\delta^*_t + \delta^* u_{e_t}) - w_o(1 - u_o) = \frac{1}{2} C_{f_o} \tag{2.15}$$

where

$$\delta^* = \int_o^{\delta_o} (1 - u) dz$$

$$\theta = \int_o^{\delta_o} u(1 - u) dz$$

$$C_{f_o} = \tau_o / \tfrac{1}{2} \rho u_o^2$$

This equation introduces the momentum defect thickness, θ, and the skin-friction coefficient, C_{f_o}, evaluated at $z = 0$. Note that w_o and u_o are the velocity components at $z = 0$ given by the nondimensional form of (2.14) with (2.5). Thus we have approximately

$$\begin{aligned} w_o &= \epsilon i k \hat{z}_s(x) e^{ikt} \\ u_o &= -\epsilon U'(0) \hat{z}_s(x) e^{ikt} \end{aligned} \tag{2.16}$$

assuming that we can write the u-component of velocity as the sum of a mean and an unsteady perturbation

$$u = U(z) + \epsilon \hat{u}_1(x,z)e^{ikt} \tag{2.17}$$

If, in addition, we assume that θ, δ^*, u_e, and C_{f_o} can be represented as in (2.17), then the terms of $0(\epsilon)$ in (2.15) yield the following perturbation equation:

$$\hat{\theta}_1'(x) + (\delta_o^* + 2\theta_o)\hat{u}_{e_1}'(x) + ik(\hat{\delta}_1^* + \delta_o \hat{u}_{e_1}) - ik\hat{z}_s = \frac{1}{2}\hat{C}_{fo_1} \tag{2.18}$$

In this equation δ_o^* and θ_o are constants and may be determined from

$$\delta_o^* = \delta_o \int_o^1 (1 - U(z^*))dz^* \tag{2.19}$$

$$\theta_o = \delta_o \int_o^1 U(z^*)(1 - U(z^*))dz^* \tag{2.20}$$

where

$$z^* = z/\delta_o$$

We may assume that the effect of the perturbation shear stress is negligible insofar as the determination of the pressure is concerned (see Chapter IV) so that we may neglect $\hat{C}_{fo_1}$ in (2.18). This equation then contains three unknowns: $\hat{\delta}_1, \hat{\theta}_1$, and $\hat{u}_{e_1}$. We need two additional equations in order to determine $\hat{\delta}_1^*$.

One equation for $\hat{u}_{e_1}$ may be found by noting that u_e is the velocity at the edge of the boundary layer. This velocity is equivalent to the velocity on the displacement surface z_D given by (2.10). With Δ_o^* constant and assuming that $\hat{\Delta}_1^* \sim 0(\delta_o) << 1$ we can state approximately that u_e is equivalent to the velocity at the actual surface in inviscid flow. Thus $\hat{u}_{e_1}$ is approximately equal to the $\hat{u}$-velocity at $z = 0$ in the linearized potential flow over the surface z_s given by (2.5). Symbolically

$$\hat{u}_{e_1} = \hat{u}_s(x,0) = f(\hat{z}_s(x)) \tag{2.21}$$

where the functional dependence upon $\hat{z}_s$ is determined by the potential flow solution.

An additional equation can be obtained by specifying a relationship between the perturbation displacement and momentum thicknesses of the form

$$H_1 = \hat{\delta}_1^* / \hat{\theta}_1 \tag{2.22}$$

where H_1 is a shape factor which must be determined by further analysis.

2.5 CLOSURE OF THE SET OF EQUATIONS

We have postulated a relationship between $\hat{\delta}_1^*$ and $\hat{\theta}_1$. Using the definitions of δ^* and θ in (2.15) and the assumed velocity profile in (2.17), we obtain the following expression for H_1:

$$H_1 = \frac{-\int_o^1 \hat{u}_1(x, z^*)dz^*}{\int_o^1 \hat{u}_1(x, z^*)(1 - 2U(z^*))dz^*} \tag{2.23}$$

The closure of this integral scheme is dependent upon the choice of a perturbation velocity profile, $\hat{u}_1(x, z\ )$.

For laminar flow we can follow Teipel's suggestion and assume a fourth order polynomial for the u-velocity components of the form

$$U = \sum_{i=0}^{4} a_i(z^*)^i \tag{2.24a}$$

$$u_1 = \sum_{i=0}^{4} A_i(z^*)^i \tag{2.24b}$$

The unknown coefficients are determined by stipulating appropriate boundary conditions for u at $z^* = 0$ and at $z^* = 1$. The resulting velocity profile is very similar to the polynomial used in the original method by von Kármán (1921) and Pohlhausen (1921). The method is ordinarily restricted to laminar flows where the shear stress can be expressed in terms of a velocity gradient. It is possible to extend the method to treat the turbulent boundary layer. For the case of steady flow Tanaka and Himeno (1970) have shown that the velocity profile can be approximated by a polynomial in the outer layer, in that part of the velocity which remains after subtracting the velocity which changes very rapidly in the neighborhood of the wall (sublayer). The coefficients of the polynomial are determined by the boundary conditions at the inside and the outside edges of the outer layer. The thickness of the inner layer (sublayer) is so thin that it is replaced by $z^* = 0$. It seems reasonable to assume that this idea can be extended to the unsteady flow of interest. The difficulty of applying this method rests with the uncertainty of our knowledge of the conditions at the edge of the sublayer, particularly the perturbation velocity component and shear stress.

Another possibility would be to determine the perturbation velocity component by solving directly for the perturbation flow. The flow is a small perturbation of the steady mean boundary layer over a flat plate. This approach goes somewhat beyond the original intent of an integral method in the sense that we would be determining the details of the boundary-layer flow, a task which is supposed to be alleviated by use of an integral method. We have no choice, however, if we are to determine $\hat{u}_1$ by purely theoretical means. We develop such a methodology in the following chapter, the output of which can be utilized for the present purpose. We find that we can determine the surface pressure directly by this method rather than using this output with (2.20) in conjunction with the integral method. This implies that an integral method is perhaps not the most direct way to attack the present problem.

In lieu of closing the set of equations by obtaining suitable information on the perturbation velocity profile, there are alternative ways to proceed. One can attempt to find additional integral equations relating the integral parameters. In the article by Reynolds mentioned earlier we find several possibilities for the choice of an additional integral equation. One choice involves the mean energy integral equation and requires information about the turbulent shear stress in calculating the dissipation of energy from the mean field to the turbulence.

Another choice involves the entrainment concept to provide an additional equation. The moment of momentum integral equation, formed by multiplication by z^*, is yet another choice and requires an assumption about the integral of the turbulent shear stress. The discussion of Reynolds for steady flow can be generalized for unsteady flow, though we have not pursued these ideas for the present integral scheme. We find that the approach taken in succeeding chapters does not suffer from the uncertainties associated with some of the semi-empirical assumptions that are required in connection with the choice of the second integral equation. Owing to these uncertainties we will not enlarge upon this analysis; instead, we proceed to a consideration of the problem based on the differential form of the equations of motion.

III. TWO-DIMENSIONAL INCOMPRESSIBLE INVISCID SHEAR FLOW OVER AN OSCILLATING SURFACE

3.1 INTRODUCTION

The goal of this chapter is to determine the surface pressure perturbations due to the unsteady boundary layer flow over an oscillating surface without considering the effects of viscosity directly. The latter will be represented indirectly by the mean shear velocity profile and its effect on the perturbation flow field.

Consider the flow over a surface that is essentially plane except for small unsteady perturbations. Refer again to Fig. 2.1 and to Fig. 3.1 where we have chosen a Cartesian coordinate system with flow in the x-direction over a surface which is executing simple harmonic motion and which can be described as follows:

$$z_s(x,t) = a\hat{z}_s(x)e^{i\omega t} \tag{3.1}$$

It is assumed that flow conditions do not vary in the y-direction. Assume that the amplitude of the surface perturbations, a, is much smaller than a characteristic length, L. The length, L, may be the wavelength of a traveling wave-train for the case of ocean waves or the panel chord for the case of panel flutter. This condition can be expressed by the requirement that the ratio of these two lengths is a small quantity; that is,

$$\epsilon = a/L \ll 1 \tag{3.2}$$

The function $\hat{z}_s$ which describes the spatial part of the surface perturbations is left unspecified at this point for greater generality. The disturbances can extend over the entire range of x or they may be limited to a finite length.

The flow is assumed to be divided into two distinct regions: a thin boundary layer adjacent to the oscillating surface and an outer flow region above the boundary layer which extends to infinity in the z-direction. Let us assume that the thickness of the boundary layer is constant over the region of the surface perturbations. Furthermore, let us assume that this thickness, call it $\delta_{b.l.}$, is large compared

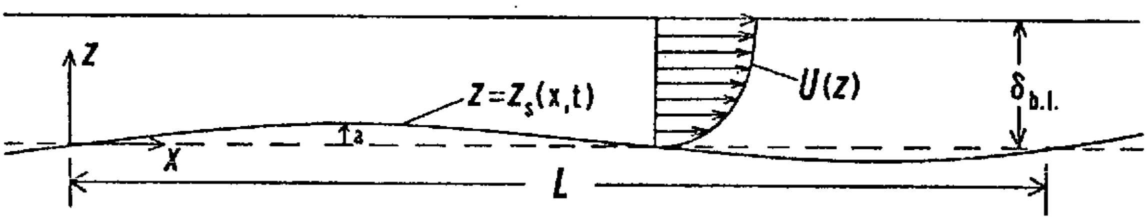

FIGURE 3.1
DETAILS OF THE SHEAR LAYER MODEL FOR FLOW OVER
AN OSCILLATING WAVY SURFACE

to the surface perturbation amplitude, a, yet small compared to the length, L. In terms of a thickness made nondimensional by L, this condition is

$$\epsilon << \delta_o << 1, \qquad \delta_o = \delta_{b.l.}/L \tag{3.3}$$

Implicit in this assumption is the additional assumption that the mean shear profile is unaffected by the motion of the surface.

3.2 FORMULATION OF THE PROBLEM

The governing equations for incompressible two-dimensional flow, neglecting viscosity, are the equations of conservation of momentum and mass. These equations can be expressed using nondimensional variables (lengths nondimensionalized by L, time by L/u_∞, velocity by u_∞, and pressure by $p/\rho u_\infty^2$) as follows:

$$u_t + uu_x + wu_z = - p_x \tag{3.4}$$

$$w_t + uw_x + ww_z = - p_z \tag{3.5}$$

$$u_x + w_z = 0 \tag{3.6}$$

We assume that the flow variables may be decomposed into a mean flow quantity and a perturbation quantity that is linear in the small nondimensional amplitude parameter, ϵ. Thus,

$$u = U(z) + \epsilon\hat{u}(x, z)e^{ikt},$$

$$w = \epsilon\hat{w}(x, z)e^{ikt}, \tag{3.7}$$

and

$$p = p(z) + \epsilon\hat{p}(x, z)e^{ikt}$$

The mean flow quantities are assumed to be solutions of the full Navier-Stokes equations. Note that in the boundary layer

$$p = \text{Constant} \quad \text{since} \quad p_z = 0 \tag{3.8}$$

if we use the boundary-layer approximation for the mean flow. The mean longitudinal velocity component or mean shear profile is assumed to vary only in the boundary layer, that is

$$U = \begin{cases} U(z), & 0 \le z \le \delta_o \\ 1, & z \ge \delta_o \end{cases} \tag{3.9}$$

To obtain the equations for the perturbation flow we substitute Eqs. (3.7) into (3.4)–(3.6). The result for the linearized perturbation quantities is

$$ik\hat{u} + U\hat{u}_x + \hat{w}U'(z) = -\hat{p}_x \tag{3.10}$$

$$ik\hat{w} + U\hat{w}_x = -\hat{p}_z \tag{3.11}$$

$$\hat{u}_x + \hat{w}_z = 0 \tag{3.12}$$

Note that this step introduces a nondimensional parameter, k, the reduced frequency,

$$k = \omega L/u_\infty \tag{3.13}$$

We will assume for the moment that $k = 0(1)$ indicating that the order of magnitude of the time derivatives is of comparable size to the space derivatives. We shall consider the limiting case as $k \to 0$ in a separate section.

The set of governing equations can be reduced to a single equation for $\hat{w}$ by elimination of the pressure between (3.10) and (3.11) and by using (3.12) to eliminate $\hat{u}$. The result is as follows:

$$D\nabla^2\hat{w} - U''(z)\hat{w}_x = 0 \tag{3.14}$$

where

$$\begin{aligned} D &= ik + U\partial/\partial x \\ \nabla^2 &= \partial^2/\partial x^2 + \partial^2/\partial z^2 \end{aligned} \tag{3.15}$$

The boundary conditions at the oscillating surface and at large distances from the surface must be specified. Since we are neglecting viscosity in this formulation we apply the inviscid tangency condition at the surface. The linearized condition is

$$\hat{w} = D\hat{z}_s(x) \quad \text{on} \quad z = \epsilon\hat{z}_s(x)e^{ikt} \tag{3.16}$$

This condition can be transferred to the mean surface $z = 0$ by expanding $\hat{w}$ and U in a Maclaurin series about $z = 0$ and retaining only the terms of $0(1)$. The result with the additional information that

$$U(0) = 0 \tag{3.17}$$

is

$$\hat{w}(x, 0) = ik\hat{z}_s(x) \tag{3.18}$$

It is interesting to note that this result is the same as the linearized form of the no-slip condition for $\hat{w}$ in viscous flow. The other boundary condition which must be satisfied is the vanishing of disturbances at infinity; that is,

$$\hat{w} = 0 \quad \text{as} \quad z \to \infty \tag{3.19}$$

We shall find it necessary to impose additional conditions at the interface between the boundary layer and the outer flow, and these will be discussed in the course of the solution.

Once the transverse velocity component, $\hat{w}$, has been determined, the perturbation pressure may be obtained by integrating the transverse momentum equation with respect to z as follows:

$$\hat{p}(x, 0) = \int_0^\infty D\hat{w}dz \tag{3.20}$$

The perturbation at infinity is assumed to be zero. The pressure at $z = 0$ is equal to the surface pressure in the linearized theory so that the evaluation of the integral in (3.20) gives the surface pressure perturbation.

3.3 SOLUTION

We seek the solution of Eq. (3.14) subject to the boundary conditions (3.18) and (3.19) and the assumption (3.9) regarding the z-variation of U. It is convenient to consider the boundary layer and the outer flow regions separately. When considering the boundary layer it is appropriate to introduce a transverse coordinate based on the boundary layer thickness as a reference length; that is,

$$z^* = z/\delta_o \tag{3.21}$$

where z is the nondimensional transverse coordinate and δ_o is the nondimensional boundary-layer thickness. Introducing Eq. (3.21) in (3.14) we obtain the following equation:

$$D(\hat{w}_{z^*z^*} + \delta_o^2 \hat{w}_{xx}) - U''(z^*)\hat{w}_x = 0, \qquad 0 \le z^* \le 1 \tag{3.22}$$

We can approximate the equation by neglecting the term of $0(\delta_o^2)$ which is a higher order term due to the assumption in Eq. (3.3). This is consistent with the boundary-layer assumption that transverse variations are much greater than longitudinal variations in the boundary layer. In mathematical terms this is equivalent to expanding $\hat{w}$ in a power series in increasing powers of δ_o and truncating the series after the term of $0(\delta_o)$. The approximate equation which applies only within the boundary layer is thus

$$D\hat{w}_{z^*z^*} - U''(z^*)\hat{w}_x = 0, \qquad 0 \le z^* \le 1 \tag{3.23}$$

Outside the boundary-layer region we assume that the x and z derivatives are of comparable orders of magnitude. The shear velocity, U, is constant so that U'' is zero. This simplifies Eq. (3.14) as follows:

$$D\nabla^2 \hat{w} = 0, \qquad z \ge \delta_o \tag{3.24}$$

where

$$D = ik + \partial/\partial x$$

It can be demonstrated that the perturbation velocity components obey Laplace's equation in the outer flow region if, in addition to the condition of incompressibility, it is assumed that the flow is irrotational. Then we have instead of Eq. (3.24) the following equation:

$$\nabla^2 \hat{w} = 0 \tag{3.25}$$

The solution of Eqs. (3.23) and (3.25) subject to the conditions (3.18) and (3.19) is accomplished by employing Fourier integral transformation on x. This reduces the partial differential equations to ordinary differential equations in z. If we define the Fourier transform of the transverse velocity as follows:

$$\tilde{w}(\alpha, z) = \int_{-\infty}^{\infty} \hat{w}(x, z)e^{-i\alpha x}dx \tag{3.26}$$

then transformation of (3.23) and (3.18) yields the following problem for the boundary-layer region:

$$(k + \alpha U)\tilde{w}_{z^*z^*} - \alpha U''(z^*)\tilde{w} = 0, \qquad 0 \leq z^* \leq 1 \tag{3.27}$$

$$\tilde{w}(\alpha, 0) = ik\tilde{z}_s(\alpha) \tag{3.28}$$

where $\tilde{z}_s(\alpha)$ is the Fourier transform of the surface amplitude function, $\hat{z}_s(x)$. Note that Eq. (3.27) can be written as an exact differential as follows:

$$d/dz^* \left\{(k + \alpha U)^2 d/dz^*[\tilde{w}/(k + \alpha U)]\right\} = 0 \tag{3.29}$$

Integration of (3.29) twice with respect to z^* yields the following:

$$\tilde{w}/(k + \alpha U) = \tilde{A}\int(k + \alpha U)^{-2}dz^* + \tilde{B} \tag{3.30}$$

where the unknown constants of integration, $\tilde{A}$ and $\tilde{B}$, are functions of the parameter α. One of these functions can be determined by satisfying the boundary condition (3.28), which yields

$$\tilde{w} = i(k + \alpha U)\left\{\tilde{z}_s - i\tilde{A}\int_0^{z^*} (k + \alpha U)^{-2}dz^*\right\}, \qquad 0 \leq z^* \leq 1 \tag{3.31}$$

The function $\tilde{A}$ will be determined by matching this solution with the outer flow solution at $z^* = 1$.

We treat the outer flow by employing the Fourier transform. The transformed version of Laplace's equation is

$$\tilde{w}_{zz} - \alpha^2\tilde{w} = 0, \qquad z \geq \delta_o \tag{3.32}$$

A solution to this equation which satisfies the condition (3.19) of vanishing velocity perturbations at infinity is

$$\tilde{w} = \tilde{w}_1 e^{-|\alpha|(z-\delta_o)}, \qquad z \geq \delta_o$$

or (3.33)

$$\tilde{w} = \tilde{w}_1 e^{-|\alpha|\delta_o(z^*-1)}, \qquad z^* \geq 1$$

The two unknown functions $\tilde{A}$ and $\tilde{w}_1$ may be determined by imposing two conditions at the interface between the boundary layer and the outer flow. The conditions are that $\tilde{w}$ and $\tilde{w}_{z*}$ should be equal at $z^* = 1$. These conditions require that the velocity perturbations and, hence, the pressure perturbations, be continuous at the interface. The result of imposing these conditions with $U'(1) = 0$ is as follows:

$$\tilde{A} = -\delta_o i|\alpha|(k+\alpha)^2[1+\delta_o|\alpha|(k+\alpha)^2\tilde{F}(\alpha,k)]^{-1}\tilde{z}_s(\alpha) \tag{3.34}$$

$$\tilde{w}_1 = i(k+\alpha)[1+\delta_o|\alpha|(k+\alpha)^2\tilde{F}(\alpha,k)]^{-1}\tilde{z}_s(\alpha) \tag{3.35}$$

where

$$\tilde{F} = \int_o^1 (k+\alpha U)^{-2} dz^*$$

We are interested in the solution for small δ_o. We can obtain the first two terms of the power series expansion of $\tilde{w}$ in powers of δ_o by expanding the binomial in (3.34) and (3.35) as follows:

$$[1+\delta_o|\alpha|(k+\alpha)^2\tilde{F}(\alpha,k)]^{-1} = 1 - \delta_o|\alpha|(k+\alpha)^2\tilde{F} + 0(\delta_o\alpha^3\tilde{F})^2 \tag{3.36}$$

We can neglect the remainder in the above expansion provided

$$|\delta_o\alpha^3\tilde{F}(\alpha,k)| \ll 1 \tag{3.37}$$

This condition is satisfied when δ_o is small, provided the combination $\alpha^3\tilde{F}$ is not large. We will assume for the moment that $k = 0(1)$ and that α is sufficiently small so that the inequality in (3.37) is satisfied. Note that for k approaching zero the integral $\tilde{F}$ becomes large in magnitude. The steady flow limit will be considered in a later section. The assumption of small α is equivalent to one of gradual variation in the surface perturbations and restricts the theory to exclude rapid variations of the surface amplitude function $\hat{z}_s(x)$. The small perturbation expansion (3.36) with the limitation (3.37) yields the following approximate result for the velocity perturbation to $0(\delta_o)$ in the boundary layer:

$$\tilde{w} = i(k + \alpha U)[1 - \delta_o |\alpha|(k + \alpha)^2 \int_o^{z^*} (k + \alpha U)^{-2} dz^*]\tilde{z}_s(\alpha) \tag{3.38}$$

The expression (3.38) evaluated at $z^* = 1$ is equivalent to the expansion of $\tilde{w}_1$ to $0(\delta_o)$, namely,

$$\tilde{w}_1 = i(k + \alpha)[1 - \delta_o |\alpha|(k + \alpha)^2 \tilde{F}(\alpha, k)]\tilde{z}_s(\alpha) \tag{3.39}$$

The Fourier transform of the surface pressure perturbation given in (3.20) is

$$\tilde{p}(\alpha, 0) = i \int_o^{\infty} (k + \alpha U)\tilde{w} dz^* \tag{3.40}$$

The evaluation of this integral is facilitated by dividing the range of integration into two parts

$$\tilde{p}(\alpha, 0) = i \int_o^{\delta_o} (k + \alpha U)\tilde{w} dz + i(k + \alpha) \int_{\delta_o}^{\infty} \tilde{w} dz \tag{3.41}$$

Substitution for $\tilde{w}$ using (3.38) and (3.33) yields

$$\tilde{p}(\alpha;0) = - \delta_o \int_o^1 (k + \alpha U)^2 dz^* \tilde{z}_s + i(k + \alpha)\tilde{w}_1/|\alpha| + 0(\delta_o^2) \tag{3.42}$$

Substitution for $\tilde{w}_1$ using (3.39) and rearranging gives

$$\tilde{p}(\alpha;0) = - (k + \alpha)^2 \tilde{z}_s/|\alpha| + \delta_o[- \int_o^1 (k + \alpha U)^2 dz^* + (k + \alpha)^4 \tilde{F}(\alpha, k)]\tilde{z}_s$$
$$+ 0(\delta_o^2) \tag{3.43}$$

The first term in the above expression is the potential flow pressure which one would obtain if there were no boundary layer and the mean velocity were constant throughout the flow (see Appendix B). The term of $0(\delta_o)$ is the effect of the mean boundary layer shear flow on the pressure, and the two expressions within the parentheses in (3.43) can be interpreted individually. The first term represents the effect of w-variations within the boundary layer, while the second expression gives the effect of w-variations in the boundary layer which appear in the outer flow by virtue of the interface conditions. We have been able to include this latter effect by simultaneously determining the boundary layer and outer flow perturbations.

3.4 AN ALTERNATE FORMULATION

The result of the previous section can be obtained using a slightly different approach which will be employed in the extension of the present problem to treat the effects of viscosity and compressibility. This approach might have some general utility in handling other problems involving perturbations of a mean shear flow. The starting point for this formulation is the set of governing equations, (3.10)-(3.12), for the perturbation quantities and the associated boundary conditions, (3.18) and (3.19). Consider the flow in the boundary layer. Using (3.11) the transverse pressure gradient in terms of the boundary-layer coordinate defined by (3.21) is as follows:

$$\hat{p}_{z*} = - \delta_o D\hat{w} \tag{3.44}$$

This implies that z*-variations of the pressure are of $0(\delta_o)$ so that within the boundary layer the pressure is of the form

$$\hat{p} = \hat{p}_o(x) + \delta_o \hat{p}_{BL}(x, z*) + \cdots \tag{3.45}$$

where $\hat{p}_o(x)$ is the inviscid surface pressure perturbation as determined from the potential flow over the oscillating surface. Now if we differentiate (3.10) with respect to x and use (3.12) to eliminate $\hat{u}$ we obtain

$$D\hat{w}_{z*} - U'(z*)\hat{w}_x = \delta_o \hat{p}_{xx} \tag{3.46}$$

Substituting for $\hat{p}$ using (3.45) and neglecting the terms of $0(\delta_o^2)$ we obtain the following equation which is equivalent to the momentum equation under the boundary-layer assumption of negligible transverse pressure gradient

$$D\hat{w}_{z*} - U'(z*)\hat{w}_x = \delta_o \hat{p}_o''(x) \tag{3.47}$$

This can be simplified by the introduction of the streamline deviation, $\delta(x, z, t)$, which is related to the perturbation velocity component, w. The perturbed flow streamlines are given by $z = \text{constant} + \delta(x, z, t)$. The condition that this surface be a stream surface is the condition of flow tangency:

$$DF/Dt = 0 \quad \text{on} \quad F = 0 \tag{3.48}$$

where

$$D/Dt = \partial/\partial t + \vec{v} \cdot \text{grad}$$

$$F = z - (\text{constant} + \delta)$$

With velocity components given in (3.7) and assuming δ is of the form

$$\delta = \epsilon \hat{\delta}(x, z) e^{ikt} \tag{3.49}$$

condition (3.48) yields the following equation neglecting terms of $0(\epsilon^2)$:

$$\hat{w} = D\hat{\delta} \tag{3.50}$$

If this result is substituted in (3.47) a simplified momentum equation is obtained:

$$D^2 \hat{\delta}_{z*} = \delta_o \hat{p}_o''(x), \qquad 0 \le z* \le 1 \tag{3.51}$$

In the outer flow $\hat{\delta}$ satisfies Laplace's equation as in the previous formulation:

$$\nabla^2 \hat{\delta} = 0, \qquad z* \ge 1 \tag{3.52}$$

The boundary conditions, (3.18) and (3.19), in terms of $\hat{\delta}$ are

$$\hat{\delta}(x, 0) = \hat{z}_s(x)$$

and

$$\hat{\delta} = 0 \quad \text{as} \quad z \to \infty \tag{3.54}$$

The linearized surface pressure perturbation is given by (3.20) using (3.50) as follows:

$$\hat{p}(x, 0) = \int_0^\infty D^2 \hat{\delta} dz \tag{3.55}$$

The solution for $\hat{\delta}$ is obtained by Fourier transformation on x. The boundary-layer equation for $\tilde{\delta}$ becomes

$$\tilde{\delta}_{z*} = \delta_o \alpha^2 (k + \alpha U)^{-2} \tilde{p}_o(\alpha), \qquad 0 \le z^* \le 1 \tag{3.56}$$

with

$$\tilde{\delta}(\alpha; 0) = \tilde{z}_s(\alpha) \tag{3.57}$$

where the Fourier transform of $\hat{\delta}$ is defined as

$$\tilde{\delta}(\alpha; z^*) = \int_{-\infty}^{\infty} \hat{\delta}(x, z^*) e^{-i\alpha x} dx \tag{3.58}$$

An integral of (3.56) subject to (3.57) is

$$\tilde{\delta} = \tilde{z}_s(\alpha) + \delta_o \alpha^2 \tilde{p}_o(\alpha) \int_0^{z^*} (k + \alpha U)^{-2} dz^*, \qquad 0 \le z^* \le 1 \tag{3.59}$$

The outer flow problem for $\tilde{\delta}$ yields a solution satisfying (3.54)

$$\tilde{\delta} = \tilde{\delta}_1 e^{-|\alpha|(z - \delta_o)}, \qquad z \ge \delta_o \tag{3.60}$$

or (3.60)

$$\tilde{\delta} = \tilde{\delta}_1 e^{-|\alpha| \delta_o (z^* - 1)}, \qquad z^* \ge 1$$

where $\tilde{\delta}_1$ is obtained by evaluating the boundary-layer solution (3.59) at $z^* = 1$. Thus,

$$\tilde{\delta}_1 = \tilde{z}_s + \delta_o \alpha^2 \tilde{p}_o \tilde{F}(\alpha, k) \tag{3.61}$$

Having obtained a solution for $\tilde{\delta}$ we can determine the surface pressure by taking the Fourier transform of (3.55)

$$\tilde{p}(\alpha;0) = -\int_{o}^{\infty} (k + \alpha U)^2 \tilde{\delta} dz \tag{3.62}$$

Dividing the range of integration, using (3.59)-(3.61), and neglecting terms of $0(\delta_o^2)$, we obtain the following expression for the pressure:

$$\tilde{p}(\alpha;0) = \tilde{p}_o(\alpha) + \delta_o \left[-\int_{o}^{1} (k + \alpha U)^2 dz^* + (k + \alpha)^4 \tilde{F}(\alpha, k) \right] \tilde{z}_s(\alpha) \tag{3.63}$$

where

$$\tilde{p}_o = -(k + \alpha)^2 \tilde{z}_s(\alpha) / |\alpha| \quad \text{(see Appendix B).}$$

This result duplicates that given by (3.43). The solution is somewhat less cumbersome than the method employed in the previous section, and the formulation emphasizes the boundary-layer nature of the problem. The present method will be useful for most unsteady flow situations but some caution must be exercised in interpreting the result for steady flow. The integral $\tilde{F}(\alpha, k)$ is singular for $k = 0$. This case will be discussed in a later section.

3.5 INVERSION OF THE FOURIER INTEGRAL TRANSFORM OF THE SURFACE PRESSURE PERTURBATION

In order to determine the x-dependence of the surface pressure amplitude we must invert the Fourier transform expressions given by (3.43) or (3.63). This results in an expression of the form

$$p(x, 0;k) = \hat{p}_o(x;k) + \delta_o \hat{p}_{BL}(x;k) \tag{3.64}$$

The inviscid pressure $\hat{p}_o$ is determined using linearized potential flow theory and can be obtained either by inversion of the Fourier transform $\tilde{p}_o$ or by superposition of sources on the x-axis. It is more convenient to use the source potential; for example, the surface pressure on a finite-chord panel is (see

Appendix B)

$$\hat{p}_o = -(ik + d/dx)^2 \frac{1}{\pi}\int_0^1 \log|x - x_1|\hat{z}_s(x_1)dx_1, \qquad 0 \le x \le 1 \tag{3.65}$$

The unsteady boundary-layer effect $\hat{p}_{BL}(x)$ is determined by inversion of the term of $0(\delta_o)$ in the Fourier transform of the surface pressure in (3.63). It is convenient to treat the two parts of this term separately; that is, in terms of the Fourier transform

$$\tilde{p}_{BL}(\alpha) = \tilde{p}_1(\alpha) + \tilde{p}_2(\alpha) \tag{3.66}$$

where

$$\tilde{p}_1 = -\int_0^1 (k + \alpha U)^2 dz^* \tilde{z}_s(\alpha)$$

$$\tilde{p}_2 = (k + \alpha)^4 \tilde{F}(\alpha, k)\tilde{z}_s(\alpha)$$

The inversion of $\tilde{p}_1$ produces the result

$$\hat{p}_1 = (ik)^2 \hat{z}_s(x) + 2ikb\hat{z}_s'(x) + c\hat{z}_s''(x) \tag{3.67}$$

where

$$b = \int_0^1 U dz^*$$

$$c = \int_0^1 U^2 dz^*$$

The inversion of $\tilde{p}_2$ yields for the finite-chord panel

$$\hat{p}_2 = \int_0^x K(x - x_1; k)(ik + d/dx_1)^4 \hat{z}_s(x_1)dx_1 \tag{3.68}$$

where

$$K(x;k) = -x\int_0^1 U^{-2} e^{-ikx/U} dz^*, \qquad x > 0 \tag{3.69}$$

The kernel, K, is convergent if k has a negative imaginary part which need only be infinitesimal in magnitude. In this case the integrand in (3.69) has a finite value at the lower limit of integration notwithstanding the fact that U(0) is zero. Appendix C presents details of the inversion of the Fourier transforms giving $\hat{p}_1$ and $\hat{p}_2$.

3.6 THE LIMITING CASE OF STEADY FLOW

Let us consider the limit as $k \to 0$ which reduces the problem to steady flow over a rigid wavy wall. We expect that there will be perturbations in pressure due to the steady boundary layer and we would like to specialize the present theory to treat this case. The motivation for considering the steady flow limit is the existence of several experimental studies of surface pressures for steady flow over sinusoidal wavy walls. This would provide a direct comparison of the theory with experiment.

If the kernel function in (3.69) is evaluated for $k = 0$ the result is a singular integral. Recall that in the formulation for small δ_o the assumption that $k = 0(1)$ was required in the series expansion of the expressions for w. For the case where $k \to 0$ the neglected terms are not insignificant. For this case the expressions in (3.34) and (3.35) must be used in conjunction with (3.31), (3.33), and (3.40) to give for the transform of the surface pressure

$$\tilde{p}(\alpha;0) = -\frac{(k+\alpha)^2/|\alpha| + \delta_o\alpha^2 H_1(c) + \delta_o^2|\alpha|(k+\alpha)^2 N_2(c)}{[1 + \delta_o(k+\alpha)^2 K_1(c)/|\alpha|]}\tilde{z}_s(\alpha) \tag{3.70}$$

where

$$H_1(c) = \int_0^1 (U - c)^2 dz^*$$

$$N_2(c) = \int_o^1 (U - c)^2 \int_{z^*}^1 (U - c)^{-2} dz^* dz^*$$

$$K_1(c) = \int_o^1 (U - c)^{-2} dz^*$$

where

$$c = - k/\alpha$$

The integrals in (3.70) arise also in the theory of hydrodynamic stability. See, for example, Lin (1955). We will restrict discussion to the case where $\alpha = 0(1)$, that is, gradual variations in the surface deformations. For small values of c the integrals $H_1(c)$ and $N_2(c)$ are $0(1)$, while the integral $K_1(c)$ is $0(c^{-1})$. To see that this is the case note that the contribution of the inner integral in $N_2(c)$ becomes large in the interval near $z^* = 0$, but the factor $(c - U)^2$ is small in this interval and tends to make this part an unimportant contribution to $N_2(c)$. Integration of the expression for $K_1(c)$ by parts yields

$$K_1(c) = - 1/(U'(0)c) + O(\log c) \tag{3.71}$$

With this information the surface pressure in (3.70) becomes

$$\tilde{p}(\alpha;0) = kU'(0)\tilde{z}_s(\alpha)/(\delta_o\alpha) \tag{3.72}$$

This gives zero pressure in the limit as $k = 0$ for finite δ_o and $U'(0)$ which indicates that the theory does not give physically meaningful results for steady flow. The same conclusion was reached by McClure (1962) who developed a theory for calculating the pressure on a surface with infinite traveling waves. His theory gives zero pressure for an inviscid fluid model (similar to the present theory) for the case of steady flow. One explanation for the failure of the inviscid fluid model for the steady case is the neglect of the viscous stress in the problem for the perturbation flow. To see that this is the case let us examine the perturbation momentum equation, (3.10), for flow near the surface. With (3.17) and (3.18) we see that near $z = 0$ for $k = 0$ the inertial terms on the left-hand side of (3.10) are zero leaving nothing to balance the pressure-gradient term on the right-hand side of the equation. This leads us to conclude that for the case where k is small we must include the perturbation viscous stress in the boundary layer, at least in the vicinity of the surface.

In light of the present discussion we can indicate the minimum amount of flow unsteadiness for which the inviscid theory presented here is applicable. The condition in (3.37) which is required for the small perturbation expansion of (3.36) can be recast using (3.71) for small k as follows:

$$\delta_o \alpha^2/(U'(0)k) \ll 1 \tag{3.73}$$

For the case of gradual variations in surface deformation; that is, for $\alpha = 0(1)$, we may simplify (3.73) to

$$\delta_o \ll U'(0)k \tag{3.74}$$

For example, for a turbulent boundary layer with $\delta_o = 0.10$ and $U'(0) = 100$ (3.74) requires that k be much larger than 10^{-3} for the theory to be applicable. We conclude that the theory should apply to most unsteady problems except those for which k is very small. The correction of the present theory due to the effects of the viscous stress in the perturbation flow is the subject of the next chapter.

IV. THE EFFECT OF VISCOSITY

4.1 INTRODUCTION

In the previous chapter we developed a theory for the unsteady boundary layer by considering the boundary layer to be an inviscid shear layer of constant thickness. The effects of viscosity were neglected and only indirectly taken into account to the extent they affect the boundary-layer thickness or the mean shear profile. We found that this theory is inapplicable for very small frequencies, however.

In the present chapter we consider the effect of including the viscous stress in the problem for the perturbed flow. We will determine the surface pressure perturbation for the case of finite but large Reynolds number and reduced frequency assumed to be of order unity. Such an analysis is useful for understanding the limit as $k \to 0$.

4.2 FORMULATION; OUTER EXPANSION; BASIC INVISCID FLOW

Consider the problem of flow over an oscillating surface and assume that the discussion of Section 3.1 is applicable. In the present analysis we assume the existence of a boundary layer of constant thickness adjacent to the surface. We assume that the flow may be decomposed into a mean flow and a perturbation flow as in (3.7). We take the boundary-layer assumption that the pressure variation across the layer is negligible so that we may eliminate the transverse momentum equation (3.11). We then have the linearized longitudinal momentum equation and the continuity equation, (3.10) and (3.12), but now with viscious terms retained. In nondimensional variables the boundary layer equations are

$$ik\hat{u} + U\hat{u}_x + \hat{w}U'(z) = -\hat{p}'(x) + \frac{1}{Re}\hat{u}_{zz} \qquad (4.1)$$

$$\hat{u}_x + \hat{w}_z = 0 \qquad (4.2)$$

where $Re = u_\infty L/\nu$ is the Reynolds number based on the reference length L. The surface boundary condition for viscous flow is the no-slip condition which is a requirement that the fluid velocity equal the velocity of the oscillating surface at the point of contact between the fluid and the impermeable surface. In terms of the two velocity components we must require that

$$u = 0$$

and (4.3)

$$w = \partial z_s/\partial t \quad \text{on} \quad z = z_s(x,t) = \epsilon \hat{z}_s(x) e^{ikt}$$

The linearized conditions may be obtained using (3.7) and by expanding the velocity components in a Maclaurin series about $z = 0$. This gives

$$\hat{u}(x,0) = -\hat{z}_s U'(0) \tag{4.4a}$$

$$\hat{w}(x,0) = ik\hat{z}_s(x) \tag{4.4b}$$

It is convenient to introduce the stream function $\psi(x,z)$ for which the continuity equation (4.2) is automatically satisfied. Thus

$$\hat{u} = \psi_z \qquad \hat{w} = -\psi_x \tag{4.5}$$

Introducing the boundary-layer coordinate defined in (3.21) and the stream function from (4.5) in the momentum equation (4.1) we obtain

$$ik\psi_{z^*} + U\psi_{xz^*} - U'(z^*)\psi_x = -f(x) + 1/R\psi_{z^*z^*z^*}, \qquad 0 \le z^* \le 1 \tag{4.6}$$

where $R = Re\delta_o^2$ and where $f(x) = \delta_o \hat{p}'(x)$. The no-slip conditions require

$$\psi_{z^*}(x,0) = -U'(0)\hat{z}_s(x) \tag{4.7a}$$

$$\psi_x(x,0) = -ik\hat{z}_s(x) \tag{4.7b}$$

We seek an asymptotic solution as the Reynolds number R becomes infinite. Hence, an (outer) expansion of the form

$$\psi(x,z^*;R) \sim \delta_1(R)\psi_1(x,z^*) + \delta_2(R)\psi_2(x,z^*) + \dots \tag{4.8}$$

is sought as $R \to \infty$ with $x, z^* > 0$ fixed. By substituting into the full problem and taking the limit as $R \to \infty$, we find that in the limit δ_1 may be zero, infinite, or finite. If δ_1 is zero we find that ψ_1 is infinite so the problem is meaningless. If δ_1 is infinite the problem is homogeneous and the solution is $\psi_1 = 0$. A significant result is obtained only if δ_1 is finite. Without loss of generality we may set

$$\delta_1(R) = 1 \tag{4.9}$$

The equation for the first approximation then becomes that for the inviscid shear layer,

$$ik\psi_{1z^*} + U\psi_{1xz^*} - U'\psi_{1x} = -f(x) \tag{4.10a}$$

$$\psi_{1x}(x, 0) = -ik\hat{z}_s(x) \tag{4.10b}$$

The no-slip condition (4.7a) has been dropped because it is unenforcible in the outer approximation. The order of the differential equation has been reduced to first order with the neglect of the viscous term, and consequently we can retain only one boundary condition. Note that the problem for ψ_1 is equivalent to the problem for $\hat{\delta}$ posed in (3.51) and (3.53). The boundary condition for $\psi_{1x}(x, 0)$ is equivalent to the linearized form of the tangency condition for inviscid flow, yet we obtained it from the no-slip condition (4.3).

In an analogous manner as before we can obtain a solution to (4.10) by use of the Fourier transform $\tilde{\psi}_1(\alpha;z^*)$. The problem for $\tilde{\psi}_1$ is

$$\tilde{\psi}_{1z^*} - [\alpha U'/(k+\alpha U)]\tilde{\psi}_1 = i\tilde{f}(\alpha)/(k+\alpha U) \tag{4.11a}$$

$$\tilde{\psi}_1(\alpha;0) = -(k/\alpha)\tilde{z}_s(\alpha) \tag{4.11b}$$

where $\tilde{f}(\alpha) = \delta_o i\alpha p_o(\alpha) = -\delta_o(i\alpha/|\alpha|)(k+\alpha)^2\tilde{z}_s$ is the transformed potential flow pressure gradient. A solution to the inhomogeneous first-order ordinary differential equation (4.11a) subject to the boundary condition (4.11b) is

$$\tilde{\psi}_1 = -(k+\alpha U)\tilde{z}_s/\alpha + i(k+\alpha U)\tilde{f}\int_o^{z^*}(k+\alpha U)^{-2}dz^* \tag{4.12}$$

Taking the inverse transform and evaluating at $z^* = 0$ we have

$$\psi_{1z^*}(x, 0) = -U'(0)\hat{z}_s(x) - f(x)/ik \tag{4.13a}$$

$$\psi_1(x, 0) = - ik \int_{-\infty}^{x} \hat{z}_s(x)dx \tag{4.13b}$$

Comparing (4.13a) to the no-slip condition (4.7a) which was dropped in the formulation of the first outer problem we find that the boundary condition is incompatible with the outer problem.

4.3 INNER EXPANSION; INNER BOUNDARY-LAYER EQUATIONS, MATCHING; BASIC INNER FLOW

The loss of the highest derivative in (4.6) is the classical hallmark of a singular perturbation problem (refer to Chapter 7 of Van Dyke (1964)). We know that the basic inviscid solution for the shear layer is not valid near the surface, where the no-slip condition had to be abandoned. There is a region of nonuniformity near the surface. The width of this region of nonuniformity (the inner boundary layer) is of order $\delta_i(R)$, where δ_i is a function that vanishes as its argument becomes infinite. We can obtain coordinates of order unity in this region by magnifying the z*-coordinate, leaving x unaltered. An appropriate magnified (inner) normal coordinate is given by $Z = z^*/\delta_i(R)$, where the stretching factor $1/\delta_i(R)$ is still to be determined. We assume that for large finite values of R corresponding to most practical problems the amplitude of the surface perturbations, ϵ, will be small compared to δ_i. This permits the continued use of the linearized boundary conditions (4.4) imposed on the surface $z^* = 0$.

We consider stretching in the inner region. Note that within the region of nonuniformity we can approximate the mean shear profile as linear, taking only the first term in a Maclaurin series expansion for small z^*. Then in terms of the magnified coordinate we have approximately

$$U = \delta_i U'_w Z$$

and (4.14)

$$U' = U'_w$$

where $U'_w = U'(0)$. Introducing this result in (4.6) and using the stretched coordinate we have

$$ik\psi_Z/\delta_i + U'_w(Z\psi_{xZ} - \psi_x) = -f(x) + 1/(R\delta_i^3)\psi_{ZZZ} \tag{4.15}$$

$$\psi_x(x,0) = -ik\hat{z}_s(x) \tag{4.16a}$$

$$\psi_Z(x,0) = -\delta_i U'_w \hat{z}_s(x) \tag{4.16b}$$

We can specify the stretching which will display the proper behavior of the stream function in the inner boundary layer. There are several alternatives. If we choose

$$\delta_i = R^{-1/3} \tag{4.17}$$

then we have three possibilities depending upon the magnitude of the parameter $\beta = kR^{1/3}$. If the parameter β is large or infinite we have an uninteresting case in which there is no effect of the viscous stress term and the lowest order inner solution is one for which $\psi_Z = 0$. If the parameter is small or zero we have a case in which the effect of the u_t-term in the momentum equation is negligible. The interesting case in the present context is the one in which $\beta \sim 0(1)$. In this condition all of the terms in (4.15) are of order unity and the two boundary conditions (4.16a) and (4.16b) contribute to the same order. The inner problem becomes

$$\psi_{ZZZ} - i\beta\psi_Z - U'_w(Z\psi_{xZ} - \psi_x) = f(x) \tag{4.18}$$

$$\left.\begin{aligned} \psi_x(x,0) &= -\delta_i i\beta\hat{z}_s(x) \\ \psi_Z(x,0) &= -\delta_i U'_w \hat{z}_s(x) \end{aligned}\right. \tag{4.19}$$

This corresponds to small reduced frequency approaching the limit of steady flow as R approaches infinity. Unfortunately, an analytical solution of (4.18) is not easily found. An additional problem associated with this case and with the case for which $\beta \to 0$ is the singularity of the basic inviscid (outer) flow as $k \to 0$. This prevents matching the inner solution and the basic outer solution of (4.13). The nature of this case is such that the region of nonuniformity is not confined to a small portion of the shear layer but rather it pervades the entire outer boundary layer. This will become clear by an alternate specification of the stretching.

If we choose

$$\delta_i = R^{-1/2} \tag{4.20}$$

and consider the case $k \sim 0(1)$ we can rewrite (4.15) as follows:

$$\psi_{ZZZ} - ik\psi_Z = \delta_i[f(x) + U_w'(Z\psi_{xZ} - \psi_x)] \tag{4.21}$$

We assume an inner expansion, valid within the inner region, of the form

$$\psi(x, z^*; R) \sim \Delta_1(R)\Psi_1(x, Z) + \Delta_2(R)\Psi_2(x, Z) + \cdots \tag{4.22}$$

as $R \to \infty$ with x, Z fixed. We determine Δ_1 by substituting this expansion into (4.21) and (4.16) and letting R tend to infinity. This gives

$$\Psi_{1ZZZ} - ik\Psi_{1Z} = \lim_{R\to\infty} [1/(R^{1/2}\Delta_1)]f(x) \tag{4.23}$$

$$\Psi_{1x}(x, 0) = - \lim_{R\to\infty}(1/\Delta_1)ik\hat{z}_s(x) \tag{4.24a}$$

$$\Psi_{1Z}(x, 0) = - \lim_{R\to\infty}[1/(R^{1/2}\Delta_1)]U_w'\hat{z}(x) \tag{4.24b}$$

The limit appearing in (4.23) and (4.24b) may be infinite, finite, or zero. The first two possibilities lead to degenerate solutions that cannot satisfy the inner boundary conditions. We choose the third possibility and take

$$\Delta_1(R) = 1 \tag{4.25}$$

Equation (4.23) for the first term of the inner expansion becomes

$$\Psi_{1ZZZ} - ik\Psi_{1Z} = 0 \tag{4.26}$$

The inner boundary conditions (4.24) become

$$\Psi_{1x}(x, 0) = - ik\hat{z}_s(x) \tag{4.27a}$$

$$\Psi_{1Z}(x, 0) = 0 \tag{4.27b}$$

We need an additional boundary condition to make the problem for Ψ_1 complete. We obtain this by applying the asymptotic matching principle to Ψ_1 for the inner expansion to $0(1)$ and the outer expansion to $0(1)$ [equation (5.24) in Van Dyke (1964)] as follows:

Outer expansion to $0(1)$: $\qquad \psi \sim \psi_1(x, z^*)$ (4.28a)

rewritten in inner variables: $\qquad = \psi_1(x, Z/\sqrt{R})$ (4.28b)

expanded for large R: $\qquad = \psi_1(x, 0) + (Z/\sqrt{R})\psi_{1z^*}(x, 0) + \ldots$ (4.28c)

inner expansion to $0(1)$: $\qquad = \psi_1(x, 0)$ (4.28d)

Inner expansion to $0(1)$: $\qquad \psi \sim \Psi_1(x, Z)$ (4.29a)

rewritten in outer variables: $\qquad = \Psi_1(x, \sqrt{R}z^*)$ (4.29b)

expanded for large R: $\qquad = \Psi_1(x, \infty) + \sqrt{R}z^*\Psi_{1Z}(x, \infty) + \cdots$ (4.29c)

outer expansion to $0(1)$ $\qquad = \sqrt{R}z^*\Psi_{1Z}(x, \infty) + \Psi_1(x, \infty)$ (4.29d)

Equating the two final results gives the matching condition

$$\Psi_{1Z}(x, \infty) = 0 \tag{4.30}$$

We can obtain a solution to the problem for Ψ_1 stated in equations (4.26), (4.27), and (4.30). With $u_1 = \Psi_{1Z}(x, Z)$ equations (4.26) and (4.30) become

$$u_{1ZZ} - iku_1 = 0 \tag{4.31}$$

$$\begin{aligned} u_1(x, 0) &= 0 \\ u_1(x, \infty) &= 0 \end{aligned} \tag{4.32}$$

This is a completely homogeneous problem for u_1 with solution $u_1(x, Z) = 0$. Thus $\Psi_1(x, Z) = \Psi_1(x)$. From (4.27a) we find that

$$\Psi_1(x) = - ik \int_{-\infty}^{x} \hat{z}_s(x)dx \tag{4.33}$$

4.4 THE SECOND TERM IN THE INNER EXPANSION

The standard matching order of steady flow boundary-layer theory requires that we proceed to the second term of the outer expansion after having determined the first term of the inner expansion, a term of $0(R^{-1/2})$. In the present problem we have found that the first term of the inner expansion is 0(1), so that we should perhaps call that the "zeroth order" term and refer to the next term in the inner expansion as the first order term. Thence, we proceed to the second term in the inner expansion. We determine the nature of the gauge function $\Delta_2(R)$ together with the matching conditions by matching the inner expansion to $0(\Delta_2)$ with the outer expansion to 0(1). We find

Outer expansion to 0(1): $$\psi \sim \psi_1(x, z^*) \tag{4.34a}$$

rewritten in inner variables: $$= \psi_1(x, Z/\sqrt{R}) \tag{4.34b}$$

expanded for large $\sqrt{R}$: $$= \psi_1(x, 0) + (Z/\sqrt{R})\psi_{1z^*}(x, 0) + \ldots \tag{4.34c}$$

inner expansion to $0(1/\sqrt{R})$: $$= \psi_1(x, 0) + (Z/\sqrt{R})\psi_{1z^*}(x, 0) \tag{4.34d}$$

rewritten in outer variables: $$= \psi_1(x, 0) + z^*\psi_{1z^*}(x, 0) \tag{4.34e}$$

Inner expansion to $0(\Delta_2)$: $$\psi \sim \Psi_1(x) + \Delta_2\Psi_2(x, Z) \tag{4.35a}$$

rewritten in outer variables: $$= \Psi_1(x) + \Delta_2\Psi_2(x, \sqrt{R}z^*) \tag{4.35b}$$

expanded for large $\sqrt{R}$: $$\begin{aligned} &= \Psi_1(x) + \Delta_2[\Psi_2(x, \infty) \\ &\quad + \sqrt{R}z^*\Psi_{2Z}(x, \infty) + \cdots] \end{aligned} \tag{4.35c}$$

We apply the asymptotic matching principle equating the inner expansion to $0(1/\sqrt{R})$ of the outer expansion to 0(1) with the outer expansion to 0(1) of the inner expansion to $0(\Delta_2)$. We see that $\Delta_2(R)$ must be some multiple of $R^{-1/2}$; we choose

$$\Delta_2 = R^{-1/2} \tag{4.36}$$

Continuing from (4.35c) we have that the outer expansion to 0(1) of the inner expansion to $0(1/\sqrt{R})$ is given by

$$\psi = \Psi_1(x) + z^*\Psi_{2Z}(x, \infty) \tag{4.35d}$$

Comparing (4.34e) and (4.35d) and using the results of the previous section we find that

$$\Psi_{2Z}(x,\infty) = \psi_{1z*}(x,0) \tag{4.37}$$

From (4.13) we find that this becomes

$$\Psi_{2Z}(x,\infty) = -U_w' \hat{z}_s(x) - f(x)/ik \tag{4.38}$$

Substituting the inner expansion (4.22) into the full equation (4.21) produces an inhomogeneous equation for Ψ_2

$$\Psi_{2ZZZ} - ik\Psi_{2Z} = f(x) + U_w'(Z\Psi_{1xZ} - \Psi_{1x}) \tag{4.39}$$

We can simplify the equation by substituting for Ψ_1 using (4.33). Hence

$$\Psi_{2ZZZ} - ik\Psi_{2Z} = f(x) + ikU_w' \hat{z}_s(x) \tag{4.40}$$

Similarly, for the inner boundary conditions we find

$$\Psi_{2x}(x,0) = 0 \tag{4.41a}$$

$$\Psi_{2Z}(x,0) = -U_w' \hat{z}_s(x) \tag{4.41b}$$

We can obtain a solution to the problem posed by (4.40), (4.41) and (4.38). With $u_2 = \Psi_{2Z}$ equations (4.40), (4.41b), and (4.38) may be rewritten as

$$u_{2ZZ} - iku_2 = f(x) + ikU_w' \hat{z}_s(x) \tag{4.42}$$

$$\left.\begin{aligned} u_2(x,0) &= -U_w' z_s(x) \\ u_2(x,\infty) &= -U_w' \hat{z}_s(x) - f(x)/ik \end{aligned}\right. \tag{4.43}$$

We can make (4.42) homogeneous by setting

$$u_2 = -f(x)/ik - U_w' \hat{z}_s(x) + v(x,Z) \tag{4.44}$$

The problem for v becomes

$$v_{ZZ} - ikv = 0 \tag{4.45}$$

$$\left.\begin{aligned} v(x,0) &= f(x)/ik \\ v(x,\infty) &= 0 \end{aligned}\right. \tag{4.46}$$

A solution of (4.45) satisfying (4.46) is easily constructed and gives

$$u_2 = -U_w' \hat{z}_s(x) - f(x)(1-e^{-\sqrt{ik}Z})/ik \tag{4.47}$$

Integrating (4.47) by parts with respect to Z and evaluating the function of integration using (4.41a) we obtain the second term of the inner expansion

$$\Psi_2(x, Z) = -(f(x)/ik + U'_w \hat{z}_s(x))Z + f(x)(1-e^{-ikZ})/(ik)^{3/2} \tag{4.48}$$

We can form the two-term inner expansion of ψ using (4.22), (4.25), (4.33), (4.36), and (4.48). Rewriting in outer variables and taking x and z^* derivatives, we have the inner representations

$$\begin{aligned}\psi_x \sim &- ikz_s(x) - (f'(x)/ik + U'_w \hat{z}_s(x))z^* \\ &+ f'(x)(1 - e^{-\sqrt{ikR}z^*})/(ik)^{3/2}R^{1/2}\end{aligned} \tag{4.49a}$$

$$\psi_{z^*} \sim - U'_w z_s(x) - f(x)(1-e^{-\sqrt{ikR}z^*})/(ik) \tag{4.49b}$$

Note that the inner representation satisfies the no-slip boundary conditions (4.7) at $z^* = 0$. Note also the exponential behavior of the inner representation within the region of nonuniformity. Examining the exponentials we find that the decay constant is the reciprocal of a characteristic length of magnitude $1/(kR)^{1/2}$. Hence, for k approaching zero the characteristic length becomes infinitely large for large fixed values of R. This indicates a failure of the expansion scheme in his limit. For $k \to 0$ we expect the region of nonuniformity to grow so that we can no longer characterize the boundary layer as an outer inviscid region and an inner viscous region. Insteady the entire boundary layer experiences the effects of viscosity.

4.5 THE SECOND TERM IN THE OUTER EXPANSION

The nature of the gauge function $\delta_2(R)$ together with the matching conditions is determined by matching the inner expansion to $0(1/\sqrt{R})$ with the outer expansion to $0(\delta_2)$. Using all previous results we find

Inner expansion to $0(1/\sqrt{R})$: $\quad \psi \sim \Psi_1(x)+(1/\sqrt{R})\Psi_2(x, Z)$ (4.50a)

Substituting for Ψ_1, Ψ_2 using (4.33) and (4.38):

$$= -ik\int_{-\infty}^{x} \hat{z}_s dx + (1/\sqrt{R})[-(f(x)/ik + U'_w \hat{z}_s(x))Z + (f(x)/(ik)^{3/2})(1-e^{-\sqrt{ik}Z})] \tag{4.50b}$$

rewritten in outer variables:

$$= -ik\int_{-\infty}^{x} \hat{z}_s dx + (1/\sqrt{R})[-(f(x)/ik + U'_w \hat{z}_s(x))\sqrt{R}z^* + (f(x)/(ik)^{3/2})(1-e^{-\sqrt{ikR}z^*})] \tag{4.50c}$$

expanded for large R:

$$= -ik\int_{-\infty}^{x} \hat{z}_s dx - (f(x)/ik + U'_w \hat{z}_s(x))z^* + (1/\sqrt{R})f(x)/(ik)^{3/2} + \ldots \tag{4.50d}$$

outer expansion to $0(1/\sqrt{R})$:

$$= -ik\int_{-\infty}^{x} \hat{z}_s dx - (f(x)/ik + U'_w \hat{z}_s(x))z^* + (1/\sqrt{R})f(x)/(ik)^{3/2} \tag{4.50e}$$

rewritten in inner variables:

$$= -ik\int_{-\infty}^{x} \hat{z}_s dx - (Z/\sqrt{R})(f(x)/ik + U'_w \hat{z}_s(x)) + (1/\sqrt{R})(x)/(ik)^{3/2} \tag{4.50f}$$

Outer expansion to $0(\delta_2)$: $\qquad \psi \sim \psi_1(x, z^*) + \delta_2\psi_2(x, z^*)$ (4.51a)

rewritten in inner variables: $\qquad = \psi_1(x, Z/\sqrt{R}) + \delta_2\psi_2(x, Z/\sqrt{R})$ (4.51b)

expanded for large R:

$$= \psi_1(x, 0) + (Z/\sqrt{R})\psi_{1z^*}(x, 0) + \cdots + \delta_2[\psi_2(x, 0) + \cdots] \tag{4.51c}$$

substituting for ψ_1 using (4.13):

$$= -ik\int_{-\infty}^{x} \hat{z}_s dx - (Z/\sqrt{R})(f(x)/ik + U'_w \hat{z}_s(x)) + \delta_2\psi_2(x, 0) + \cdots \tag{4.51d}$$

Comparing (4.50f) and (4.51d) shows that $\delta_2(R)$ must be some multiple of $R^{-1/2}$; we choose

$$\delta_2 = R^{-1/2} \tag{4.52}$$

Using this result we find the inner expansion to $0(1/\sqrt{R})$ of the outer expansion to $0(1/\sqrt{R})$:

$$\psi = -ik\int_{-\infty}^{x} \hat{z}_s dx - (Z/\sqrt{R})(f(x)/ik + U'_w \hat{z}_s(x)) + (1/\sqrt{R})\psi_2(x,0) \tag{4.51e}$$

It then follows that

$$\psi_2(x,0) = f(x)/(ik)^{3/2} \tag{4.53}$$

Substituting the outer expansion (4.8) into the full equation (4.6) yields a homogeneous equation for ψ_2,

$$ik\psi_{2x*} + U\psi_{2xz*} - U'\psi_{2x} = 0 \tag{4.54}$$

The problem for ψ_2 is given by (4.54) and (4.53). Taking the Fourier transform of these equations we find

$$\tilde{\psi}_{2z*} - [\alpha U'/(k+\alpha U)]\tilde{\psi}_2(\alpha;z^*) = 0 \tag{4.55a}$$

$$\tilde{\psi}_2(\alpha;0) = \tilde{f}(\alpha)/(ik)^{3/2} \tag{4.55b}$$

A solution to (4.55a) satisfying (4.55b) is

$$\tilde{\psi}_2 = i(k+\alpha U)\tilde{f}(\alpha)/(ik)^{5/2} \tag{4.56}$$

Hence, upon inversion

$$\psi_2 = (ik + Ud/dx)f(x)/(ik)^{5/2} \tag{4.57}$$

We can also form the two-term outer expansion of ψ, although it is more convenient to work directly with the Fourier transform

$$\psi = -\,i(k+\alpha U)\tilde{z}_s(\alpha)/(i\alpha) + i(k+\alpha U)\tilde{f}\Big[\int_0^{z^*} (k+\alpha U)^{-2}dz^* + R^{-1/2}/(ik)^{5/2}\Big], \qquad 0 \le z^* \le 1 \tag{4.58}$$

4.6 SURFACE PRESSURE

The pressure is determined from the outer flow solution in the same manner as discussed in the previous chapter. Recall that

$$\tilde{p}(\alpha;0) = \delta_o \int_0^1 (ik + i\alpha U)\tilde{w}dz^* + i(k+\alpha)\delta_o \int_1^\infty \tilde{w}dz^* \tag{3.41}$$

where $\tilde{w}$, the Fourier transform of the $\hat{w}$-velocity component, can be obtained from (4.58) for the boundary layer, and (3.33) for the potential flow. Thus

$$\tilde{w} = -\,i\alpha\tilde{\psi} = \begin{cases} (ik+i\alpha U)\Big\{1-\delta_o(\alpha^2/|\alpha|)(k+\alpha)^2\Big[\int_0^{z^*}(k+\alpha U)^{-1}dz^* \\ \qquad + R^{-1/2}/(ik)^{5/2}\Big]\Big\}\tilde{z}_s(\alpha), & 0 \le z^* \le 1 \\ \tilde{w}_1 e^{-|\alpha|\delta_o(z^*-1)}, & z^* \ge 1 \end{cases} \tag{4.58}$$

where

$$\tilde{w}_1 = \tilde{w}(\alpha;1) = i(k+\alpha)\Big\{1 - \delta_o \frac{\alpha^2}{|\alpha|}(k+\alpha)^2\Big[\int_0^1 (k+\alpha U)^{-2}dz^* + R^{-1/2}/(ik)^{5/2}\Big]\Big\}\tilde{z}_s(\alpha)$$

Substituting in (3.41) and neglecting terms of $0(\delta_o^2)$ we find

$$\tilde{p}(\alpha;0) = \tilde{p}_o + \delta_o\tilde{p}_{BL} + \delta_o R^{-1/2}\tilde{p}_v \tag{4.59}$$

where the first two terms are identical to the result obtained in the previous chapter: $\tilde{p}_o$ is the potential flow pressure and $\tilde{p}_{BL}$ is the pressure due to the effect of the shear layer (the effect of the first term in the outer expansion for the boundary layer). See, for example, (3.43). The remaining term in (4.59) is the effect of including viscous stress in the perturbed flow (the second term in the outer expansion) and is

$$\tilde{p}_v = (k + \alpha)^4 \tilde{z}_s(\alpha)/(ik)^{5/2} \tag{4.60}$$

The inverse transform yields

$$\hat{p}(x, 0) = \hat{p}_o(x) + \delta_o \hat{p}_{BL}(x) + \delta_o R^{-1/2} \hat{p}_v(x) \tag{4.61}$$

where $\hat{p}_o$ and $\hat{p}_{BL}$ are given in Section 3.5 and where

$$\hat{p}_v(x) = (ik + d/dx)^4 \hat{z}_s(x)/(ik)^{5/2} \tag{4.62}$$

An alternate way to express this result is as follows:

$$\hat{p}(x, 0) = \hat{p}_o(x) + \delta_o \hat{p}_{BL}(x) + Re^{-1/2} \hat{p}_v(x) \tag{4.63}$$

where $Re = U_\infty L/\nu$. By introducing the Reynolds number based on reference length L (see (4.6)), we have clearly separated the viscous effect from the effect of the perturbation due to the inviscid shear layer.

4.7 DISCUSSION

We can estimate the relative importance of the viscous effect and the effect of the shear layer. For the case where $k \sim 0(1)$ we find that

$$\left| Re^{-1/2} \hat{p}_v / \delta_o \hat{p}_{BL} \right| \sim 0(Re^{-1/2}/\delta_o) \tag{4.64}$$

assuming $\hat{p}_v$ and $\hat{p}_{BL}$ are both $0(1)$. For the case of a typical boundary layer with $\delta_o = 10^{-1}$ and $Re = 10^6$ the ratio is equal to 10^{-2}. The viscous effect is practically negligible compared to the effect of the shear flow. For sufficiently high Reynolds numbers and for boundary layers that are not too thin we find that the effect of including viscous stress in the perturbed flow is negligible provided that the flow is sufficiently unsteady.

It is interesting to see the effect of flow unsteadiness as compared to viscosity. In terms of the Fourier transforms we find

$$\left|Re^{-1/2}\tilde{p}_V/\delta_o\tilde{p}_{BL}\right| \sim \begin{cases} 0(U'_w/(\delta_o k^{3/2} Re^{1/2})) & \text{as } k \to 0 \\ 0(1/(\delta_o k^{5/2} Re^{1/2})) & \text{as } k \to \infty \end{cases} \tag{4.65}$$

As $k \to 0$ we find that the effect of including the viscous stress becomes more important and the character of the flow changes. The nonuniformity grows and the effects of viscosity are experienced throughout the shear layer. For $k \sim 0(1)$ or greater we find that the viscous effect is negligible.

V. EFFECTS OF THE TURBULENT REYNOLDS STRESSES

5.1 INTRODUCTION

The aim of this chapter is to assess the role of perturbations in the background Reynolds stresses in modifying the pressure perturbations on an oscillating surface. The intent is to formulate the problem for the case of two-dimensional incompressible flow including the effects of the turbulent fluctuations, to discuss the problem of closure of the set of equations, and to make a coarse estimate of the effect rather than to obtain an accurate solution. In formulating the problem we draw on the methodology of the preceding two chapters where the effects of turbulence were neglected entirely in the perturbation flow. In that formulation the effect of turbulence is assumed to play an indirect role and is exhibited by the choice of an appropriate mean velocity profile for turbulent flow.

Benjamin (1959) and Miles (1957) have proposed the use of a turbulent mean velocity profile in a small perturbation theory for the shear flow over a surface with traveling waves. McClure (1962) discussed some of the conceptual difficulties that arise in such an analysis, including the fact that there is no sharp critical layer (where $U(z) = c$) in turbulent flow. He formulated the problem for a turbulent shear flow over a perturbed surface and proposed a solution analagous to the laminar case. Based on an experimental study of supersonic flow over a rigid wavy wall he concluded that one can use the mean quantities for flow over an unperturbed surface if the amplitude of the surface disturbances is sufficiently small. We will use this result in the present analysis and assume that the mean profile is essentially unaffected by the small-amplitude wavy surface.

5.2 FORMULATION

The theoretical foundations for the treatment of a periodic disturbance in a turbulent shear flow have been presented by Hussain and Reynolds (1970) and others and we shall draw heavily upon their work for the present section. They propose that the flow variables may be decomposed as the sum of three contributions. For the velocity and pressure fields they write

$$u_i = \bar{u}_i + \tilde{u}_i + u'_i \tag{5.1a}$$

$$p = \bar{p} + \tilde{p} + p' \tag{5.1b}$$

where $(\bar{\ })$ is the mean value at the location (x, y, z), $(\tilde{\ })$ is the statistical contribution of the periodic disturbance, and $(\ )'$ is the background turbulence fluctuation. They define the time average of $f(\vec{r}, t)$, where f is a flow field variable, as

$$\bar{f}(\vec{r}) = \lim_{T\to\infty} 1/T \int_0^T f(\vec{r}, t)dt \tag{5.2}$$

and, the phase average of f as

$$\langle f(\vec{r}, t)\rangle = \lim_{N\to\infty} 1/N \sum_{n=1}^{N} f(\vec{r}, t + n\tau) \tag{5.3}$$

where τ is the period of the perturbation wave. The background turbulence is assumed to be random and its contribution to the phase average of a large ensemble is therefore zero. Hence, the perturbation f is defined by

$$\langle f\rangle = \bar{f} + \tilde{f} \tag{5.4}$$

The governing equations for the perturbation waves, the mean field, and the turbulence fluctuations can be obtained by substitution of the decompositions (5.1) into the continuity and momentum equations (the Navier-Stokes equations). Assuming the density and viscosity to be constant, normalizing the variables on a suitable characteristic length L and velocity u_∞, and appropriately averaging and manipulating the resulting equations Hussain and Reynolds obtain equations for the mean field, the perturbation equations, and the turbulence equations. We quote their result for the perturbation equations

$$\partial\tilde{u}_i/\partial x_i = 0 \tag{5.5}$$

$$\partial \tilde{u}_i/\partial t + \bar{u}_j \partial \tilde{u}_i/\partial x_j + \tilde{u}_j \frac{\partial \bar{u}_i}{\partial x_j} = - \partial \tilde{p}/\partial x_i + 1/\mathrm{Re}\, \partial^2 \tilde{u}_i/\partial x_j^2$$

$$+ \partial/\partial x_j (\overline{\tilde{u}_i \tilde{u}_j} - \tilde{u}_i \tilde{u}_j) - \partial/\partial x_j (\langle u_i' u_j' \rangle - \overline{u_i' u_j'}) \tag{5.6}$$

where $\mathrm{Re} = u_\infty L/\nu$ is the Reynolds number. Note the appearance of the last term in (5.6) involving the difference of the phase and time averages of the Reynolds stress of the background turbulence. With the definition (5.4) one can look upon this difference as the oscillation or perturbation of the background Reynolds stress. Accordingly, we define

$$\tilde{r}_{ij} = \langle u_i' u_j' \rangle - \overline{u_i' u_j'} \tag{5.7}$$

As there is presently no theory available for determining $\tilde{r}_{ij}$ a closure problem arises. This is discussed in Section 5.3.

Prior to consideration of the closure problem let us specialize the formulation for waves of small amplitude by neglecting the terms quadratic in $\tilde{u}_i$ in (5.6). The term involving $\tilde{r}_{ij}$ remains to be specified. Consider a parallel mean flow, $\bar{u}_i = (U(z), 0, 0)$, and specialize to two-dimensional flow for which $\tilde{u}_i = (\tilde{u}, 0, \tilde{w})$. Assume that the perturbation quantities may be represented as

$$\tilde{f} = \epsilon \hat{f}(x, z) e^{ikt} \tag{5.7}$$

where ϵ is the small-amplitude parameter defined in Chapter 3, and where $\hat{f}$ represents the complex amplitude of the relevant quantity $\tilde{f}$, and k is the reduced frequency of the oscillation. Substituting (5.7) for the perturbation quantities in (5.5) and (5.6) we obtain

$$\hat{u}_x + \hat{w}_z = 0 \tag{5.8}$$

$$ik\hat{u} + U\hat{u}_x + \hat{w}U'(z) = - \hat{p}_x + 1/\mathrm{Re} \nabla^2 \hat{u} - \partial \hat{r}_{xx}/\partial x - \partial \hat{r}_{xz}/\partial z \tag{5.9}$$

$$ik\hat{w} + U\hat{w}_x = - \hat{p}_z + 1/\mathrm{Re} \nabla^2 \hat{w} - \partial \hat{r}_{xz}/\partial x - \partial \hat{r}_{zz}/\partial z \tag{5.10}$$

The boundary conditions are the no-slip conditions at the surface

$$z = z_s(x, t) = \epsilon \hat{z}_s(x) e^{ikt} \tag{5.11}$$

and vanishing disturbances at infinity. The linearized forms of the surface conditions are given by (4.4); namely,

$$\hat{u}(x, 0) = - U'(0)\hat{z}_s(x) \tag{5.12a}$$

$$\hat{w}(x, 0) = ik\hat{z}_s(x) \tag{5.12b}$$

5.3 CLOSURE OF THE SET OF GOVERNING EQUATIONS

There are several possibilities for evaluating the turbulent stress perturbations. One straightforward method is to derive an equation for $\tilde{r}_{ij}$ by manipulating the Navier-Stokes equations (see, for example, Hinze (1959)). Using this approach Hussain and Reynolds (1970) obtain an equation that is linear in the $\tilde{r}_{ij}$. They claim that it is futile to seek closure through this equation because of the appearance of still unknown terms on the right-hand side. Recently Davis (1972) has proposed a way out of this dilemma by relating the unknown terms on the right-hand side of this "stress conservation equation" to the quantities $\tilde{r}_{ij}$ and $\tilde{u}_i$. He suggests a relation on the basis of dimensional arguments and uses this model to compute the flow over a wave. A shortcoming of his approach is the fact that only one boundary condition can be applied at the surface indicating that this closure scheme with its associated approximations does not adequately model the flow.

Another possibility is to apply the concept of an eddy viscosity, or perhaps a combination of an eddy viscosity and the elastic behavior of turbulence, to the flow over an oscillating surface. Hussain and Reynolds (1970) propose that the Reynolds stress perturbations are related to the wave strain rates by

$$\tilde{r}_{ij} = - 2\epsilon\tilde{s}_{ij} \tag{5.13a}$$

where

$$\tilde{s}_{ij} = 1/2(\partial\tilde{u}_i/\partial x_j + \partial\tilde{u}_j/\partial x_i) \tag{5.13b}$$

and where the kinematic eddy viscosity $\epsilon(z)$ is viewed as a property of the mean velocity field and is presumed known. Following Hussain and Reynolds, Davis (1972) proposes a model based on the assumption that the turbulent stress of a fluid element is determined by the rate of strain it has recently experienced. If the "memory" of the fluid is long, the constitutive relation will be that of a viscoelastic fluid; however, if the memory of the fluid is short, the turbulent stresses will be primarily determined by the local rate of strain and the fluid will behave in a viscous manner. In the limit of zero memory the relation proposed in (5.13) is recovered. Davis found that such eddy viscoelasticity models are strongly dependent on the details of the mean velocity profile very near the surface since the value of the horizontal velocity component $\hat{u}$ at the surface is determined by U', the gradient of the primary flow at the surface, as indicated in (5.12a). Davis compared results based on this model with the field measurements of Dobson (1969) and found that the surface pressure predicted by the eddy viscoelasticity models is in reasonable agreement with experimental values. He found little difference in the results depending on the assumption that the fluid has a finite memory or zero memory. Hence, we will use the case of zero memory and assume an eddy viscosity relation of the form given by (5.13).

5.4 AN APPROXIMATE ANALYTICAL SOLUTION

In order to proceed with the solution of (5.8)-(5.10) subject to (5.12) and the closure assumption (5.13) we need to make some additional simplifying assumptions. In the previous chapters we postulated the existence of a thin boundary layer near the wavy surface where the x-derivatives are small in comparison to the z-derivatives and where the z-pressure gradient is assumed to be negligible. Under these assumptions the z-momentum equation, (5.10), becomes trivial, and we find that the only important Reynolds stress in the remaining momentum equation is the shear stress which can be written nondimensionally as

$$\hat{r}_{xz} = \overline{E}\hat{u}_z \tag{5.14}$$

where

$$\overline{E} = \epsilon/u_\infty L = E/Re$$

Substitution in (5.9) gives the boundary-layer momentum equation

$$ik\hat{u} + U\hat{u}_x + \hat{w}U'(z) = -\hat{p}'(x) + 1/Re[\hat{u}_{zz} + (E\hat{u}_z)_z] \tag{5.15}$$

The continuity equation and boundary conditions are as before

$$\hat{u}_x + \hat{w}_z = 0 \tag{5.16}$$

$$\left.\begin{aligned} \hat{u} &= -U'(0)\hat{z}_s(x) \\ \hat{w} &= ik\hat{z}_s(x) \end{aligned}\right\} \text{ at } z = 0 \tag{5.17}$$

As in the previous chapters we assume that these equations apply within the boundary layer, $0 \le z \le \delta_o$, and we assume that the flow is inviscid and irrotational outside the layer, governed by equations (3.19) and (3.24).

Considering the boundary-layer problem we introduce in (5.15) the stream function defined in (4.5) and the z*-coordinate defined in (3.21) to obtain

$$ik\psi_{z*} + U\psi_{xz*} - U'(z^*)\psi_x = -f(x) + 1/R[\psi_{z*z*z*} + (E\psi_{z*z*})_{z*}], \tag{5.18}$$

$$0 \le z^* \le 1$$

where R and f are defined in (4.6). The no-slip conditions (5.17) are

$$\left.\begin{aligned} \psi_{z*} &= -U'(u)\hat{z}_s(x) \\ \psi_x &= -ik\hat{z}_s(x) \end{aligned}\right\} \text{ at } z^* = 0 \tag{5.19}$$

Note the similarity to the problem posed in (4.6) and (4.7) for the laminar case; the presence of the term in $E(z^*)$ complicates the turbulent case.

It is instructive to consider the variation of $E(z^*)$ in the boundary layer. Near the wall E is extremely small indicating that the laminar stress dominates. As z^* increases E begins to grow rapidly as the effect of the turbulence begins to dominate over the effect of the viscosity. Near the outer edge of the boundary layer E may be 10–100 times as large as ν. In predictions of steady turbulent boundary layers one postulates a suitable expression for the eddy viscosity; for example, one can take the model of Van Driest (1956) for the wall region

$$E = (kz^+)^2[1 - e^{-z^+/A^+}]^2 |\partial u^+/\partial z^+| \tag{5.20}$$

where

$$z^+ = u_\tau z/\nu, \qquad u^+ = U/u_\tau,$$

$$u_\tau = \tau_w/\rho,$$

and k, A^+ are constants, and match this to some estimate of the eddy viscosity for the outer portion of the boundary layer through an equation of the form

$$E = KRe_{\delta *} \tag{5.21}$$

We could use expression (5.20) for the present study, but this requires precise knowledge of the primary velocity gradient in the wall region. The complexity of the expression prevents a straightforward analytical solution.

One way out of this difficulty is to take E = constant. We can assume that E is approximately 10-100. In this case equation (5.18) reduces to the laminar form with the Reynolds number replaced by an effective Reynolds number based upon an enhanced viscosity; that is,

$$R_e = R/(E+1) \simeq R/E \tag{5.22}$$

This would reduce the Reynolds number in (5.18) by a factor of 10-100. We still have a small parameter multiplying the highest derivative in (5.18) which gives rise to a singular perturbation in very much the same manner as with the laminar viscous term. We can solve the problem by introducing a thin "eddy viscous" layer near the wall. The width of this region is of order $\delta_i(R_e)$. In analogy to the laminar case we stretch the z^*-coordinate by a factor $1/\delta_i$ and choose

$$\delta_i = (R_e)^{-1/2} \tag{5.23}$$

This permits us to replace the Reynolds number R with the effective Reynolds number R_e in all of the results given in Chapter 3.

5.5 EFFECT ON THE SURFACE PRESSURE

It is possible to obtain an estimate of the effect of the constant eddy viscosity on the surface pressure. We can employ the result in (4.63) to give

$$\hat{p}(x,0) = \hat{p}_o(x) + \delta_o \hat{p}_{BL}(x) + (Re_e)^{-1/2} \hat{p}_{EV}(x) \tag{5.24}$$

where

$$Re_e = u_\infty L/(\epsilon + \nu) \cong Re/E,$$

and where

$$\hat{p}_{EV}(x) = (ik + d/dx)^4 \hat{z}_s(x)/(ik)^{5/2} \tag{5.25}$$

is taken from (4.62). The subscript "EV" refers to "eddy viscous" and implies the dominance of the turbulence over the effect of viscosity.

We can estimate the relative importance of the eddy viscous term compared to the other terms. For $k \sim 0(1)$, $\delta_o = 10^{-1}$, $Re = 10^6$, $E = 10\text{–}100$, we find, using (4.64), that the eddy viscous term is about .03-.10 times the inviscid shear layer effect. This indicates that the effect of the Reynolds stress perturbations is smaller than the effect of the shear flow, though it is not negligible. For the largest value of the eddy viscosity, $E = 100$, we find that the shear term is about 10 times larger than the eddy viscous term in (5.24). For decreasing flow unsteadiness, as $k \to 0$, we find from (4.65) that the effect of the eddy viscosity becomes more important.

5.6 DISCUSSION

The approximate analysis of the previous two sections gives us an assessment of the importance of including the Reynolds stress terms in the perturbation equations for the boundary layer over a wavy surface. We find that for sufficient flow unsteadiness the effect of including the Reynolds stress perturbations is small but not negligible. As in the case of laminar flow the analysis breaks down when the flow unsteadiness diminishes. For a more accurate analysis employing variable eddy viscosity $\epsilon(z)$ one would have to resort to a numerical analysis of the governing equations with an assumed eddy viscosity or some other appropriate closure assumption for the perturbation Reynolds stresses. This approach was taken by Hussain and Reynolds (1970), Saeger and Reynolds (1971), and Davis (1972), but the whole question is still somewhat inconclusive as Davis indicates. For the present work it was decided that a numerical analysis including the Reynolds stresses was beyond the scope or intent of this study. The significant effect appears to be the perturbation due to the mean shear profile. For the application to panel flutter the Reynolds number and reduced frequency will be roughly equal to the numbers used in the estimates of the previous section, so that we can expect the relative importance of the Reynolds stresses to be about the same as indicated for the incompressible analysis. One should not conclude, however, that the role of the Reynolds stresses is not very important in the problem of the wind-driven water waves. For geophysical flows there is no boundary-layer thickness and the only characteristic scale is the height above the boundary. For this reason one must work directly with the Navier-Stokes equations (5.8)-(5.10) in such a case, and the effect of including the Reynolds stresses may be quite significant. We will discuss this further in the section on wind-driven water waves in Chapter 8.

VI. EFFECTS OF COMPRESSIBILITY

6.1 INTRODUCTION

In the previous chapters we have considered several aspects of the incompressible flow over an oscillating surface. Examined separately were the effects of an inviscid shear flow, the result of including viscous effects in the perturbed flow, and the effect of the turbulent Reynolds stresses on the perturbed flow. We have established that for sufficient flow unsteadiness the inclusion of the Reynolds stresses has a small effect on the pressure. The most important effect in the perturbed flow appears to be due to the mean shear profile. We assume that the relative importance of these three effects is the same for compressible flow. In this chapter we consider the two-dimensional compressible inviscid shear flow over an oscillating surface by extending the method developed in Chapter 3 for the incompressible case.

6.2 FORMULATION

The formulation of the problem of two-dimensional compressible flow over an oscillating surface closely parallels the formulation of Section 3.4 in which we consider the shear layer to be a thin boundary layer. Assume that the remarks made in Section 3.1 apply to the present case. We assume that the fluid is a perfect gas with constant specific heats and consider the dimensional form of the equations for two-dimensional inviscid flow. The continuity equation is

$$\partial\rho/\partial t + \partial(\rho u)/\partial x + \partial(\rho w)/\partial z = 0 \qquad (6.1)$$

The two components of the momentum equation are

$$\rho(u_t + uu_x + wu_z) = - p_x \qquad (6.2)$$

$$\rho(w_t + uw_x + ww_z) = - p_z \qquad (6.3)$$

If the equation of mechanical energy is subtracted from the equation of conservation of total energy we obtain the equation which describes the rate of change of the internal energy

$$\rho c_v(T_t + uT_x + wT_z) = - p(u_x + w_z) \qquad (6.4)$$

We complete the set of equations with the equation of state

$$p = \rho RT \tag{6.5}$$

As in Chapter 3 nondimensional variables are employed using freestream values for the flow quantities. Thus,

$$\begin{aligned} x &= x/L & u &= u/u_\infty & \rho &= \rho/\rho_\infty \\ z &= z/L & w &= w/u_\infty & T &= T/T_\infty \\ t &= u_\infty t/L & p &= p/(\rho_\infty u_\infty^2) \end{aligned} \tag{6.6}$$

using the same symbols rather than introducing new ones. We represent the flow quantities as the sum of a mean flow quantity and a small perturbation. In terms of the nondimensional variables

$$\begin{aligned} u &= U(z) + \epsilon\hat{u}(x, z)e^{ikt} \\ w &= \epsilon\hat{w}(x, z)e^{ikt} \\ p &= p(z) + \epsilon\hat{p}(x, z)e^{ikt} \\ \rho &= \rho(z) + \epsilon\hat{\rho}(x, z)e^{ikt} \\ T &= T(z) + \epsilon\hat{T}(x, z)e^{ikt} \end{aligned} \tag{6.7}$$

Using the boundary-later approximation for the mean flow we note that

$$p = \text{constant since } \partial p/\partial z = 0 \tag{6.8}$$

This leads to the equation of state for the mean flow in nondimensional variables

$$\rho T = 1 \tag{6.9}$$

The total enthalpy is conserved for a fluid particle in the mean flow. We can express this form of the conservation of energy in terms of nondimensional variables as

$$T + (\gamma - 1)/2\ M_\infty^2 U^2 = 1 + (\gamma - 1)/2\ M_\infty^2 \tag{6.10}$$

where $\gamma = c_p/c_v$ is the ratio of specific heats, and M_∞ is the Mach number of the freestream. The mean flow is completely specified by Eqs. (6.8)-(6.10) once the details of the velocity profile, $U(z)$, are known.

We can now proceed to derive the equations for the perturbation flow. Nondimensionalizing Eqs. (6.1)-(6.5), substituting the flow quantities (6.7), and neglecting the terms of $0(\epsilon^2)$, we obtain the linearized equations

$$ik\hat{\rho} + U\hat{\rho}_x + \rho(\hat{u}_x + \hat{w}_z) + \hat{w}\rho'(z) = 0 \tag{6.11}$$

$$ik\hat{u} + U\hat{u}_x + \hat{w}U'(z) = -\hat{p}_x/\rho \tag{6.12}$$

$$ik\hat{w} + U\hat{w}_x = -\hat{p}_z/\rho \tag{6.13}$$

$$ik\hat{T} + U\hat{T}_x + \hat{w}T'(z) = -(\gamma - 1)(\hat{u}_x + \hat{w}_z) \tag{6.14}$$

$$\hat{\rho}/\rho + \hat{T}/T = \gamma M_\infty^2 \hat{p} \tag{6.15}$$

The surface boundary condition is the same as in Chapter 3. The flow obeys the tangency condition at the surface

$$z = \epsilon \hat{z}_s(x) e^{ikt} \tag{6.16}$$

and the linearized form of this condition is

$$\hat{w}(x, 0) = ik\hat{z}_s(x) \tag{6.17}$$

Another boundary condition must be applied far away from the surface. In the case of subsonic disturbances, the velocity perturbations are zero at infinity, while in the case of supersonic disturbances where the solutions are wavelike, the condition requires that the disturbances radiate outwards from the surface to infinity.

As in Chapter 3 we can obtain a single governing equation for the $\hat{w}$-velocity perturbation. It is convenient to treat the boundary layer and the outer flow separately. In the boundary layer we assume that the pressure gradient in the z-direction is $0(\delta_o)$. This leads to the approximation

$$\hat{p} = \hat{p}_o(x) + \delta_o \hat{p}_{BL}(x, z) \tag{6.18}$$

where $\hat{p}_o$ is the potential flow pressure and $\hat{p}_{BL}$ is the perturbation due to the boundary layer. In the analysis of the boundary layer equations we assume that the pressure amplitude is approximately equal to $\hat{p}_0$. The governing equations (6.11)-(6.15) are then

$$D\hat{\rho}/\rho + (\hat{u}_x + \hat{w}_z) + (\rho'(z)/\rho)\hat{w} = 0 \tag{6.19}$$

$$D\hat{u} + U'(z)\hat{w} = -\hat{p}_0'(x)/\rho \tag{6.20}$$

$$D\hat{T}/T + (T'(z)/T)\hat{w} = -(\gamma - 1)(\hat{u}_x + \hat{w}_z) \tag{6.21}$$

$$\hat{\rho}/\rho + \hat{T}/T = \gamma M_\infty^2 \hat{p}_o \tag{6.22}$$

where $D = ik + U(z)\partial/\partial x$. Here we have used (6.9) in eliminating ρT in the energy equation. We next add (6.19) and (6.21) and substitute for $D\hat{\rho}/\rho + D\hat{T}/T$ using (6.22). We operate on the resulting equation using D, then eliminate $D\hat{u}_x$ from the resulting equation by differentiating the momentum equation (6.20) with respect to x and substituting for $D\hat{u}_x$. This results in an equation for $\hat{w}$

$$D\hat{w}_z - U''\hat{w}_x + 1/\gamma(\rho'/\rho + T'/T)D\hat{w} = 1/\rho\hat{p}_0'' - M_\infty^2 D^2 \hat{p}_o \tag{6.23}$$

We can introduce the streamline deviation, $\hat{\delta}$, from the relation developed in Chapter 3,

$$\hat{w} = D\hat{\delta} \tag{6.24}$$

Substituting in (6.23) we obtain

$$D^2\hat{\delta}_z + (1/\gamma)(\rho'/\rho + T'/T)D^2\hat{\delta} = [(1/\rho)d^2/dx^2 - M_\infty^2 D^2]\hat{p}_o(x) \tag{6.25}$$

The surface boundary condition (6.17) in terms of $\hat{\delta}$ is

$$\hat{\delta}(x, 0) = \hat{z}_s(x) \tag{6.26}$$

Note the similarity to the incompressible case. If T and ρ are both constant and $M_\infty = 0$ in (6.25) we recover the incompressible equation for $\hat{\delta}$.

Consider now the outer potential flow in which all of the mean flow quantities are independent of z. The linearized perturbation equations (6.11)-(6.15) are

$$D\hat{\rho} + (\hat{u}_x + \hat{w}_z) = 0 \tag{6.27}$$

$$D\hat{u} = -\hat{p}_x \tag{6.28}$$

$$D\hat{w} = -\hat{p}_z \tag{6.29}$$

$$D\hat{T} = -(\gamma - 1)(\hat{u}_x + \hat{w}_z) \tag{6.30}$$

$$\hat{\rho} + \hat{T} = \gamma M_\infty^2 \hat{p} \tag{6.31}$$

where $D = ik + \partial/\partial x$. We can use these equations to obtain an equation for $\hat{w}$. First we add (6.27) and (6.30) and substitute for $D\hat{\rho} + D\hat{T}$ using (6.31). We differentiate the resulting equation with respect to z and eliminate $\hat{p}_z$ using (6.29). We now have an equation in $\hat{u}$ and $\hat{w}$. To eliminate $\hat{u}$ we assume that the outer flow is irrotational, that is,

$$\hat{u}_z = \hat{w}_x \tag{6.32}$$

Differentiating (6.32) with respect to x and substituting for $\hat{u}_{xz}$ in the equation involving $\hat{u}$ and $\hat{w}$ we obtain

$$\nabla^2\hat{w} - M_\infty^2 D^2 \hat{w} = 0 \tag{6.33}$$

Introducing the streamline deviation using (6.24) we obtain

$$D(\nabla^2\hat{\delta} - M_\infty^2 D^2 \hat{\delta}) = 0 \tag{6.34}$$

Assuming $\hat{\delta} = 0$ for all the streamlines far upstream we conclude that the quantity in the parentheses in (6.34) is zero for all the fluid. Thus,

$$\nabla^2\hat{\delta} - M_\infty^2 D^2 \hat{\delta} = 0, \qquad z \geq \delta_o \tag{6.35}$$

Expanding the operators in (6.35) we obtain

$$(M_\infty^2 - 1)\hat{\delta}_{xx} - \hat{\delta}_{zz} + 2ikM_\infty^2\hat{\delta}_x - k^2 M_\infty^2 \hat{\delta} = 0 \tag{6.36}$$

We recognize that this equation for $\hat{\delta}$ is the same as the equation for the amplitude of the perturbation potential in linearized potential flow.

We obtain the pressure by integrating the z-momentum equation (6.13). Assuming $\hat{p}$ is zero at infinity we have

$$\hat{p}(x,0) = \int_0^\infty \rho D\hat{w}dz \tag{6.37}$$

Introducing $\hat{w}$ from (6.24) and separating the range of integration into two parts we have

$$\hat{p}(x,0) = \int_0^{\delta_o} \rho D^2\hat{\delta}dz + D^2\int_{\delta_o}^\infty \hat{\delta}dz \tag{6.38}$$

where we have used the fact that ρ and D do not vary with z in the outer flow.

6.3 SOLUTION

We use the Fourier transform to obtain the solution of the problem formulated in Section 6.2. The technique is an extension of the method developed in Chapter 3 for the incompressible case. It may here be convenient also to take the alternate view that the Fourier transform is the solution due to an infinite traveling wave train of phase velocity $c = k/\alpha$. Consider the boundary layer for which the transformation of (6.25) and (6.26) yields

$$\tilde{\delta}_z + P(z)\tilde{\delta} = Q(\alpha;z), \qquad 0 \le z \le \delta_o \tag{6.39}$$

$$\tilde{\delta}(\alpha;0) = \tilde{z}_s(\alpha) \tag{6.40}$$

where

$$P(z) = (1/\gamma)(\rho'/\rho + T'/T)$$

$$Q(\alpha;z) = [\alpha^2\rho^{-1}(k+\alpha U)^{-2} - M_\infty^2]\tilde{p}_o(\alpha)$$

and where $\tilde{z}_s$ and $\tilde{p}_o$ are the Fourier transforms of the surface amplitude and potential flow pressure amplitude respectively. We recognize that equation (6.39) is a linear, first-order ordinary differential equation in the independent variable, z, with the transform variable α as a parameter. The solution to this equation subject to the boundary condition (6.40) is

$$\tilde{\delta} = \tilde{z}_s + \delta_o [\alpha^2 \int_o^{z*} \rho^{-1}(k + \alpha U)^{-2} dz* - M_\infty^2 z*]\tilde{p}_o, \qquad 0 \le z* \le 1 \tag{6.41}$$

In obtaining the solution we have used (6.9) to eliminate ρT. Note also that we have expressed the result in terms of $z*$ to emphasize that the z-variation of $\tilde{\delta}$ is contained in the perturbation term of $0(\delta_o)$.

The outer flow equation (6.35) transforms as

$$\tilde{\delta}_{zz} - \lambda^2 \tilde{\delta} = 0, \qquad z \ge \delta_o \tag{6.42}$$

where $\lambda^2 = \alpha^2 - M_\infty^2(\alpha + k)^2$. The general solution to (6.42) is

$$\tilde{\delta} = Ae^{\lambda z} + Be^{-\lambda z}, \qquad \lambda^2 > 0 \tag{6.43a}$$

or

$$\delta = Ce^{i\mu z} + De^{-i\mu z}, \qquad \lambda^2 = -\mu^2 < 0 \tag{6.43b}$$

depending upon the particular value of α. In order to specify the constants in the general solution we should consider separately two cases depending upon whether the freestream is subsonic or supersonic relative to the wave.

In the subsonic case ($M_\infty < 1$) it is convenient to set

$$\lambda^2 = \beta^2(\alpha - \lambda_1)(\alpha - \gamma_2) \tag{6.44}$$

where

$$\beta^2 = 1 - M_\infty^2$$

$$\gamma_1 = kM_\infty/(1 - M_\infty)$$

$$\gamma_2 = - kM_\infty/(1 + M_\infty)$$

This simplifies the problem of choosing the appropriate form of the solution in (6.43) which applies for a given value of α. We note that (6.43a) is appropriate for $\alpha > \mathrm{Re}(\gamma_1)$ or $\alpha < \mathrm{Re}(\gamma_2)$. The nature of this solution is "subsonic" and we conclude that A must be zero for the solution to be finite at infinity. This is similar to the incompressible case. If α lies in the range $\mathrm{Re}(\gamma_2) < \alpha < \mathrm{Re}(\gamma_1)$, then (6.43b) is appropriate for the solution which has a "supersonic" character.

We choose $C = 0$ to satisfy the radiation condition of waves propagating outward to infinity. It is interesting to note that this "supersonic" disturbance attenuates to zero at infinity if we assume that k is complex with a negative imaginary part. We can summarize the solution for a subsonic freestream as

$$\tilde{\delta} = \tilde{\delta}_1 e^{-\lambda(z-\delta_o)}, \qquad \alpha < \mathrm{Re}(\gamma_2) \text{ or } \alpha > \mathrm{Re}(\gamma_1) \tag{6.45}$$

with the understanding that $\lambda = i\mu$ when $\mathrm{Re}(\gamma_2) < \alpha < \mathrm{Re}(\gamma_1)$. We specify $\tilde{\delta}_1$ by evaluating the boundary layer solution (6.41) at the edge of the layer. This gives

$$\tilde{\delta}_1 = \tilde{z}_s + \delta_o[\alpha^2 \int^1 \rho^{-1}(k + \alpha U)^{-2} dz^* - M_\infty^2]\tilde{p}_o \tag{6.46}$$

In the case of a supersonic freestream ($M_\infty > 1$) it is convenient to consider (6.42) as follows:

$$\tilde{\delta}_{zz} + \sigma^2\tilde{\delta} = 0 \tag{6.47}$$

where

$$\sigma^2 = \beta^2(\alpha - \gamma_1)(\alpha - \gamma_2) = -\lambda^2$$

and where

$$B^2 = M_\infty^2 - 1$$

and

γ_1, γ_2 as defined in (6.44)

The general solution to (6.47) is

$$\tilde{\delta} = Ae^{i\sigma z} + Be^{-i\sigma z}, \qquad \sigma^2 > 0 \tag{6.48a}$$

or

$$\tilde{\delta} = Ce^{\tau z} + De^{-\tau z}, \qquad \sigma^2 = -\tau^2 < 0 \tag{6.48b}$$

As in the case of a subsonic freestream, the general solution can be specialized by the same arguments relating to finiteness at infinity for "subsonic" disturbances and outward propagation in the case of "supersonic" disturbances. The solution which satisfies these conditions and matches the boundary-layer solution at the interface is

$$\tilde{\delta} = \tilde{\delta}_1 e^{-\tau(z-\delta_o)}, \qquad \mathrm{Re}(\gamma_1) < \alpha < \mathrm{Re}(\gamma_2) \tag{6.49}$$

with the understanding that $\tau = i\sigma$ when $\alpha < \mathrm{Re}(\gamma_1)$ or $\alpha > \mathrm{Re}(\gamma_2)$. $\tilde{\delta}_1$ is given by (6.46).

6.4 THE SURFACE PRESSURE

Having determined the solutions for the streamline deviation we can calculate the surface pressure amplitude using (6.38). The Fourier transform of that expression is

$$\tilde{p}(\alpha;0) = -\delta_o \int_o^1 \rho(k+\alpha U)^2 \tilde{\delta} dz^* - (k+\alpha)^2 \int_{\delta_o}^{\infty} \tilde{\delta} dz. \tag{6.50}$$

Substituting for $\tilde{\delta}$ using (6.41) in the first integral and (6.45) and (6.49) in the second integral we obtain

$$\tilde{p}(\alpha;0) = \begin{cases} -\delta_o \int_o^1 \rho(k+\alpha U)^2 dz^* \tilde{z}_s - (k+\alpha)^2 \tilde{\delta}_1/\lambda + 0(\delta_o^2), & M_\infty < 1 \\ -\delta_o \int_o^1 \rho(k+\alpha U)^2 dz^* \tilde{z}_s - (k+\alpha)^2 \tilde{\delta}_1/\tau + 0(\delta_o^2), & M_\infty > 1 \end{cases} \tag{6.51}$$

where the terms of $0(\delta_o^2)$ arise from the z-variation of $\tilde{\delta}$ in the first integral. We substitute for $\tilde{\delta}_1$ using (6.46) and we obtain an expression for $\tilde{p}_o$ by evaluating (6.50) for $\delta_o = 0$ with $\tilde{\delta}$ from (6.45) or (6.49). Neglecting the terms of $0(\delta_o^2)$ we obtain

$$\tilde{p}(\alpha;0) = \tilde{p}_o + \delta_o \tilde{p}_{BL} \tag{6.52}$$

where

$$\tilde{p}_o = \begin{cases} -(k+\alpha)^2 \tilde{z}_s/\lambda, & M_\infty < 1 \\ -(k+\alpha)^2 \tilde{z}_s/\tau, & M_\infty > 1 \end{cases}$$

$$\tilde{p}_{BL} = \tilde{p}_1 + \tilde{p}_2$$

where

$$\tilde{p}_1 = -\int_0^1 \rho(k+\alpha U)^2 dz^* \tilde{z}_s$$

$$\tilde{p}_2 = \begin{cases} (k+\alpha)^4 (\alpha^2 \int_0^1 \rho^{-1}(k+\alpha U)^{-2} dz^* - M_\infty^2)\tilde{z}_s/\lambda^2, & M_\infty < 1 \\ (k+\alpha)^4 (\alpha^2 \int_0^1 \rho^{-1}(k+\alpha U)^{-2} dz^* - M_\infty^2)\tilde{z}_s/\tau^2, & M_\infty > 1 \end{cases}$$

Note that we can write a single expression for $\tilde{p}_2$ for both subsonic and supersonic freestream since $\tau^2 = -\sigma^2 = \lambda^2$. Substituting for λ^2 using (6.44) we obtain

$$\tilde{p}_2 = \frac{(k+\alpha)^4 (\alpha^2 \int_0^1 \rho^{-1}(k+\alpha U)^{-2} dz^* - M_\infty^2)\tilde{z}_s}{(1 - M_\infty^2)(\alpha - \gamma_1)(\alpha - \gamma_2)} \tag{6.53}$$

The physical counterparts of these expressions can be obtained by inversion of the Fourier transforms in (6.52). Thus

$$\hat{p}(x,0) = \hat{p}_o(x) + \delta_o \hat{p}_{BL}(x) \tag{6.54}$$

The potential flow pressure, $\hat{p}_o$, may be obtained more conveniently by other means owing to the difficulty of inverting the Fourier transform. In the case of supersonic flow the problem of determining the potential flow pressure proves quite tractable. A particularly efficient approach employing Laplace transformation on x (see Section 13.3 of Ashley and Landahl (1965)) yields the following result for a finite-chord panel located between $x = 0$ and $x = 1$:

$$\hat{p}_o = 1/B \int_0^x K_o(x - x_1; k, M_\infty)(ik + d/dx_1)^2 \hat{z}_s(x_1) dx_1 \tag{6.55}$$

where

$$K_o(x;k,M_\infty) = e^{-ikM_\infty^2 x/B^2} J_o(kM_\infty x/B^2)$$

and

$$B = (M_\infty^2 - 1)^{1/2}, \quad M_\infty > 1$$

The pressure due to the boundary layer, $\hat{p}_{BL}$, may be obtained by inverting the Fourier transforms in (6.52) and (6.53), (see Appendix D). This gives

$$\hat{p}_{BL}(x) = \hat{p}_1(x) + \hat{p}_2(x) \tag{6.56}$$

The first term is due to the effect of perturbations within the boundary layer and is given by

$$\hat{p}_1 = (ik)^2 a\hat{z}_s(x) + 2ikb\hat{z}_s'(x) + c\hat{z}_s''(x) \tag{6.57}$$

where

$$a = \int_o^1 \rho dz^*, \qquad b = \int_o^1 \rho U dz^*, \qquad c = \int_o^1 \rho U^2 dz^*$$

We can relate the mean flow density profile to the shear profile using (6.9) and (6.10). This gives

$$\rho = [1 + (\gamma - 1)/2\ M_\infty^2(1 - U^2)]^{-1} \tag{6.58}$$

The second term in (6.56) is due to the effect of the boundary layer on the outer flow. We can express this by a convolution integral. For the case of a surface deformation which extends to infinity on the x-axis,

$$\hat{p}_2 = \int_{-\infty}^{\infty} K(x - x_1;k,M_\infty)(ik + d/dx_1)^4 \hat{z}_s(x_1)dx_1 \tag{6.59a}$$

and for a finite-chord panel located between $x = 0$ and $x = 1$,

$$\hat{p}_2 = \int_o^1 K(x - x_1;k,M_\infty)(ik + d/dx_1)^4 \hat{z}_s(x_1)dx_1 \tag{6.59b}$$

where

$$K(x;k,M_\infty) = \int_0^1 \rho^{-1}U^{-2}F_1(x,U;k,M_\infty)dz^* + K_2(x;k,M_\infty)$$

The functions, F_1 and K_2, are the result of inverting the Fourier transform in (6.53). Expressions for these functions are given in Appendix D for both subsonic and supersonic flow. We note here that the most significant difference in the results for these two cases is that in the supersonic case the kernel, K, exhibits the property of no upstream influence. For this case the function K is zero for negative values of the argument $x - x_1$ and we may replace the upper limit in the integral in (6.59) with x. Another interesting property of the kernel function is the fact that the function is well-behaved in the transonic limit as $M_\infty \to 1$. Apparently the essential nonlinearity of steady, two-dimensional transonic flow disappears in the oscillatory case when k is sufficiently large. We obtain the same result as $M_\infty \to 1$ using the expressions for subsonic or supersonic flow. This serves as a partial check on the algebra. Finally, we note that in the limit as $M_\infty \to 0$ we obtain the incompressible result of (3.69) which serves as an additional check.

6.5 DISCUSSION

The limits of applicability of the present theory can be ascertained by examining the consequences of the assumption that δ_o is small. The first-order analysis will be applicable provided the boundary-layer perturbation pressure is small compared to the potential flow result, that is,

$$|\delta_o \tilde{p}_{BL}/\tilde{p}_o| \ll 1 \qquad (6.60)$$

This will occur for flow that is sufficiently unsteady. To determine the degree of flow unsteadiness that is required consider the Fourier transform expressions in (6.52) and (6.53). We observe that $\tilde{p}_2$ becomes large for small k so that this is the dominant part of the boundary-layer effect for small k. With this understanding we find that condition (6.60) is approximately

$$\left| \frac{\delta_o \alpha^4 \tilde{F}(\alpha, k)}{B\sqrt{(\alpha - \gamma_1)(\alpha - \gamma_2)}} \right| << 1 \tag{6.61}$$

where

$$\tilde{F}(\alpha, k) = \int_0^1 \rho^{-1}(k + \alpha U)^{-2} dz*$$

For small k, $\tilde{F}(\alpha, k) \sim 0(1/(\alpha k U'(0))$ so that condition (6.61) is

$$\left| \frac{\delta_o \alpha^3}{kU'(0)B\sqrt{(\alpha - \gamma_1)(\alpha - \gamma_2)}} \right| << 1 \tag{6.62}$$

Consider the case of low supersonic flow for which γ_1 and γ_2 are $0(k)$. Assuming gradual variations in the surface so that $\alpha \sim 0(1)$ we have the condition

$$\delta_o/(kU'(0)B) << 1 \tag{6.63}$$

which is similar to condition (3.74) in the incompressible case. For transonic flow $\gamma_1 \sim 0[k/(M_\infty - 1)]$ and $\gamma_2 \sim 0(k)$. In the limit as $M_\infty \to 1$ with k small but nonzero we express condition (6.62) as

$$\delta_o/(k^{3/2}U'(0)) << 1, \qquad M_\infty \to 1 \tag{6.64}$$

This relation gives the minimum amount of flow unsteadiness required in order that the theory apply for transonic flow. Using the numbers in the example at the end of Chapter 3 we find that k must be larger than 10^{-2} in transonic flow, that is, a slightly larger amount of unsteadiness is required in this case than in the incompressible case or in the case of low supersonic flow.

VII. THREE-DIMENSIONAL COMPRESSIBLE INVISCID SHEAR FLOW OVER AN OSCILLATING RECTANGULAR PANEL

7.1 INTRODUCTION

In the previous chapter we considered the two-dimensional compressible inviscid shear flow over an oscillating surface, obtaining expressions for the perturbation surface pressure. We extend the analysis to treat the flow over an oscillating rectangular panel to obtain an expression for the surface pressure as a function of the panel transverse displacement. This expression could be of use in an investigation of panel flutter.

Refer to Fig. 7.1 where we have a thin rectangular panel of chord length L and span b performing transverse oscillations of the form

$$z(x, y, t) = az_s(x, y)e^{i\omega t} \tag{7.1}$$

As in the previous chapter the flow is in the x-direction and the boundary-layer thickness is constant. We assume that

$$\begin{aligned} &\epsilon = a/L \ll 1, \\ &\delta_o = \delta_{b.1.}/L \ll 1, \end{aligned} \tag{7.2}$$

and

$$\epsilon \ll \delta_o$$

7.2 FORMULATION

The formulation of the three-dimensional case closely parallels the treatment of the two-dimensional case given in the previous chapter. In terms of the Cartesian coordinate system of Fig. 7.1 we have the three-dimensional version of the complete set of governing equations, a modified version of the equations (6.1)-(6.5). These are the equations of continuity, the three-component equations of motion, the energy equation, and an equations of state for a perfect gas:

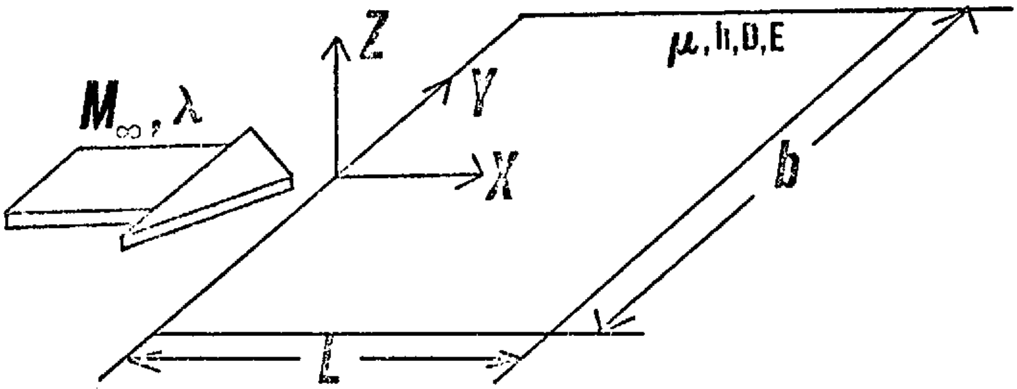

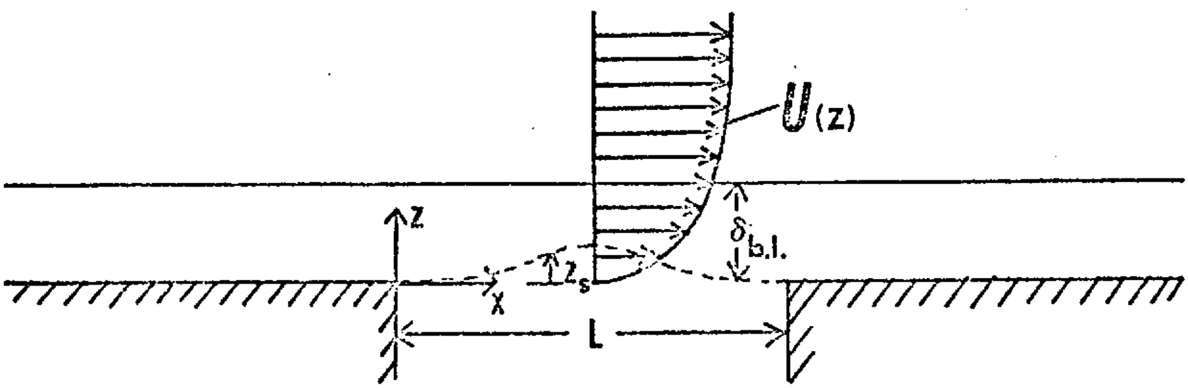

FIGURE 7.1
FLOW OVER AN OSCILLATING RECTANGULAR PANEL
AND DETAILS OF THE SHEAR LAYER MODEL

$$\rho_t + (\rho u)_x + (\rho v)_y + (\rho w)_z = 0 \tag{7.3}$$

$$\rho[u_t + uu_x + vu_y + wu_z] = -p_x \tag{7.4}$$

$$\rho[v_t + uv_x + vv_y + wv_z] = -p_y \tag{7.5}$$

$$\rho[w_t + uw_x + vw_y + ww_z] = -p_z \tag{7.6}$$

$$\rho w[T_t + uT_x + vT_y + wT_z] = -p(u_x + v_y + w_z) \tag{7.7}$$

$$p = \rho RT \tag{7.8}$$

We nondimensionalize lengths by L, velocity components by u_∞, time by L/u_∞, and the remaining variables as in (6.6) and assume that the nondimensional flow quantities may be represented as in (6.7) with the modification that the perturbation variables depend upon x, y, and z. Thus

$$\begin{aligned}
u &= U(z) + \epsilon\hat{u}(x,y,z)e^{ikt} \\
v &= \epsilon\hat{v}(x,y,z)e^{ikt} \\
w &= \epsilon\hat{w}(x,y,z)e^{ikt} \\
p &= p(z) + \epsilon\hat{p}(x,y,z)e^{ikt} \\
\rho &= \rho(z) + \epsilon\hat{\rho}(x,y,z)e^{ikt} \\
T &= T(z) + \epsilon\hat{T}(x,y,z)e^{ikt}
\end{aligned} \tag{7.9}$$

The mean flow is completely specified by (6.8)-(6.10), since it depends only upon the transverse coordinate, z. We obtain the equations for the perturbation flow by substituting (7.9) in the nondimensionalized version of (7.7)-(7.8) and linearizing

$$ik\hat{\rho} + U\hat{\rho}_x + \rho(\hat{u}_x + \hat{v}_y + \hat{w}_z) + \hat{w}\rho'(z) = 0 \tag{7.10}$$

$$ik\hat{u} + U\hat{u}_x + \hat{w}U'(z) = -\hat{p}_x/\rho \tag{7.11}$$

$$ik\hat{v} + U\hat{v}_x = -\hat{p}_y/\rho \tag{7.12}$$

$$ik\hat{w} + U\hat{w}_x = -\hat{p}_z/\rho \tag{7.13}$$

$$ik\hat{T} + U\hat{T}_x + \hat{w}T'(z) = -(\gamma-1)(\hat{u}_x + \hat{v}_y + \hat{w}_z)/\rho \tag{7.14}$$

$$\hat{\rho}/\rho + \hat{T}/T = \gamma M_\infty^2 \hat{p} \tag{7.15}$$

We consider the boundary-layer flow and the potential flow separately as in the previous chapter. For the boundary layer we assume that the perturbation pressure is approximately

$$\hat{p} = \hat{p}_o(x,y) + \delta_o \hat{p}_{BL}(x,y,z) \tag{7.16}$$

which is equivalent to (6.18). For the analysis of the boundary-layer equations we neglect the second term and assume that $\hat{p}$ is given by $\hat{p}_o(x,y)$, the potential flow pressure at $z = 0$. This approximation leads to a governing equation for $\hat{w}$ after manipulating the equations as in the previous chapter:

$$D\hat{w}_z - U'(z)\hat{w}_x + (1/\gamma)(\rho'/\rho + T'/T)D\hat{w} = (1/\rho)(\hat{p}_{o_{xx}} + \hat{p}_{o_{yy}}) - M_\infty^2 D^2 \hat{p}_o \tag{7.17}$$

Note the similarity to (6.23), the only difference being the additional term in $\hat{p}_{o_{yy}}$ in the present case. For the tangency condition at the surface

$$z = \epsilon \hat{z}_s(x,y)e^{ikt} \tag{7.18}$$

we have, upon linearization,

$$\hat{w}(x,y,0) = ik\hat{z}_s(x,y) \tag{7.19}$$

Introducing the streamline deviation, (6.24), in (7.17) and (7.19) we obtain

$$D^2\hat{\delta}_z + 1/\gamma(\rho'/\rho + T'/T)D^2\hat{\delta} = [1/\rho(\partial^2/\partial x^2 + \partial^2/\partial y^2) - M_\infty^2 D^2]\hat{p}_o(x,y) \tag{7.20}$$

$$\hat{\delta}(x,y,0) = \hat{z}_s(x,y) \tag{7.21}$$

For the potential flow in which the mean flow quantities are constant we manipulate the equations (7.10)-(7.15) as in the previous chapter assuming in addition that the flow is irrotational so that

$$\hat{u}_z = \hat{w}_x \tag{7.22}$$

and

$$\hat{v}_z = \hat{w}_y$$

The assumption of an unperturbed flow far upstream leads to

$$\nabla^2\hat{\delta} - M_\infty^2 D^2\hat{\delta} = 0, \qquad z \geq \delta_o \tag{7.23}$$

This result is identical to (6.35) with the understanding that now

$$\nabla^2 = \partial^2/\partial x^2 + \partial^2/\partial y^2 + \partial^2/\partial z^2 \tag{7.24}$$

The boundary conditions for the potential flow are the condition that the perturbations diminish at infinity for subsonic disturbances and that the condition of outward radiation applies for the wave-like supersonic disturbances.

The perturbation pressure is obtained by integrating (7.13) with respect to z. The result is identical to (6.38)

$$\hat{p}(x,y,0) = \int_0^{\delta_o} \rho D^2\hat{\delta}dz + D^2\int_{\delta_o}^{\infty} \hat{\delta}dz \tag{7.25}$$

7.3 SOLUTION

In the previous chapter we obtained solutions for the two-dimensional case in terms of a Fourier transform on x. We generalize that technique to the present case by employing Fourier transforms on x and y. For any perturbation quantity $\hat{f}$ the Fourier transform is defined as follows:

$$\tilde{f}(\alpha,\beta;z) = \int_{-\infty}^{\infty} \hat{f}(x,y,z)e^{-i\alpha x - i\beta y}dxdy \tag{7.26}$$

We can reduce (7.20) and (7.23) to ordinary differential equations in z. Transforming the boundary-layer problem, (7.20) and (7.21), we obtain

$$\tilde{\delta}_z + P(z)\tilde{\delta} = Q(\alpha, \beta; z) \tag{7.27}$$

$$\tilde{\delta}(\alpha, \beta; 0) = \tilde{z}_s(\alpha, \beta) \tag{7.28}$$

where

$$P(z) = (1/\gamma)(p'/\rho + T'/T)$$

$$Q(\alpha, \beta; z) = [(\alpha^2 + \beta^2)\rho^{-1}(k + \alpha U)^{-2} - M_\infty^2]\tilde{p}_o(\alpha, \beta)$$

Noting the similarity to (6.39) we obtain a solution similar to (6.41):

$$\tilde{\delta} = \tilde{z}_s + \delta_o\left[(\alpha^2 + \beta^2)\int_o^{z^*} \rho^{-1}(k + \alpha U)^{-2} dz^* - M_\infty^2 z^*\right]\tilde{p}_o, \tag{7.29}$$

$$0 \le z^* \le 1$$

We treat the potential flow problem, (7.23), by transforming on x and y and obtaining

$$\tilde{\delta}_{zz} + \sigma^2\tilde{\delta} = 0, \qquad z \ge \delta_o \tag{7.30}$$

where

$$\sigma^2 = M_\infty^2(\alpha + k)^2 - (\alpha^2 + \beta^2) \tag{7.31}$$

Assuming for the moment that k is purely real, we can express the general solution of (7.30) as

$$\tilde{\delta} = Ae^{i\sigma z} + Be^{-i\sigma z}, \qquad \sigma^2 > 0 \tag{7.32a}$$

or

$$\tilde{\delta} = Ce^{\tau z} + De^{-\tau z}, \qquad \sigma^2 = -\tau^2 < 0 \tag{7.32b}$$

We can specialize the general solution by considering the boundary conditions. Let us assume that the freestream is supersonic. We can express (7.31) as

$$\sigma^2 = \sigma_{2D}^2(\alpha) - \beta^2 \tag{7.33}$$

where

$$\sigma_{2D}^2 = B^2(\alpha - \gamma_1)(\alpha - \gamma_2)$$

The parameters B, γ_1, and γ_2 are defined in the previous chapter. The solution (7.32a) corresponds to the case of supersonic disturbances and the region of validity is a region in the α-β plane for which the expression in (7.33) is positive. We choose $A = 0$ to satisfy the radiation condition. For the case of a subsonic disturbance we take the solution in (7.32b) and note that the region of validity in the α-β plane consists of the points for which the expression in (7.33) is negative. We choose $C = 0$ in order to satisfy the condition of vanishing disturbances at infinity. In summary we have

$$\tilde{\delta} = \tilde{\delta}_1(\alpha, \beta) e^{-i\sigma(z-\delta_o)}, \qquad \sigma^2(\alpha, \beta) > 0 \tag{7.34a}$$

$$\delta = \delta_1(\alpha, \beta) e^{-\tau(z-\delta_o)}, \qquad \sigma^2(\alpha, \beta) < 0 \tag{7.34b}$$

where $\tilde{\delta}_1$ is the boundary-layer solution, (7.29), evaluated at $z^* = 1$. We can follow a similar line of reasoning to obtain the solutions for the case of a subsonic freestream

$$\tilde{\delta} = \tilde{\delta}_1 e^{-\lambda(z-\delta_o)}, \qquad \lambda^2 > 0 \tag{7.35a}$$

$$\tilde{\delta} = \tilde{\delta}_1 e^{-i\mu(z-\delta_o)}, \qquad \lambda^2 = -\sigma^2 < 0 \tag{7.35b}$$

7.4 SURFACE PRESSURE

We use the previous results in conjunction with (7.25) to obtain an expression for the surface pressure transform. The transformed expression of (7.25) is

$$\tilde{p}(\alpha, \beta; 0) = -\delta_o \int_0^1 \rho(k + \alpha U)^2 \tilde{\delta} dz^* - (k + \alpha)^2 \int_{\delta_o}^{\infty} \tilde{\delta} dz \tag{7.36}$$

Substituting for $\tilde{\delta}$ using (7.29) and either (7.34) or (7.35), neglecting terms of order (δ_o^2), we obtain the result to first order in δ_o:

$$\tilde{p}(\alpha, \beta; 0) = \tilde{p}_o(\alpha, \beta) + \delta_o \tilde{p}_{BL}(\alpha, \beta) \tag{7.37}$$

where

$$\tilde{p}_o = \begin{cases} -(k+\alpha)^2 \tilde{z}_s(\alpha,\beta)/\lambda, & M_\infty < 1 \\ -(k+\alpha)^2 \tilde{z}_s(\alpha,\beta)/\tau, & M_\infty > 1 \end{cases}$$

$$\tilde{p}_{BL} = \tilde{p}_1 + \tilde{p}_2$$

$$\tilde{p}_1 = -\int_0^1 \rho(k+\alpha U)^2 dz^* \tilde{z}_s(\alpha,\beta)$$

$$\tilde{p}_2 = -1/\sigma^2(\alpha,\beta)(k+\alpha)^4 [(\alpha^2+\beta^2)\int_0^1 \rho^{-1}(k+\alpha U)^{-2} dz^* - M_\infty^2] \tilde{z}_s(\alpha,\beta)$$

Note that the expression for the boundary-layer effect applies for both subsonic and supersonic flow. It is interesting to note that in the limit of incompressible flow as M_∞ approaches zero we obtain the following result for the boundary-layer effect:

$$\tilde{p}_{BL}(\alpha,\beta) = \left[-\int_0^1 (k+\alpha U)^2 dz^* + (k+\alpha)^4 \int_0^1 (k+\alpha U)^{-2} dz^*\right] \tilde{z}_s(\alpha,\beta) \qquad (7.38)$$

In this case the expression multiplying $z_s(\alpha,\beta)$ is independent of β. The Fourier inversion of (7.38) yields results identical to those obtained in the two-dimensional case, equations (3.67) and (3.68), with $\hat{z}_s(x)$ replaced by $\hat{z}_s(x,y)$. The inversion for compressible flow is not nearly as simple.

7.5 GENERALIZED AERODYNAMIC FORCE

The Fourier transform expression for the surface pressure may be formally inverted to obtain

$$\hat{p}(x,y,0) = 1/(2\pi)^2 \int_{-\infty}^{\infty} \tilde{p}(\alpha,\beta;0) e^{ix\alpha + iy\beta} d\alpha d\beta \qquad (7.39)$$

Our experience in inverting the transforms in the two-dimensional case has shown that the $\tilde{p}_2$-term gives some difficulty. Inspection of this term in the present case shows that the inversion is complicated by the dependence of σ upon α and β. We will not attempt to invert the expressions for the pressure, but rather we will try to find a more efficient way to use the Fourier transforms directly.

In the analysis of the phenomenon of panel flutter we are interested in the "generalized aerodynamic forces" rather than the pressure itself. If we represent the nondimensional panel deflection as a sum over some assumed modal amplitude functions

$$z_s(x, y, t) = \sum_m \sum_n \epsilon_{mn} \psi_m(x) \psi_n(y) e^{ikt} \tag{7.40}$$

then we can define a nondimensional generalized force Q_{mnpq} as

$$\begin{aligned} Q_{mnpq} &= \hat{Q}_{mnpq} e^{ikt} \\ \hat{Q}_{mnpq} &= \int_0^1 \int_0^1 \hat{p}_{mn} \psi_p(x) \psi_q(y) dx dy \end{aligned} \tag{7.41}$$

where $\hat{p}_{mn}$ is the nondimensional pressure due to $\epsilon_{mn}\psi_m\psi_n$. Dowell (1967) has shown that a great deal of economy may be achieved by performing the integration over x and y in (7.41) before inverting the transform in (7.39). Then $\hat{Q}_{mnpq}$ may be written as

$$\hat{Q}_{mnpq} = H_{mnpq}(k, M_\infty, \delta_o)\epsilon_{mn}$$

where

$$H_{mnpq} = 1/(2\pi)^2 \int_{-\infty}^{\infty} K(\alpha, \beta; k, M_\infty, \delta_o) G_{mnpq} d\alpha d\beta$$

$$G_{mnpq} = \int_0^1 \psi_m e^{-i\alpha x} dx \int_0^1 \psi_p e^{i\alpha x} dx \int_0^1 \psi_n e^{-i\beta y} dy \int_0^1 \psi_q e^{i\beta y} dy \tag{7.43}$$

where

$$K(\alpha, \beta; k, M_\infty, \delta_o) = \tilde{p}(\alpha, \beta; 0; k, M_\infty, \delta_o)/\tilde{z}_s(\alpha, \beta)$$

from equation (7.37). This device permits us to use the Fourier transform expression directly in calculating the generalized force rather than inverting to obtain the surface pressure prior to calculating the generalized force. In Chapter 9 we apply this method in calculating the boundary-layer contribution to the generalized force for the case of an infinite-span panel in two-dimensional supersonic flow.

VIII. APPLICATION OF THE THEORY TO WIND-DRIVEN WATER WAVES

8.1 INTRODUCTION

The previous chapters have presented the basic ingredients for a theoretical attack upon the problem of predicting the pressure over an oscillating surface in flow situations ranging from incompressible low-speed flow to compressible supersonic flow, including two and three space dimensions, and including separately the important boundary-layer effects; namely, the effects of the mean shear velocity profile, the viscous stresses, and the turbulent Reynolds stresses. To give some substance to these theoretical developments and to study a geophysical problem of current interest we apply the theory to the air-sea interaction problem and predict the pressure distribution over a moving water surface over which a steady wind is blowing. Our goal is threefold. First we would like to gain some experience in working out an example using the theory to show how one might actually employ this approach. Second we would like to compare the theory with the inviscid theory of Miles (1957, 1959b) and note any differences or similarities. Finally we would like to compare the theory with experiment. For the latter we examine the laboratory studies of Shemdin and Hsu (1967) and Yu and Hsu (1971) based on data taken in the Stanford wind-water channel. In this application to wind-wave interaction we use the inviscid shear flow theory developed in Chapter 3 for two-dimensional incompressible flow and we do not include the terms for the viscous stresses and Reynolds stresses in the perturbed flow.

8.2 SPECIALIZATION OF THE THEORY FOR TRAVELING SURFACE WAVES

Consider the case of a wind blowing over a water surface such as a lake or the open ocean and refer to figure 2.1 for a simplified representation of this flow situation. We can idealize the problem by assuming that the waves are two-dimensional, that conditions do not vary in the y-direction, and that the waves extend infinitely far in the x-direction. We represent the wave surface nondimensionally by choosing the wave amplitude function

$$\hat{z}_s(x) = e^{-i\alpha x} \tag{8.1}$$

where the relevant quantities have been nondimensionalized by the wavelength, L, of the surface waves. Substituting this expression in the generalized expression for an oscillating surface [see equation (3.16)] we obtain

$$z_s(x,t) = \epsilon\, e^{-i(\alpha x-kt)} \tag{8.2a}$$

$$= \epsilon\, e^{-i\alpha(x-ct)} \tag{8.2b}$$

where $c = k/\alpha$. We recognize this as the representation for a traveling wave disturbance propagating in the x-direction with phase velocity (nondimensional), c. Note that $\alpha = 2\pi$ due to the fact that the reference length is the wavelength, L.

We proceed to specialize the theory developed in Chapter 3 to treat the present problem. Refer to Chapter 3 for the basic assumptions that were used to develop the theory and examine Figure 3.1 for a view of the essential features of the flow near the traveling wave. We can obtain an expression for the perturbation pressure at the surface in a variety of ways. One rather straightforward approach using the methodology of 3.4 would be to reformulate the problem by assuming that the streamline deviation may be represented as

$$\delta(x,z,t) = \epsilon\hat{\Delta}(z)e^{-i(\alpha x-kt)} \tag{8.3}$$

and the perturbation pressure may be represented as

$$p(x,z,t) = \epsilon\hat{\pi}(z)e^{-i(\alpha x-kt)} \tag{8.4}$$

Substituting $\hat{\delta} = \hat{\Delta}(z)e^{-i\alpha x}$ and $\hat{p} = \hat{\pi}(z)e^{-i\alpha x}$ in (3.51) through (3.55) we obtain

$$\hat{\Delta}'(z^*) = \delta_0\alpha^2(k-\alpha U)^{-2}\hat{\pi}_0(0), \quad 0 \le z^* \le 1 \tag{8.5}$$

$$\hat{\Delta}(0) = 1 \tag{8.6}$$

$$\hat{\Delta}''(z^*) - (\alpha\delta_0)^2\,\hat{\Delta} = 0, \qquad z^* \geq 1 \tag{8.7}$$

$$\hat{\Delta}(\infty) = 0 \tag{8.8}$$

$$\hat{\pi}(0) = -\delta_0 \int_0^\infty (k-\alpha U)^2\,\hat{\Delta}(z^*)dz^* \tag{8.9}$$

The solution to (8.5) through (8.8), matching $\hat{\Delta}$ at $z^* = 1$, is

$$\begin{aligned}\hat{\Delta}(z^*) &= 1 + \delta_0\alpha^2\hat{\pi}_0(0)\int_0^{z^*} (k-\alpha U)^{-2}dz^*, \qquad 0 \leq z^* \leq 1 \\ &= \hat{\Delta}(1)e^{-\alpha\delta_0(z^*-1)} \qquad\qquad z^* \geq 1\end{aligned} \tag{8.10}$$

Substituting these expressions in (8.9), evaluating the resulting integrals, and neglecting terms of $0(\delta_0^2)$ we obtain

$$\hat{\pi}(0) = -(k-\alpha)^2/\alpha + \delta_0\left[-\int_0^1 (k-\alpha U)^2dz^* + (k-\alpha)^4\int_0^1 (k-\alpha U)^{-2}dz^*\right] \tag{8.11}$$

Comparing this expression with (3.63) note that the present result is equivalent to the Fourier transform of the pressure amplitude provided we interpret the Fourier transform variable, α, as the negative of the wave number of the traveling surface wave. In terms of the wave phase speed, c, the above expression is

$$\hat{\pi}(0) = -\alpha(1-c)^2 + \alpha^2\delta_0[-H_1(c) + (1-c)^4K_1(c)] \tag{8.12}$$

where

$$H_1(c) = \int_0^1 (U-c)^2dz^* \tag{8.13}$$

$$K_1(c) = \int_0^1 (U-c)^{-2}dz^* \tag{8.14}$$

We recognize the integrals $H_1(c)$ and $K_1(c)$ as the familiar integrals from the theory of hydrodynamic stability mentioned in Section 3.6. Note that the first term in (8.12) is the potential flow pressure while the remaining terms are the first-order perturbation due to the boundary layer.

We can obtain the expressions for the boundary-layer effect in an alternate manner by substituting (8.1) in (3.67) and (C-23). The evaluation of the first term is rather straightforward, while the second term involves a double integral over x_1 and z^*. The integral is evaluated by interchanging the order of integration and performing the integration over x_1 by making a change of variables, $t = x - x_1$. This resulting integral is evaluated by parts and the remaining integration over z^* gives the desired result, $K_1(c)$.

8.3 EVALUATION OF THE EXPRESSION FOR THE SURFACE PRESSURE COEFFICIENT

We now consider the evaluation of the expressions $H_1(c)$ and $K_1(c)$. Expanding the binomial in (8.13) we obtain

$$H_1(c) = c^2 - 2b_1c + c_1 \tag{8.15}$$

where

$$b_1 = \int_0^1 U dz^*$$

$$c_1 = \int_0^1 U^2 dz^*$$

The expression for $K_1(c)$ given by (8.14) may be re-written as

$$K_1(c) = \int_0^1 z^{*\prime}(U)(U-c)^{-2} dU \tag{8.16}$$

This integral has a singularity at $U = c$, but the singularity can be circumvented by taking a path of integration that is indented <u>over</u> the singular point c. Refer to Miles (1959a) and to Chapter 8 of Lin (1955) for a discussion of this delicate question. The choice of indenting the contour over the singularity at $U = c$ is similar to the problem of where to locate the singularity, $\gamma_0 = -k/U$, in connection with the inversion of the Fourier transform expressions considered in Chapter 3 (see Appendix C). In that case we assume that the reduced frequency, k, is complex with an infinitesimally small negative imaginary part which is equivalent to disturbances which grow with time. In the present context we assume that the imaginary part of c is negative corresponding to growing disturbances in the limit as $\mathrm{Im}(c) \to 0$. Indenting the contour over the singular point is equivalent to locating the singularity just below the real axis in the complex U-plane.

Integrating (8.16) once by parts along the appropriate path and then separating out the singular portion, I_s, we obtain

$$K_1(c) = -z^{*\prime}(0)/c - z^{*\prime}(1)/(1+c) + I_s + \int_0^1 \frac{(z^{*\prime\prime}-z_c^{*\prime\prime})dU}{(U-c)} \tag{8.17}$$

where

$$I_s = z_c^{*\prime\prime}\int_0^1 dU/(U-c) \tag{8.18}$$

Integrating I_s <u>over</u> the singular point yields

$$I_s = z_c^{*\prime\prime}\{\log[(1-c)/c]-i\pi\} \tag{8.19}$$

Note that the imaginary component of the pressure is proportional to

$$z_c^{*\prime\prime} = -U_c^{\prime\prime}/(U_c^{\prime})^3 , \tag{8.20}$$

which is related to the curvature of the wind profile (U'') at the elevation where the wind speed is equal to the wave speed. This is an essential feature of Miles' (1957) theory for the generation of surface waves by a parallel shear flow on the basis of the inviscid Orr-Sommerfeld equation (see Section 8.4).

We can evaluate the integrals $H_1(c)$ and $K_1(c)$ in (8.15) and (8.17) for a mean shear velocity profile, $U(z^*)$, representative of turbulent flow over water. We choose the logarithmic profile, which has the support of both theory [Miles (1957)] and experiment [Shemdin and Hsu (1967); Kendall (1970); Stewart (1970), Yu and Hsu (1971)]. The form we shall use for the present case in terms of the nondimensional variables is

$$U = U_1 \log (z^*/z_0^*) \tag{8.21}$$

where $U_1 = u_*/(u_\infty \kappa)$, and where u_* is Prandtl's shearing stress velocity, κ Kármán's universal turublence constant, and z_0^* an effective roughness parameter. Using (8.21) to evaluate (8.15) and (8.19) we obtain (see Appendix E)

$$H_1(c) = c^2 - 2b_1 c + c_1 \tag{8.15}$$

where

$$b_1 = 1 - U_1 \tag{8.22}$$

$$c_1 = 1 - 2U_1 + 2U_1^2 \tag{8.23}$$

and

$$K_1(c) = K_1^R(c) + iK_1^I(c) \tag{8.24}$$

where

$$K_1^R(c) = -z_0^*/(U_1 c) - z_0^* e^{1/U_1}/[U_1(1-c)]$$

$$+ \frac{z_0^* e^{c/U}}{U_1^2} \{\log[(1-c)/c] + f[(1-c)/U_1] - f(-c/U_1)\} \tag{8.25}$$

$$K_1^I(c) = -\pi z_c^{*''} = -\pi z_0^* e^{c/U_1}/U_1^2 . \tag{8.26}$$

where

$$f(w) = \sum_{n=1}^{\infty} \frac{w^n}{n \cdot n!} \tag{8.27}$$

We now have all the necessary ingredients for evaluating the surface pressure coefficient according to the present first-order theory in terms of the boundary layer thickness parameter, δ_0. The pressure coefficient is obtained by multipying the expression in (8.4) by the factor 2 to account for the appropriate reference quantity, the freestream dynamic pressure, $1/2\rho_\infty u_\infty^2$. The surface pressure coefficient is found using this correction to (8.4), evaluating at $z^* = 0$, using (8.12), (8.15), and (8.24), and is given by

$$C_{p_s}(x,t) = -2\alpha\epsilon\{(1-c)^2 + \alpha\delta_0[H_1(c)-(1-c)^4(K_1^R(c) + iK^I(c))]\} e^{i(kt-\alpha x)} \quad (8.28)$$

We are interested in the magnitude of the pressure coefficient and the phase shift between the pressure and the wave elevation, $z_s(x,t)$ [see (8.2)]. Taking the real part of (8.28) and (8.2) we have

$$C_{p_s} = |C_{p_s}| \cos[(kt - \alpha x) + \varphi] \quad (8.29)$$

$$z_s = \epsilon \cos(kt-\alpha x) \quad (8.30)$$

An equivalent representation is

$$C_{p_s} = |C_{p_s}| \cos[(\alpha x-kt) + \theta] \quad (8.31)$$

$$z_s = \epsilon \cos(\alpha x-kt) \quad (8.32)$$

where

$$|C_{p_s}| = (R^2 + I^2)^{1/2} \quad (8.33)$$

$$\theta = \pi - \gamma \quad (8.34)$$

$$\gamma = \tan^{-1}(I/R) \quad (8.35)$$

and where

$$R = 2\alpha\epsilon\{(1-c)^2 + \alpha\delta_0[H_1(c)-(1-c)^4 K_1^R(c)\} \quad (8.36)$$

$$I = -(2\alpha\epsilon)\alpha\delta_0(1-c)^4 K_1^I(c) \tag{8.37}$$

The representation (8.31) through (8.32) is the same form as that used in the Miles theory and in the experiments and allows direct comparison with those results. Note that $|C_{p_s}|$ is the magnitude of the pressure coefficient while θ is the phase shift relative to the surface wave. In the limit as $\delta_0 \to 0$ we recover the potential flow result; namely,

$$|C_{p_{s_0}}| = 2\alpha\epsilon(1-c)^2 \tag{8.38}$$

$$\theta_0 = \pi \tag{8.39}$$

Without actually evaluating (8.33) numerically we cannot draw any immediate conclusions as to the effect of a finite value of δ_0 in modifying the pressure magnitude predicted by (8.38) for $\delta_0 = 0$. However, we can see qualitatively what will be the effect of a small value of δ_0 upon the phase angle predicted by (8.34). For small δ_0 we find (note that $K_1^I(c)$ is negative) that γ is small and positive, thus θ is slightly less than its potential flow value of π. Note that for $c \to 1$ we find $\gamma \to 0$ and $\theta \to \pi$. This seems to indicate that the present theory predicts zero wave growth for wave phase speeds equal to the wind speed. It will be interesting to see how this result compares with experimental results and with the Miles' theory.

8.4 RELATIONSHIP OF THE THEORY TO MILES' INVISCID STABILITY MODEL

Miles (1957) treated the motion of the wavy water surface as a two-dimensional mass-spring system with the wave-induced aerodynamic pressure $\tilde{p}_a$ as the forcing function. He assumed that the surface displacement z_s and pressure p_a both vary sinusoidally and can be represented in terms of dimensional variables as

$$z_s(x,t) = ae^{i\alpha_w(x-Ct)} \tag{8.40}$$

$$p_a(x,t) = (\alpha_1 + i\beta)\rho_a u_1^2 \alpha_w z_s \tag{8.41}$$

where a is the wave amplitude, α_w the wave number, C the wave celerity, $(\alpha_1 + i\beta)$ a dimensionless pressure coefficient, ρ_a the air density, u_1 the reference velocity at the edge of the viscous sublayer, and $\alpha_w z_s$ the wave slope. The equation of motion for the water surface is

$$Lz_s + m z_{s_{tt}} = -p_a \tag{8.42}$$

where L is a linear operator such that Lz_s represents the restoring force while m is the effective mass per unit area such that $mz_{s_{tt}}$ is the inertia term. By substituting (8.40) and (8.41) into (8.42) Miles obtained a first approximation for deep water gravity waves

$$C = C_0 \left[1 + \frac{1}{2} \frac{\rho_a}{\rho_0} (\alpha_1 + i\beta)(u_1/C)^2 \right] \tag{8.43}$$

where

$$C_0^2 = g/\alpha_w \tag{8.45}$$

This gives the following expression for the wave elevation

$$z_s = a \exp\left[\frac{1}{2} \frac{\rho_a}{\rho_0} \beta \left(\frac{u_1}{C}\right)^2 \alpha_w C_0 t \right] \exp[i\alpha_w (x - C_0 t)] \tag{8.45}$$

We therefore interpret the imaginary part of Miles' pressure coefficient, β, as a wave growth parameter. The primary problem of Miles' effort was to determine β from an analysis of the wind field.

Starting from the equations of motion governing the two-dimensional flow in an inviscid incompressible fluid of constant density [cf. equations (3.4) through (3.6)], assuming small perturbations of a shear flow $U(z)$, introducing a stream function, ψ, and assuming by virtue of linearity that ψ and p exhibit the same dependence on x and t as z_s in (8.40) Miles obtained after elimination of the pressure

(8.46)

$$(U-C)\psi_{zz} - [\alpha_w^2(U-C) + U_{zz}]\psi = 0, \tag{8.46}$$

the inviscid form of the Orr-Sommerfeld equation. The boundary conditions are that the disturbance shall die out at infinity and that the air-water interface (originally at $z = z_0$) shall remain a streamline. The surface boundary condition is approximately

$$\psi_x/(U-C) = i\alpha_w z_s \quad \text{at} \quad z \simeq z_0. \tag{8.47}$$

We note that (8.46) and (8.47) are equivalent to the formulation presented in Chapter 3. If we substitute

$$\hat{w}(x, z) = -\psi_x \tag{8.48}$$

and

$$\hat{\psi} = \psi(z)e^{-i\alpha x} \tag{8.49}$$

in (3.14) and (3.16) we obtain using $c = k/\alpha$ the nondimensional version of (8.46) and (8.47). The two formulations are identical at this point.

Miles obtained an implicit solution of (8.46) which yielded

$$\beta = -\pi|\varphi_c|^2 \; U_c''/U_c' \tag{8.49}$$

where

$$\varphi = \psi/(u_1 z_s) \tag{8.50}$$

and where the derivatives are with respect to the variable $\xi = \alpha_w z$ and the subscript c indicates the quantities at $z = z_c$. We infer from Miles' result that only those waves with phase speeds in the range for which $-U''$ is large may be expected to grow. With a given velocity field β can be evaluated and the wave growth rate predicted. Miles (1957) attempted an approximate determination of β, however he chose not to seek an approximate solution for the case of thin boundary layers as we have done, indicating that such a technique "is not well suited to the relatively thick turbulent boundary-layer profiles that are of interest in the present problem." He chose instead to seek an approximate solution for φ_c using the approximation

$$\varphi = (U-C)e^{-\xi}/u_1 \tag{8.51}$$

and prescribing a logarithmic mean velocity distribution of the form given by (8.21). Under these assumptions an integral approximation for β in terms of ξ_c was found. In a subsequent paper, Miles (1959b) obtained a numerical integration of the inviscid Orr-Sommerfeld equation which yielded values of β that were generally smaller than those estimated in Miles (1957).

For the purpose of comparing with Miles we must obtain an expression for β. Comparing (8.28) and (8.41) we obtain after a little manipulation

$$\beta = \alpha\delta_0(1-c)^4 K_1^I(c)/U_1^2 \tag{8.52}$$

where

$$K_1^I(c) = \pi z_c^{*''} \tag{8.53}$$

Note that the expression in (8.53) has the opposite sign from (8.26) which arises from the differences in the sign of the expression in the exponential [cf. (8.2b) and (8.40)]. The result in (8.52) is given in terms of the nondimensional variables used in connection with this theory. We can simplify this by noting that for a logarithmic profile

$$z_c^{*''} = z_c^*/U_1^2 \tag{8.54}$$

Substituting this in (8.52) and noting that the combination

$$\alpha\delta_0 z_c^* = 2\pi \frac{\delta_{b.1}}{L} \frac{z_c}{\delta_{b.1}} = \xi_c \tag{8.55}$$

we obtain

$$\beta = \pi(1-c)^4 \xi_c/U_1^4 \tag{8.56}$$

Miles (1957) obtained an approximate expression for $\beta(\xi_c)$ for small values of the arguments ξ_c which could be compared with the above expression, however, one must specify both U_1 and z_0^* in order to evaluate the present theory.

An alternative is to proceed to express β as a function of the dimensionless wave speed, $c/U_1(=C/u_1)$. The wave number for gravity waves may be determined from (8.45)

$$\alpha_w = g/C^2 \tag{8.57}$$

Evaluating the logarithmic velocity profile for z_c and multiplying by (8.57) yields

$$\xi_c = \Omega(U_1/c)^2 e^{c/U_1} \tag{8.58}$$

where we have introduced the dimensionless wind-profile parameter

$$\Omega = gz_0/u_1^2 \tag{8.59}$$

Substituting (8.58) in (8.56) we obtain

$$\beta(c/U_1, U_1, \Omega) = \pi\Omega(U_1^{-1} - c/U_1)^4 e^{c/U_1}/(c/U_1)^2 \tag{8.60}$$

We can compute β vs. c/U_1 for fixed values of U_1 and Ω and compare with similar results obtained by Miles (1959b). Miles (1957) indicates that an adequate approximation for the upper limit of validity of (8.21) is $u_\infty = 10u_1$ (dimensional variables); therefore, we choose $U_1 = 0.1$ in (8.60). Choosing a typical value for Ω used by Miles, $\Omega = 10^{-2}$, we evaluate (8.60) for various values of c/U_1. These results and values obtained by Miles (1959b) taken from his Figure 4 are presented in the accompanying table

c/U_1	β [Eq. (8.60)]	β_M[Miles (1959b)]	β/β_M
1	537	3.25	163
2	239	3.40	71
4	139	3.00	46
6	90	2.00	45
8	23	.65	35
9	3	.20	15
10	0	~.02	0

Apparently the two theories are not equivalent as far as the prediction of the wave growth parameter is concerned. The present theory predicts values for β which are many times larger than the values predicted by Miles' theory over almost the entire range of wave speeds. Only for $c/U_1 \to 10$ (corresponding to $c \to 1$) do the two theories predict values of β that are comparable, but in that case the values are negligibly small. We will defer drawing conclusions from this comparison until we have examined these theories in the light of experimental evidence. However, we can indicate a possible explanation for the different results. Earlier in this section we indicated that the two theories were equivalent as far as the governing equation and boundary conditions are concerned. The main difference arises from the assumption of thin (in wavelengths) boundary layers made in the present theory. We should try to determine whether or not the application of these theories to treat gravity waves is consistent with this assumption.

We obtain an expression for δ_0 by multiplying $\delta_{b.1.}$ by the wave number given by (8.57), then dividing by 2π to give

$$\delta_0 = \delta_{b.1.}\, g/(2\pi C^2) \tag{8.61}$$

Introducing u_1 and u_∞, this becomes

$$\delta_0 = \frac{(\delta_{b.1.} g/u_\infty^2)(u_\infty/u_1)^2}{2\pi(C/u_1)^2} \tag{8.62}$$

We use Miles' suggestion that $u_\infty = 10\ u_1$ is a rough but adequate approximation for the wind speed at two meters above the water, hence we take $\delta_{b.1.} = 2m.$ This leaves two other variables to be specified: c/U_1 and u_∞. We take the wind speed $u_\infty = 10m./sec.$ as a rough estimate of that quantity for the open ocean. Putting these numbers in (8.62) we obtain approximately

$$\delta_0 \simeq \frac{3}{(c/U_1)^2} \tag{8.63}$$

For values of δ_0 equal to or smaller than 0.10 we find from (8.63) that c/U_1 must be equal to or greater than 5. This implies that for these conditions at least half of the range of c/U_1 in the preceding table is appropriate to the thin boundary-layer regime. Obviously, this numerical exercise is not intended to be exhaustive, but it does indicate that the large difference between the two theoretical predictions of the wave growth parameter is not necessary due to the thin boundary-layer assumption. Examination of the two theories in the light of experimental evidence will perhaps clarify the situation somewhat.

8.5 COMPARISON BETWEEN THEORY AND EXPERIMENT

Having obtained expressions for the aerodynamic pressure over progressive water waves and having made a preliminary comparison with Miles' theory, we now attempt a comparison of the two theories with some experimental measurements conducted in the Stanford wind-wave channel by Shemdin and Hsu (1967) and Yu and Hsu (1971). We will not describe the experimental facilities and instrumentation in detail as that information may be obtained in the two references previously mentioned and in the earlier report of Hsu (1965); however, we will note the essential features. The channel is 115 feet long and the nominal water depth is 3 feet. Deep water waves are generated by a mechanical wave generator which permits the wave amplitudes and periods to be pre-selected. The wind is generated by drawing air with a fan at the downstream end of the channel. The key feature of the experimental method is the use of a wave following device to measure the instantaneous pressure at a fixed relative distance above the oscillating water surface to achieve meaningful results. In addition to the pressure sensing system (refer to the references for details) there is a system to measure the mean velocity and a wave height gauge.

To produce test conditions that satisfy Miles' inviscid model the velocity of the freestream must not be less than the wave celerity and the pressure probe must be inside the critical layer $(z < z_c)$ and outside the viscous sublayer. The measured mean velocity profiles follow the logarithmic law with respect to the mean water level [equation (8.21)] in agreement with Miles' model and the present theory. In evaluating these theories for the conditions of the experiment we take experimentally-determined values for the profile parameters, U_1 and z_0^*.

The results of a comparison between experiment and theory are presented in Figures 8.1 through 8.7. The results for the pressure coefficient magnitude, $|C_{p_s}|$, and the phase shift, θ, are displayed as functions of the wave phase speed-freestream wind speed ratio, $c = C/u_\infty$. The present theory was evaluated using equations (8.33) through (8.38) and (8.15) through (8.27) and the numerical results were obtained using a computer for accuracy in evaluating the series in (8.27). The Miles' theory results were obtained by Shemdin and Hsu (1967) and Yu and Hsu (1971) and are reproduced here for comparison. Figures 8.1 and 8.2 correspond to the experiment of Shemdin and Hsu (1967) in which data was taken mainly from the lower range of c and for which the boundary layer was relatively thin, $\delta_0 \simeq .06$. Examination of Figure 8.1 shows reasonable agreement between theory and experiment for the wave-induced pressure magnitudes for c between 0.2 and 0.4. The potential flow pressure variation is also presented. The present theory and Miles' theory are in close agreement for this particular case. For c greater than

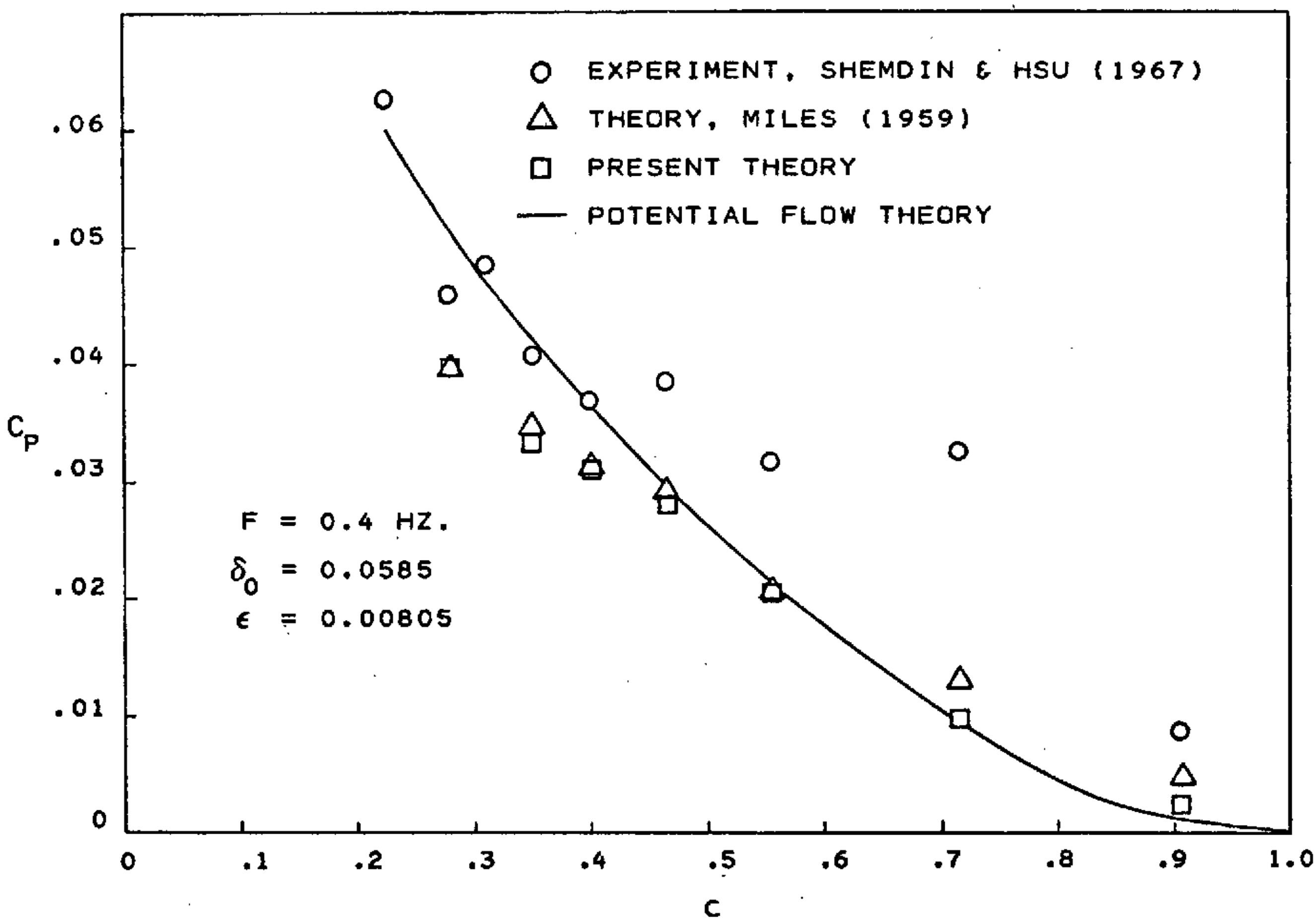

FIGURE 8.1
COMPARISON OF THEORETICAL AND EXPERIMENTAL WAVE-INDUCED PRESSURE MAGNITUDE VS. WAVE PHASE SPEED

0.4 the experimental pressure values are much larger than the values predicted by the theories, and this could indicate some sort of general trend if the experimental point at $c \simeq 0.9$ is considered to be spurious. The phase shift variation for this case is presented in Figure 8.2. Again the agreement between theory and experiment is reasonable for c smaller than 0.4. The most striking feature, however, is the difference between the two theoretical predictions of phase shift. The Miles theory predicts a gradual decrease in phase shift with increasing wave phase speed, while the present theory predicts increasing phase shift with increasing wave phase speed. This behavior deserves some additional comment.

At first it was felt that the behavior of the phase shift for the present theory was due to the use of experimental values for the profile parameters U_1 and z_0^*. To resolve this problem we proceeded to perform a sensitivity analysis using the computer to evaluate the present theory by fixing one of the parameters and varying the other parameter. Some of the results of this study are presented in Figures 8.3a and 8.3b. In figure 8.3a we vary z_0^* with U_1 fixed, while in Figure 8.3b we vary U_1 with z_0^* fixed. In both cases we obtain the same behavior for the phase shift variation; namely, the curves show θ decreasing with increasing c for c less than 0.5 and θ increasing for larger values of c. This exercise shows that the theory is quite sensitive to the profile parameters; for example at $c = 0.3$ a 15% increase in U_1 causes a 45% increase in θ at constant z_0^*. This points out the importance of accuracy in measuring the mean velocity profile and also suggests that an area for possible future study would be the sensitivity of the theory to the type of profile used in the model, as there is some indication that the experimental data exhibit a systematic deviation from a least-square logarithmic fit [cf. Shemdin and Hsu (1967)].

Having eliminated the profile parameters as the source of unexplained behavior of the present theory insofar as phase variation is concerned, we will defer further discussion of this matter until the next section and proceed with

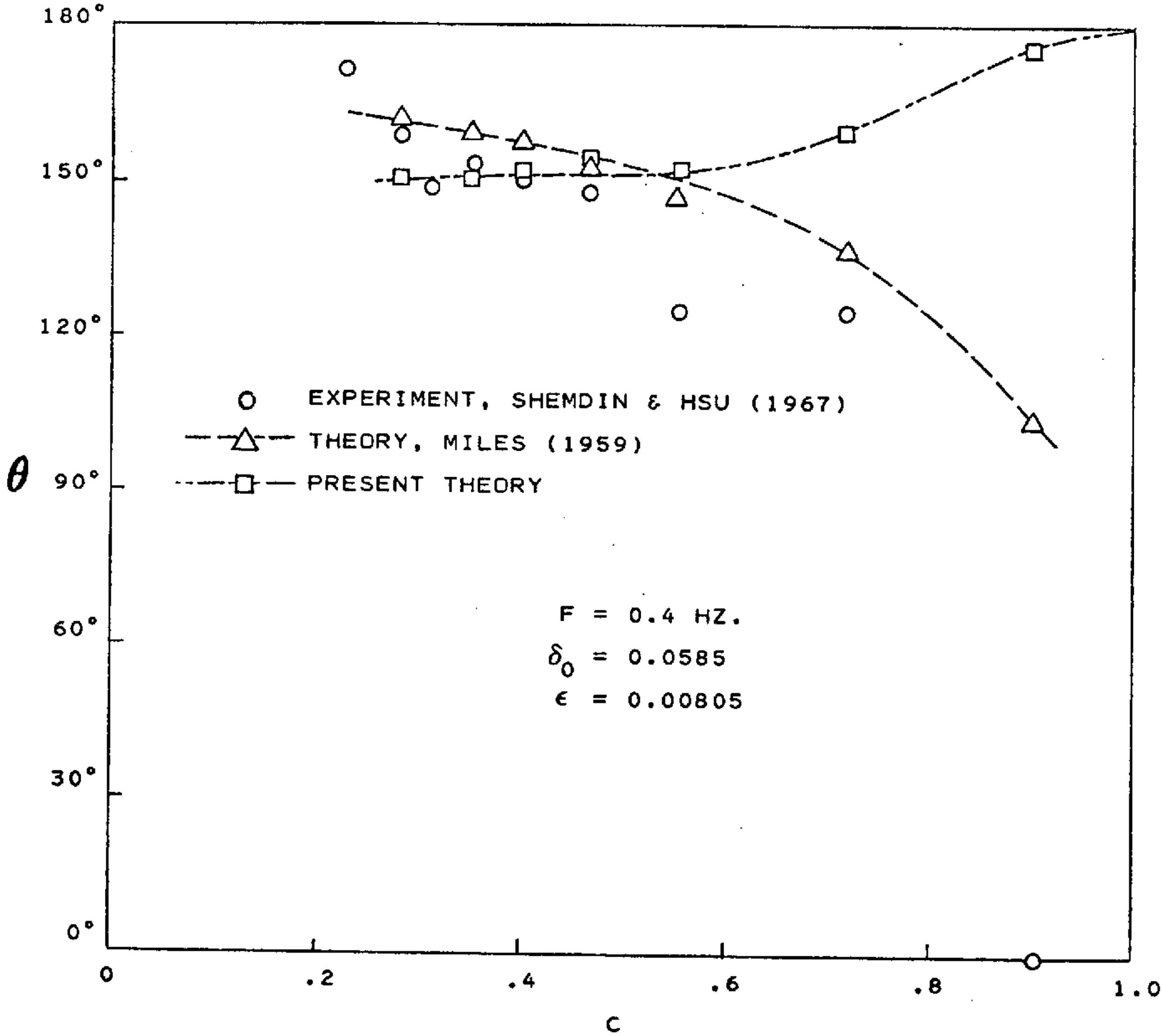

FIGURE 8.2
COMPARISON OF THEORETICAL AND EXPERIMENTAL WAVE-INDUCED PHASE SHIFT VS. WAVE PHASE SPEED

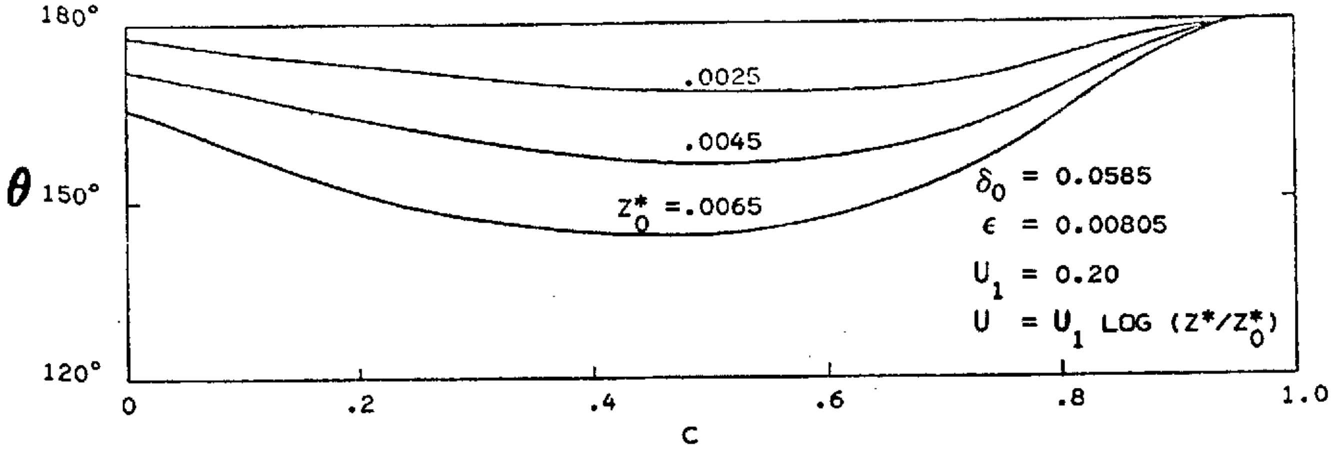

FIGURE 8.3A
WAVE-INDUCED PHASE SHIFT VS. PHASE SPEED
FOR VARIOUS VALUES OF EFFECTIVE ROUGHNESS

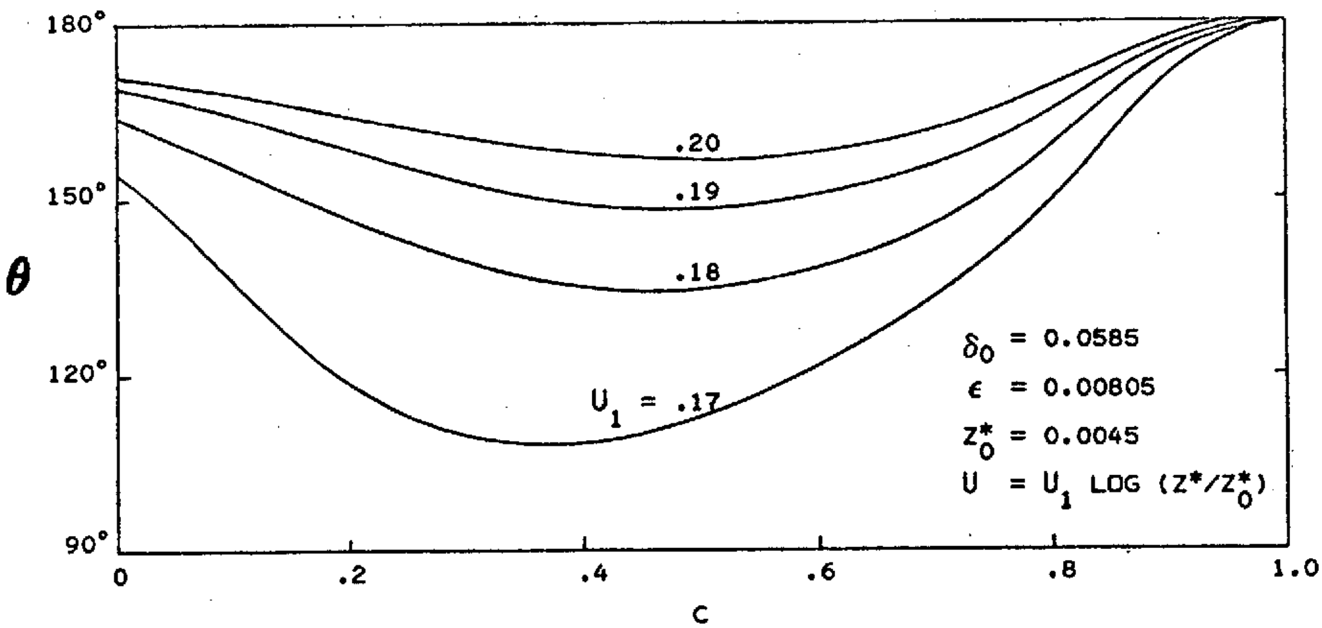

FIGURE 8.3B
WAVE-INDUCED PHASE SHIFT VS. PHASE SPEED
FOR VARIOUS VALUES OF THE REFERENCE VELOCITY

additional comparison of theory and experiment. Figures 8.4 through 8.7 correspond to the recent experiments of Yu and Hsu (1971). These experiments are an extension of and improvement over the earlier measurements of Shemdin and Hsu (1967). The earlier measurements were limited by the range of c (most of the data were obtained for c less than 0.5) and were obtained with the probe near the outer edge of the critical layer. The more recent measurements were obtained with the pressure probe at a fixed distance of 1/4 inch above the wave surface and for c in the range of 0.6 to 1.0. Figures 8.4 and 8.5 show the pressure magnitude and phase shift variation for 0.8 Hz. waves and $\delta_0 \simeq .18$, while Figure 8.6 and 8.7 show the variation for 1.2 Hz. waves and thicker boundary layer, $\delta_0 \simeq .41$. In both cases the phase shift behavior is similar to the case observed in Figure 8.2. The experimental values of θ are smaller than the theoretical values and tend to decrease slightly with increasing wave speed. The present theory gives improved agreement with the experiment over Miles' theory for values of c less than about 0.70 but the trend of increasing phase shift with increasing wave speed for larger values of c indicates a failure of the present theory to adequately model the experimental behavior. Note that Miles' theory also predicts increasing phase shift with increasing wave speed for values of c greater than 0.9 indicating a failure of his theory in this range.

The behavior of the pressure magnitude is far more striking. The experimental data are an order of magnitude larger than the theoretical predictions. The data indicate an increase in pressure magnitude for increasing wave speed, while the theories predict a decrease. Notwithstanding this disagreement between theory and experiment, the present theory is significantly closer to the experiment with regard to magnitude than is Miles' theory. Furthermore the present theory predicts an increase in magnitude over the potential flow theory while Miles' theory represents a decrease from the potential flow values. Comparing the potential flow theory with the experimental results we would at least expect an inviscid shear flow theory to represent some improvement over potential flow theory.

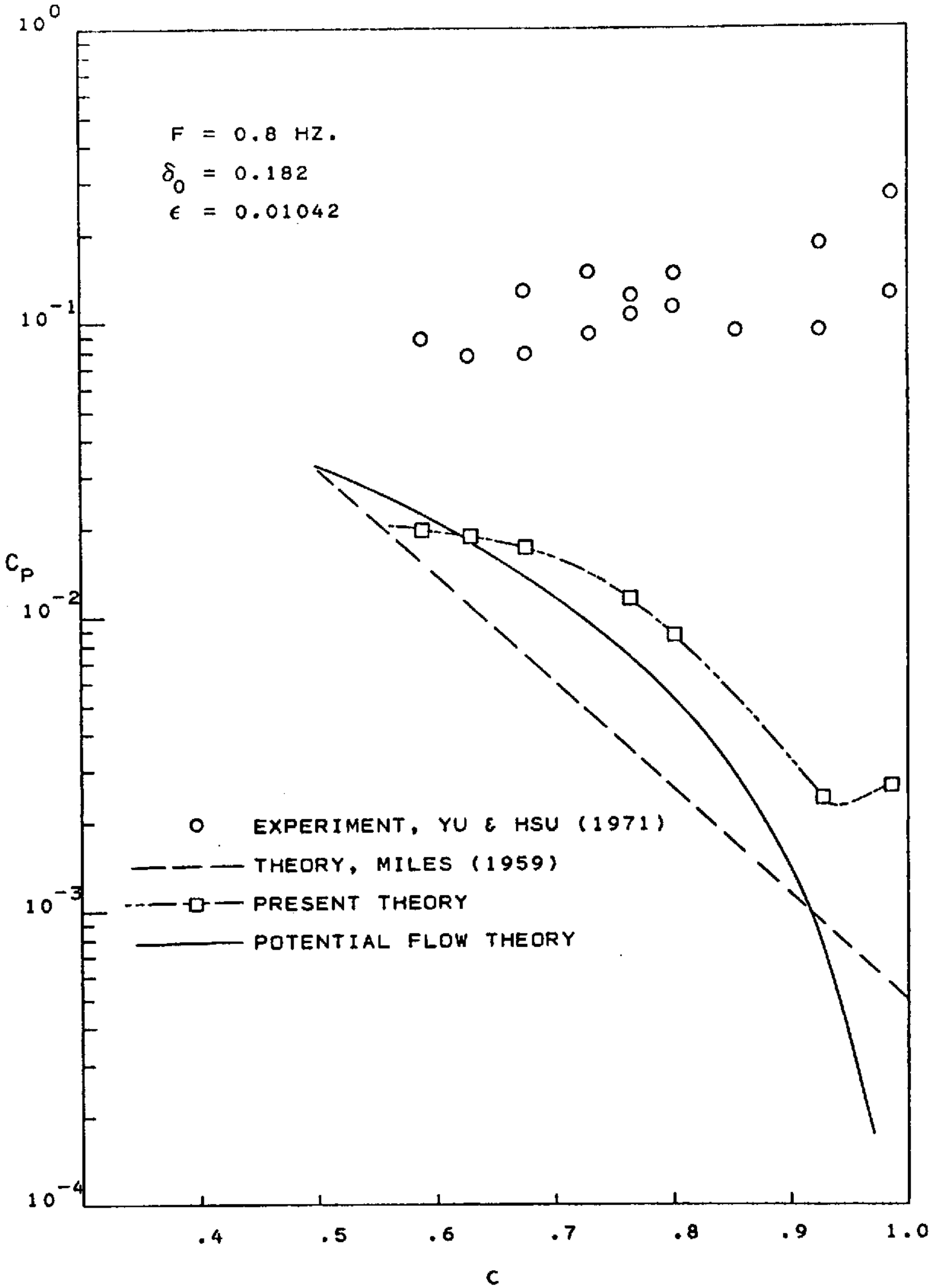

FIGURE 8.4
COMPARISON OF THEORETICAL AND EXPERIMENTAL WAVE-INDUCED PRESSURE MAGNITUDE VS. WAVE PHASE SPEED

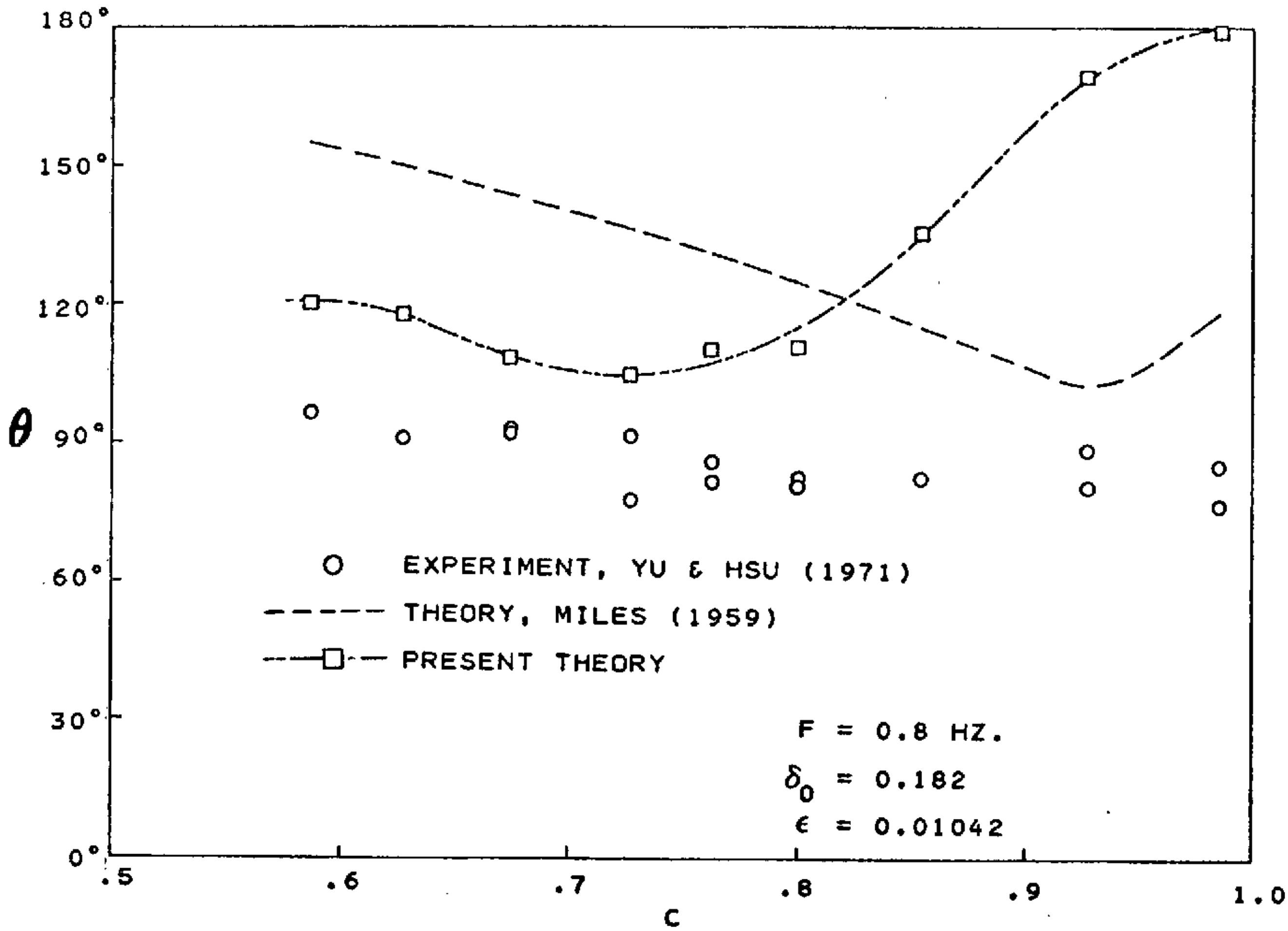

FIGURE 8.5
COMPARISON OF THEORETICAL AND EXPERIMENTAL WAVE-INDUCED PHASE SHIFT VS. WAVE PHASE SPEED

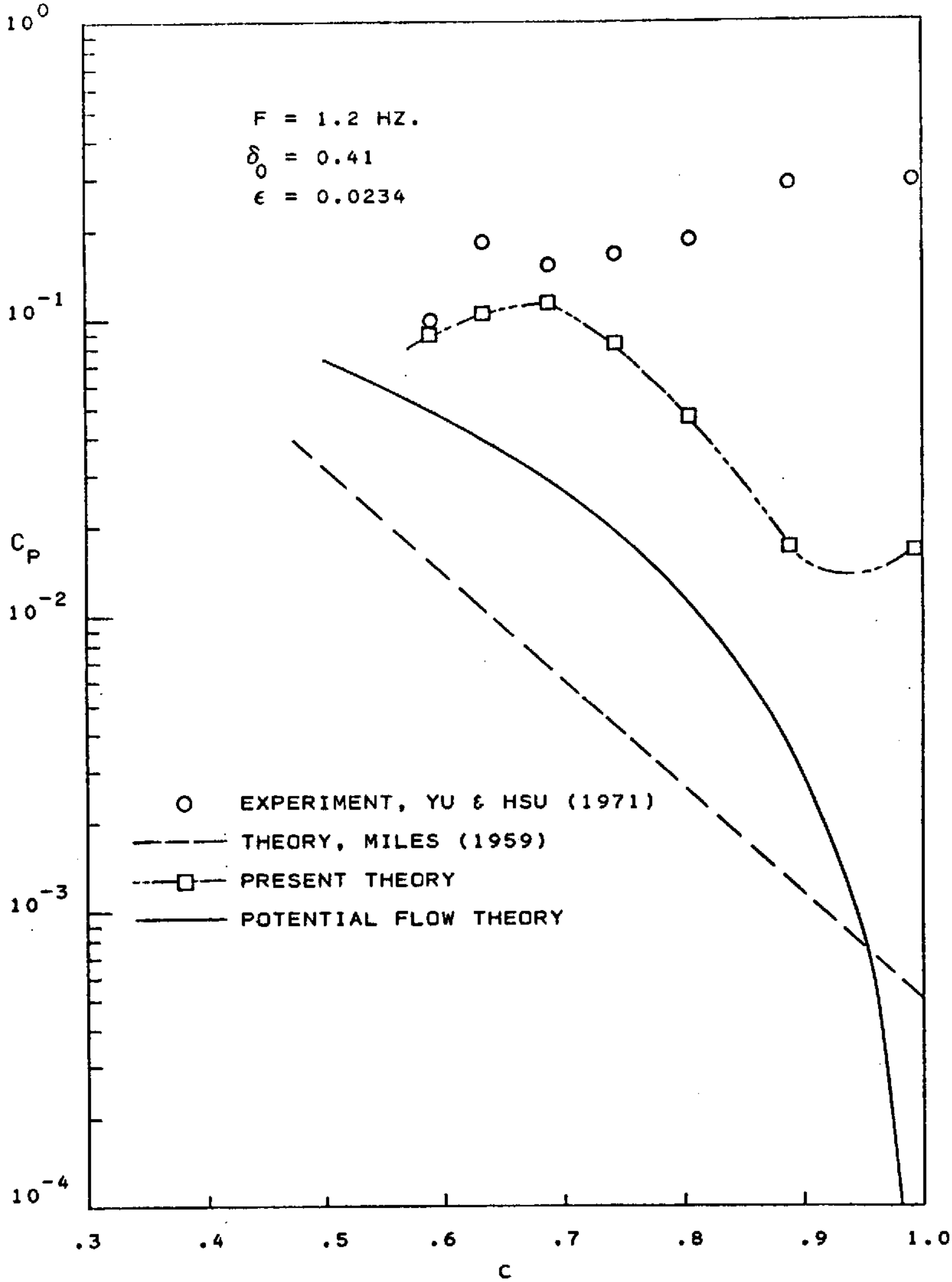

FIGURE 8.6
COMPARISON OF THEORETICAL AND EXPERIMENTAL WAVE-INDUCED PRESSURE MAGNITUDE VS. WAVE PHASE SPEED

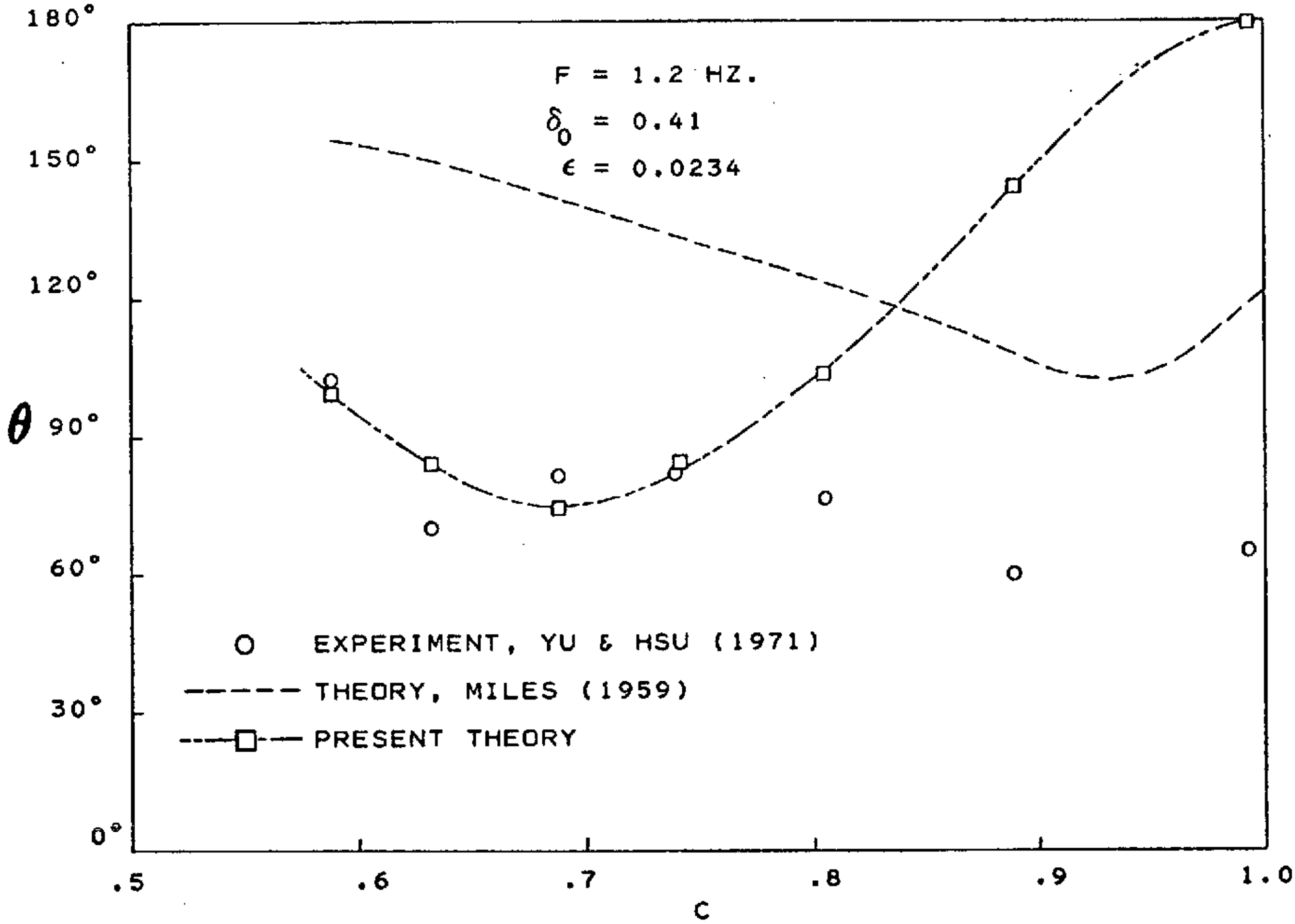

FIGURE 8.7
COMPARISON OF THEORETICAL AND EXPERIMENTAL WAVE-INDUCED PHASE SHIFT VS. WAVE PHASE SPEED

8.6 DISCUSSION

The comparisons presented in the previous sections are by no means exhaustive but they do indicate a rather fundamental failure of an inviscid shear flow theory to adequately model the turbulent flow over progressive water waves. Of academic interest at this point are the reasons for the differences between Miles' theory and the present theory. One aspect of Miles' results that is a little puzzling is the prediction of phase shift values approaching 90° for c near 0.90. This would imply large energy transfer from the wind to the water since $\theta = 90^{\circ}$ is the most efficient phase shift for maximum energy exchange. However, the predicted values of the wave growth parameter, β, for wave phase speeds in this range are rather small. The only obvious explanation for this behavior is the fact that Miles' theory predicts small values of pressure magnitude for $c \simeq 0.90$ which tends to explain the small predicted values of β. The behavior of the present theory on this account is more reasonable in that for $c \to 1$ the predicted phase shift tends to 180° and the wave growth parameter tends to zero.

We did not make comparisons of the present theory with other experimental studies, notably the data obtained by Kendall (1970) and Saeger and Reynolds (1971). The Kendall data is for relatively thick boundary layers, $\delta_0 \simeq 0.75$, and is inappropriate for comparison with the present theory. We might even question the comparison of the present theory with Yu and Hsu (1971) for the 1.2 Hz. waves since the boundary layer is relatively thick. Of more significance, however, is the nature of the moving surface boundary used in the various experiments. Yu and Hsu (1971) compare with the data obtained by Kendall and Saeger and with the earlier data obtained by Shemdin and Hsu (1967) and indicate that there are two distinct groups of data trends with regard to the phase-shift relation. The Kendall-Saeger data represents one group and the Shemdin-Yu data represents the other group. The difference appears to be caused by the differences in boundary conditions in that the former group have fixed walls as boundaries with progressive waves moving on them, while the latter have truly deformable boundaries. The solid wavy wall can only influence the fluid flow above it in a fixed manner, while the water surface can change form when acted upon by the wind. This deformation of the sea surface when the wind is blowing is a coupling process which modifies the structure of the turbulent Reynolds stress in the airstream and eventually results in a different momentum transfer rate to the water surface.

The large differences between the experiment and the inviscid theories for air pressures over moving water waves and the possible mechanism suggested here point to the inadequacy of an inviscid theory. Recall the order of magnitude analysis of Chapter 5 indicating that for the low-speed situation of the wind-water wave problem the turbulent Reynolds stress term in the first-order peturbation is significant and should not be neglected. The probable role of the Reynolds stress in the "coupling" process occurring at the air-sea boundary is important and must be considered in any successful attempt to model the real world. The recent attempts of Hussain and Reynolds (1972) and Davis (1972) to model the Reynolds stress terms are promising and this effort should be continued with guidance supplied by complementary experimental effort. Yu and Hsu are currently conducting an experimental investigation of the turbulent structure of the wind in their wind-water channel and have obtained some preliminary data which indicate that the magnitude of the wave-induced Reynolds stress, $-\rho\,\widetilde{u}\widetilde{v}$, is significantly larger than that predicted by the inviscid model.

IX. APPLICATION OF THE THEORY TO PANEL FLUTTER

9.1 INTRODUCTION

This chapter is the most exciting part of the present thesis in that it represents the realization of several years of effort on the title problem, the original goal of which was to try to ascertain the effect of the unsteady boundary layer on the stability of the motion of an oscillating panel. We have discovered in the earlier chapters that it is not a simple task to apply the theory to an elementary example in the hope of evaluating the soundness of the assumptions and obtaining solutions for the resulting equations. The results of the preceding chapter, an application to wind-driven water waves, are somewhat disappointing in the sense that the present theory does not agree with Miles' theory or with experiment. Hopefully the results discussed in the present chapter will lend some confidence to the present effort insofar as the goal of obtaining "useful" results as well as "interesting" results is concerned.

In the discussion to follow we apply the two-dimensional inviscid shear flow theory to the calculation of the generalized aerodynamic forces, the quantity of interest which is directly related to the aerodynamic pressure. We obtain results for a clamped, infinite-span panel at a low supersonic freestream Mach number for which the unsteady boundary-layer effect is quite significant, and we compare with similar results obtained by Dowell (1970). We discuss an approximate flutter analysis based on a one-mode Galerkin solution to the governing equation for the panel motion and compare flutter predictions with Dowell's (1971) theory and with the experiments of Muhlstein et al. (1968).

9.2 CALCULATION OF GENERALIZED AERODYNAMIC FORCES

For the application of the theory to panel flutter we have already stated (Section 7.5) that the quantities of interest are the generalized aerodynamic forces rather than the pressure itself. This will be elucidated when we discuss the equation of motion for an oscillating panel in Section 9.6. In the analysis that follows we assume that the panel in question is of infinite span; i.e., $b \to \infty$ for the theory developed in Chapter 7 and in Figure 7.1. The panel with infinite span is often referred to as a "two-dimensional plate-column", emphasizing the fact that the flow depends only upon two space variables and that the panel is actually a cylinder. We assume further that the panel is clamped at the two ends, $x = 0, 1$, so that the boundary conditions which the nondimensional panel deflection must satisfy are

$$z_s(x,t) = \partial z_s/\partial x = 0, \quad x = 0, 1 \tag{9.1}$$

With a little elaboration we can specialize the development of section 7.5 for a rectangular panel to the case of a plate-column. Assume that the nondimensional panel displacement may be represented as the sum over a finite set of N assumed modal functions

$$z_s(x,t) = \sum_{m=1}^{N} \epsilon_m \psi_m(x) e^{ikt} \tag{9.2}$$

where $\psi_m(x)$ is the mode shape for the m-th mode and where ϵ_m is the modal amplitude for the m-th mode. We have assumed that the motion is simple harmonic in time. Then the nondimensional generalized force, Q_{mn}, is defined as

$$Q_{mn}(t) = \int_0^1 p_m(x,t)\psi_n(x)dx \tag{9.3}$$

where p_m is the nondimensional pressure due to the m-th mode deflection

$$z_{s_m} = \epsilon_m \psi_m(x) e^{ikt} \tag{9.4}$$

We can represent the pressure as a linear operator, $\hat{p}$, operating on the deflection, z_{s_m}, since we are dealing with a linearized aerodynamic theory; thus

$$p_m = \hat{p}[\epsilon_m \psi_m e^{ikt}] \tag{9.5a}$$

$$= \epsilon_m \hat{p}[\psi_m(x);k,M_\infty,\delta_0]e^{ikt} \tag{9.5b}$$

This permits us to express the generalized force as

$$Q_{mn} = \epsilon_m H_{mn}(k;M_\infty,\delta_0)e^{ikt} \tag{9.6}$$

where

$$H_{mn}(k;M_\infty,\delta_0) = \int_0^1 \hat{p}[\psi_m(x);k,M_\infty,\delta_0]\psi_n(x)dx \tag{9.7}$$

Note that the function H_{mn} is actually the mechanical admittance (hence, the familiar symbol H) since it represents the ratio of the output amplitude to the input amplitude for sinusoidal motion. Assuming the output to be of the form

$$Q_{mn}(t) = \hat{Q}_{mn}(k)e^{ikt} \tag{9.8}$$

and substituting in (9.6), we have

$$H_{mn} = \hat{Q}_{mn}(k)/\epsilon_m \tag{9.9}$$

Rather than evaluating (9.7) directly using an expression for the pressure operator, $\hat{p}$, we achieve a considerable economy of effort by representing $\hat{p}_m$ as an inverse Fourier transform as follows:

$$\hat{p}_m = \frac{1}{2\pi} \int_{-\infty}^{\infty} \tilde{p}_m e^{i\alpha x} d\alpha \tag{9.10}$$

where $\tilde{p}_m(\alpha;k,M_\infty,\delta_0)$ is the Fourier transform of the surface pressure due to the m-th mode deflection. Substituting (9.10) in (9.7) and interchanging the order of integration we obtain

$$H_{mn} = \frac{1}{2\pi} \int_{-\infty}^{\infty} \tilde{p}_m \int_0^1 \psi_n(x)e^{i\alpha x}dxd\alpha \tag{9.11}$$

In analogy to (7.44) we can express $\tilde{p}_m$ as

$$\tilde{p}_m = \tilde{K}(\alpha; k, M_\infty, \delta_0)\tilde{\psi}_m(\alpha) \tag{9.12}$$

where $\tilde{K}$ is the Fourier transform of the pressure kernel and where $\tilde{\psi}_m(\alpha)$ is the Fourier transform of the m-th mode shape given by

$$\tilde{\psi}_m(\alpha) = \int_{-\infty}^{\infty} \psi_m(x)e^{-i\alpha x}dx \tag{9.13}$$

where

$$\psi_m(x) = 0, \quad \begin{cases} x \le 1 \\ x \ge 1 \end{cases} \tag{9.14}$$

This latter statement indicates that the panel deflection is zero everywhere except between $x = 0$ and 1. Substituting (9.12) through (9.14) in (9.11) we obtain

$$H_{mn} = \frac{1}{2\pi}\int_{-\infty}^{\infty} \tilde{K}(\alpha; k, M_\infty, \delta_0)G_{mn}(\alpha)d\alpha \tag{9.15}$$

where

$$G_{mn}(\alpha) = \int_0^1 \psi_m(x)e^{-i\alpha x}dx \int_0^1 \psi_n(x)e^{i\alpha x}dx \tag{9.15}$$

We obtain an expression for the kernel, $\tilde{K}$, by noting that

$$\tilde{K} = \tilde{p}(\alpha;0)/\tilde{z}_s(\alpha) \tag{9.17}$$

where $\tilde{p}$ is the Fourier transform of the surface pressure for two-dimensional flow developed in Chapter 6 [see (6.52) and (6.53)]; thus, for our first-order theory we have

$$\tilde{K}(\alpha; k, M_\infty, \delta_0) = \tilde{K}_0(\alpha; k, M_\infty) + \delta_0\tilde{K}_{BL}(\alpha; k, M_\infty) \tag{9.18}$$

where

$$\widetilde{K}_0 = -\frac{-(k+\alpha)^2}{iB(\alpha-\gamma_1)^{1/2}(\alpha-\gamma_2)^{1/2}} \tag{9.19}$$

$$\widetilde{K}_{BL} = \widetilde{K}_1 + \widetilde{K}_2 \tag{9.20}$$

where

$$\widetilde{K}_1 = -\int_0^1 \rho(k+\alpha U)^2 dz^* \tag{9.21}$$

$$\widetilde{K}_2 = (k+\alpha)^4 \frac{[-\alpha^2 \int_0^1 \rho^{-1}(k+\alpha U)^{-2} dz^* + M_\infty^2]}{B^2(\alpha-\gamma_1)(\alpha-\gamma_2)} \tag{9.22}$$

and where

$$B = (M_\infty^2 - 1)^{1/2} \tag{9.23}$$

$$\gamma_1 = -kM_\infty/(M_\infty - 1) \tag{9.24}$$

$$\gamma_2 = -kM_\infty/(M_\infty + 1) \tag{9.25}$$

$$\rho = [1 + (\gamma-1)/2\ M_\infty^2(1-U^2)]^{-1} \tag{9.26}$$

Having determined a means of obtaining the generalized forces using the present theory, we proceed to evaluate the expressions analytically. Note that the linear representation in (9.18) implies that the generalized forces are of the form

$$H_{mn} = H_{mn_0} + H_{mn_{BL}} \tag{9.27}$$

where

$$H_{mn_0} = \frac{1}{2\pi} \int_{-\infty}^{\infty} \widetilde{K}_0 G_{mn} d\alpha \tag{9.28}$$

$$H_{mn_{BL}} = \delta_0 \frac{1}{2\pi} \int_{-\infty}^{\infty} \widetilde{K}_{BL} G_{mn} d\alpha \tag{9.29}$$

The first term is the inviscid force given by the linearized potential flow theory, while the second term represents the first-order correction due to the boundary layer. In evaluating the inviscid term using (9.28) care must be taken in treating the singularities of $\widetilde{K}_0$. Examination of (9.19) reveals that the function $\widetilde{K}_0$ has branch points at γ_1 and γ_2 in the complex γ-plane. This integral is not easily evaluated analytically. Rather than evaluating the integral (9.28) numerically, one can obtain the inviscid term using (9.7); thus,

$$H_{mn_0} = \int_0^1 \hat{p}_0[\psi_m;k,M_\infty]\psi_n(x)dx \tag{9.30}$$

with the expression for the potential flow pressure given in (6.55); namely,

$$\hat{p}_0 = 1/B \int_0^x K_0(x-x_1;k,M_\infty)(ik + d/dx_1)^2 \psi_m(x_1)dx_1 \tag{9.31}$$

where

$$K_0(x;k,M_\infty) = e^{-ikM_\infty^2 x/B} J_0(kM_\infty x/B^2) \tag{9.32}$$

The double integral in (9.30) can be evaluated numerically.

We obtain the boundary-layer contribution to the generalized force by evaluating (9.29) analytically. The details of these developments are presented in Appendix F with discussion of the application of the residue theorem and the special treatment which allows inclusion of the contributions of the apparent singularities of the function $G_{mn}(\alpha)$. We carry out the evaluation using mode functions satisfying the end conditions (9.1); namely,

$$\psi_m(x) = \cos[(m-1)\pi x] - \cos[(m+1)\pi x] \tag{9.33}$$

We obtain detailed expressions only for the case $m = n = 1$, corresponding to work done on the first mode due to first mode deformation, since our main objective is the comparison with similar results obtained by Dowell (1970) for sinusoidal motion. The derivation for this case is explicit enough to allow one to calculate H_{mn} for other combinations of m and n, although the task is rather tedious. We do not reproduce here any of the detailed equations associated with the derivations as they are complicated (see Appendix F); rather, we have indicated some of the general features and we now proceed to a discussion of the numerical results.

For the actual calculations we evaluate the real and imaginary parts of the admittance function H_{11} according to the linear superposition of (9.27). Thus,

$$H_{11} = H_{11}^R + iH_{11}^I \tag{9.34}$$

where

$$H_{11}^R = H_{11_0}^R + H_{11_{BL}}^R \tag{9.35}$$

and

$$H_{11}^I = H_{11_0}^I + H_{11_{BL}}^I \tag{9.36}$$

We use (9.30) for the inviscid contributions. As discussed previously we compute the inviscid terms numerically using the theoretical expression for the supersonic potential flow pressure given in (9.31) and (9.32). In this calculation we use a Gaussian integration subroutine to evaluate the pressure, and we use an adaptive Simpson subroutine for the integration over the panel chord in (9.30). The mode function for this case is obtained from (9.33) for $m = 1$ and is given by

$$\psi_1(x) = 1 - \cos(2\pi x) \tag{9.37}$$

We must also specify values for the parameters M_∞ and γ. We choose $M_\infty =$ 1.20 to correspond to the case of low supersonic flow where the effect of the boundary layer on panel flutter stability is most pronounced, and we take $\gamma = 1.40$ assuming the air to be a diatomic gas. These values correspond to the case treated by Dowell and allow us to compare directly with his results.

The boundary-layer perturbations are obtained by the analytical evaluation of the integral in (9.29) as discussed in Appendix F. Note that the function $\tilde{K}_{BL}$ depends upon $U(z^*)$ and requires an additional integration with respect to z^*. For the purposes of comparison with Dowell we choose the 1/7 power law mean velocity profile

$$U = (z^*)^{1/7} \tag{9.38}$$

representative of the turbulent flow over the undisturbed surface. Measurements of the mean velocity profile by Muhlstein et al. (1968) for $M_\infty = 1.20$ indicate that the 1/7 power profile is a reasonable representation of the observed profile. The integration with respect to z^* over the boundary layer is simplified by changing variables

$$dz^* = z^{*\prime}\, dU \tag{9.39}$$

Solving (9.38) for z^* and taking the derivative we have

$$z^{*\prime} = 7U^6 \tag{9.40}$$

The integration in (9.21) is accomplished analytically; however, the analytical integration of (9.22) causes some difficulty. As explained in Appendix F this could be accomplished using the method of partial fractions. In fact an attempt was made using an algebra routine on a PDP 1011 Computer, and we soon discovered that the task, though not hopeless, was certainly not worth the effort that would be required in the resulting algebraic accounting process. We realized this as soon as the core capacity of the computer was exceeded in the course of attempting to determine the constants in the partial fraction expansions. We decided that a numerical integration for this calculation would be more efficient, and we proceeded to compute the desired integrals making another change of variables

$$U = 1/t \tag{9.41}$$

and integrating (9.22) from $t = 1$ to $t = \infty$ (actually $t = N$ where N is a number sufficiently large so that the contribution to the value of the integral for $t = N$ to $t = \infty$ is negligible). We used an adaptive Simpson routine for this integration with an initial choice of $N = 25$ and accuracy (relative error) equal to 10^{-3}. To test the accuracy of the numerical integration we made some calculations with $N = 100$ and accuracy $= 10^{-4}$ and observed no significant changes. The results for the two calculations were identical up to the first 5 digits.

The results are presented in Figures 9.1 and 9.2 in which the real and imaginary components of the mechanical admittance, H_{11} (generalized force $\hat{Q}_{11}$ for unit modal amplitude in the first mode) are presented as a function of reduced frequency, k, for three values of boundary-layer thickness, $\delta_0 = 0$, .05, and 0.10. The range of these parameters was chosen in order to compare with Dowell's results (Section 9.3). The effect of the boundary layer is rather significant at this Mach number. It is well known that for the inviscid theory at low supersonic Mach number the flutter is of a single-degree-of-freedom type due to negative aerodynamic damping in the first mode. The boundary-layer effect on this behavior is most readily observed by considering the imaginary component of H_{11} in Figure 9.2. For the inviscid case H^I_{11} is negative for a range of $k = 0 \rightarrow .745$ indicating negative aerodynamic damping for that range of k. For the viscous case with $\delta_0 = .05$ the range of k for which negative aerodynamic damping can occur is reduced by about 32% and for $\delta_0 = .10$ the range of k is reduced by about 46% of the inviscid case. We will compare this feature of the present results with Dowell in the following section. An important consequence of this reduction in the range of reduced frequency over which negative damping can occur is the stabilizing effect of the boundary layer on panel flutter. This will be verified in our analysis of panel flutter and comparison with experiment in later sections.

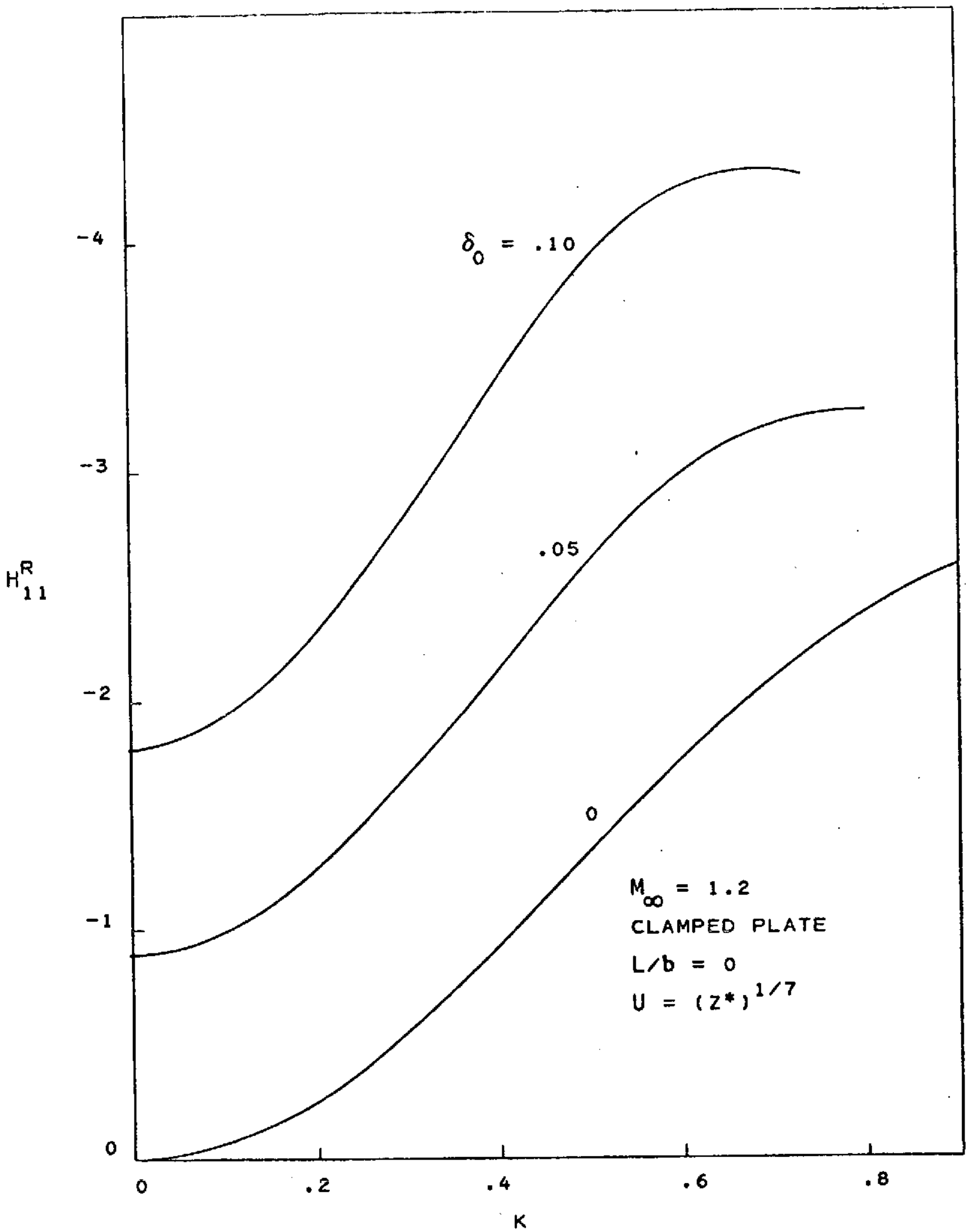

FIGURE 9.1
REAL COMPONENT OF MECHANICAL ADMITTANCE VS. REDUCED FREQUENCY

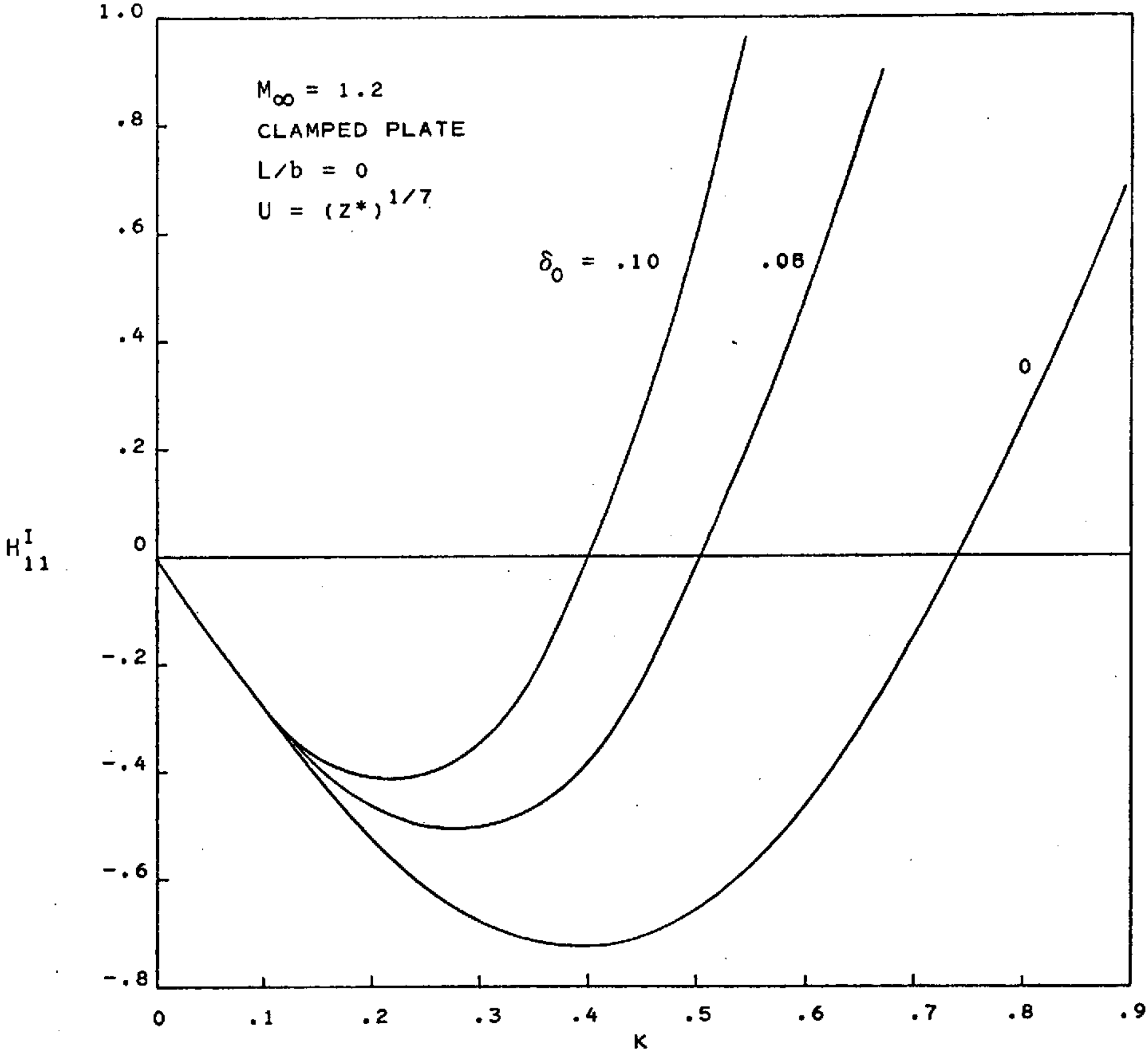

FIGURE 9.2
IMAGINARY COMPONENT OF MECHANICAL ADMITTANCE VS. REDUCED FREQUENCY

9.3 COMPARISON WITH DOWELL'S THEORY

We can compare the results of the previous section with the recent work of Dowell (1970, 1971). Dowell formulates the problem starting with the three dimensional equations for nonlinear, inviscid flow [see, for example, (7.3) through (7.8)]. He assumes that the flow quantities can be represented as the sum of a mean flow quantity and a perturbation quantity; for example the x-component of velocity is

$$u = U(z) + \hat{u}(x,y,z,t) \tag{9.42}$$

Substituting the assumed form of the flow quantities in the governing equations and linearizing in the perturbed quantities, he obtains a set of perturbation equations which he eventually reduces to a single (nondimensional) equation for the perturbation pressure

$$\frac{M_\infty^2}{T} D^3\hat{p} - D\nabla^2\hat{p} + 2\frac{\partial^2\hat{p}}{\partial x\partial z}\frac{dU}{dz} - D\frac{\partial\hat{p}}{\partial z}\frac{1}{T}\frac{dT}{dz} = 0 \tag{9.43}$$

where the mean flow velocity, U, and temperature, T, are related as in (6.10) and where

$$\begin{aligned} D &= \partial/\partial t + U\,\partial/\partial x \\ \nabla^2 &= \partial^2/\partial x^2 + \partial/\partial z^2 + (L/b)^2\,\partial^2/\partial y^2 \end{aligned} \tag{9.44}$$

He specifies a wall boundary condition (linearized)

$$\hat{w} = D\hat{z}_s \tag{9.45}$$

on $z = \hat{z}_s(x,y,t)$ which he uses along with the linearized and nondimensional form of (7.6) to obtain a wall boundary condition for the pressure

$$\partial\hat{p}/\partial z = D^2\hat{z}_s \tag{9.46}$$

on $z = \hat{z}_s(x,y,t)$.

Note that Dowell's formulation differs somewhat from the present theory in that Dowell does not specialize to simple harmonic motion as we have done in (7.9). Also he does not assume thin (in panel chord lengths) boundary layers. His basic solution procedure is to employ Fourier transformation in x and y, numerical integration in z and t, and numerical integration to invert the Fourier transforms. In obtaining the generalized forces he achieves some economy of effort by performing the integrals over x and y in his counterpart to (7.41) before inverting the transform in his counterpart to (7.39).

Another difference between the two formulations is the manner in which Dowell applies the linearized wall boundary condition on the instantaneous plate surface, $z = z_s(x, y, t)$, rather than on the fixed reference surface, $z_s = 0$. He emphasizes that this is the most important approximation in the analysis and claims that application of the boundary condition on $\hat{z}_s = 0$ is physically unacceptable for the present problem because it grossly overestimates the stabilizing effect of the boundary layer. He explains this by noting that the mean velocity at $\hat{z}_s = 0$ is zero, and stating that in such a case the fluid loading appears to be of the virtual mass type and thus provides no mechanism of instability. In comparing with Dowell's results we should try to ascertain whether his conjecture about the relationship between $\hat{z}_s$ and stability is correct. We should also point out that application of the boundary condition exactly on the instantaneous plate surface $z_s(x, y, t)$ is difficult since the plate motion is, as yet, undetermined. Dowell uses an approximate scheme to circumvent this difficulty by obtaining from a nonlinear flutter analysis a compatibility condition for which only a single value of plate deflection corresponding to a single value of dynamic pressure will be compatible with his assumed $\hat{z}_s$. There is still some ambiguity in this scheme since $\hat{z}_s$ varies continuously with space and time. To circumvent this difficulty Dowell arbitrarily chooses to equate $\hat{z}_s$ to the maximum center plate deflection since the results are not very sensitive to the precise deflection chosen. With the salient features of Dowell's method summarized here, we now turn to a comparison of results for the generalized aerodynamic forces.

Dowell (1970, 1971) presents results for the generalized forces Q_{11} and Q_{12} for a unit step function (in time) in the first mode. We cannot compare directly with these results since the present theory yields the response to simple harmonic motion (the mechanical admittance) rather than the response to a step function (indicial admittance). Fortunately there is a connection between the mechanical and indicial admittances which is especially useful when the sinusoidal behavior of the system is readily available. This is pointed out in the book by Bisplinghoff and Ashley (1962) where it is shown that the indicial admittance must be

$$A_{mn}(t) = \frac{1}{2\pi} \int_{-\infty}^{\infty} \frac{H_{mn}(k)e^{ikt}}{ik} dk \tag{9.47}$$

where convergence is ensured by requiring the integration path to make a small semicircular loop below the origin. The formula in (9.47) provides a means of converting the results in Section 9.2 to a form suitable for comparison with Dowell; however, the indicated integration is rather tedious, though it can be obtained analytically. Fortunately it is not necessary to pursue this for the purpose of comparison, as Dowell (1970) presents some results for sinusoidal motion in the first mode.

In his Figure 6 [see Figure 9.5] Dowell presents results for the imaginary component of $\hat{Q}_{11}$ for unit modal amplitude vs. the reduced frequency, k, analagous to Figure 9.2 of the present work. The only significant difference in the conditions assumed is that Dowell chooses $\hat{z}_s = .01$, while the present results are for $\hat{z}_s = 0$ ($\hat{z}_s$, the point of application of the surface boundary condition). We compare with Dowell in Figure 9.3 for $\delta_0 = .05$ and Figure 9.4 for $\delta_0 = .10$. Note that for the thinner boundary layer the two theories are in reasonable agreement, while for the thicker boundary layer there is considerable difference between the two results. From Figure 9.3 we infer that Dowell's theory predicts that the boundary-layer effect is slightly more stabilizing (less negative aerodynamic damping) than does the present theory for k less than about 0.4,

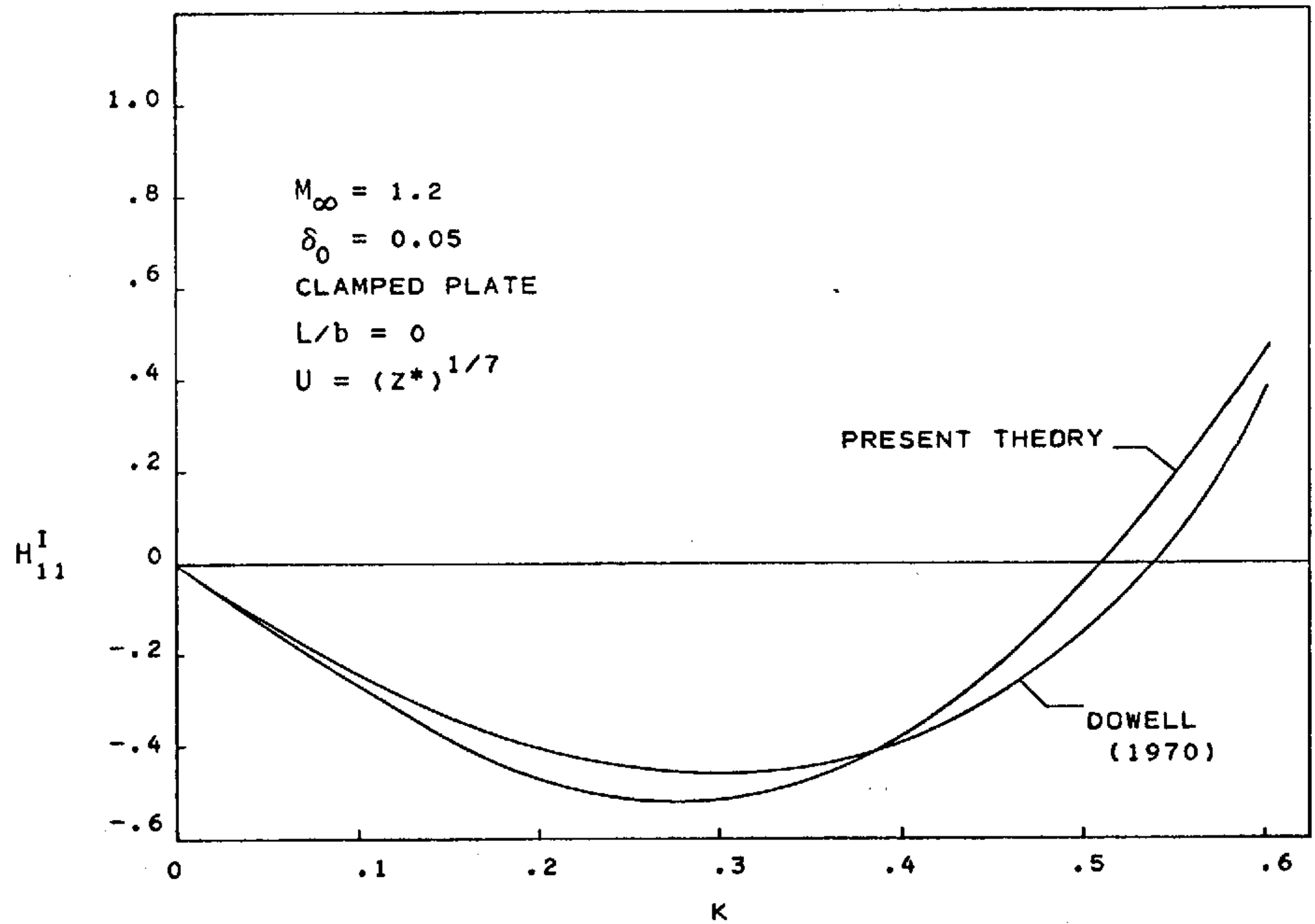

FIGURE 9.3
COMPARISON OF THEORETICAL IMAGINARY COMPONENTS OF MECHANICAL ADMITTANCE VS. REDUCED FREQUENCY FOR δ_0 = .05

while the opposite is true for larger values of k. The net result is that Dowell shows a slightly larger range of k for which negative aerodynamic damping occurs (about 6% larger than the present range of about .51). From these observations one might tentatively conclude that Dowell's theory predicts a slightly greater stabilizing influence of the boundary layer than the present theory would indicate for this particular case of a thin boundary layer.

This conclusion tends to be confirmed for the case of the thicker boundary layer in Figure 9.4. For this case there appears to be a fundamental difference in the two results. Dowell's theory predicts no negative aerodynamic damping for the range of reduced frequency of interest. His theory predicts a stronger effect of the boundary layer on Q_{11} (which is known to govern the single-degree-of-freedom flutter at low supersonic Mach number). In fact, it appears that his theory predicts that the system is no longer a single-degree-of-freedom system in that the range of k for which negative aerodynamic damping can occur has been virtually eliminated. The present theory predicts a range of $k = 0 \rightarrow .405$ for which $\hat{Q}_{11}$ is negative. Note that the present theory predicts larger (positive) values of $\hat{Q}_{11}$ than Dowell for k greater than about 0.5. This same phenomenon was observed in Figure 9.3 and may indicate that the present theory predicts a more stabilizing effect of the boundary layer than Dowell's theory for larger values of reduced frequency.

One possible explanation for the large differences in the two theories for the thicker boundary layer is the fact that the present theory is only correct to first-order in δ_0, while Dowell's theory is exact in that parameter. The condition, (6.63), establishing a relationship between values of the parameters for which the first-order theory is applicable at small values of reduced frequency is not easily applied to the present calculations because of the fact that the velocity gradient $U'(0)$ is infinite for the 1/7 power law profile. However, it cautions us to be careful in applying the theory for small values of k and indicates that for a given (small) value of k and for a given velocity profile, the small perturbation hypothesis might be violated if δ_0 becomes too large. It is not clear from these considerations, however, why we should observe such

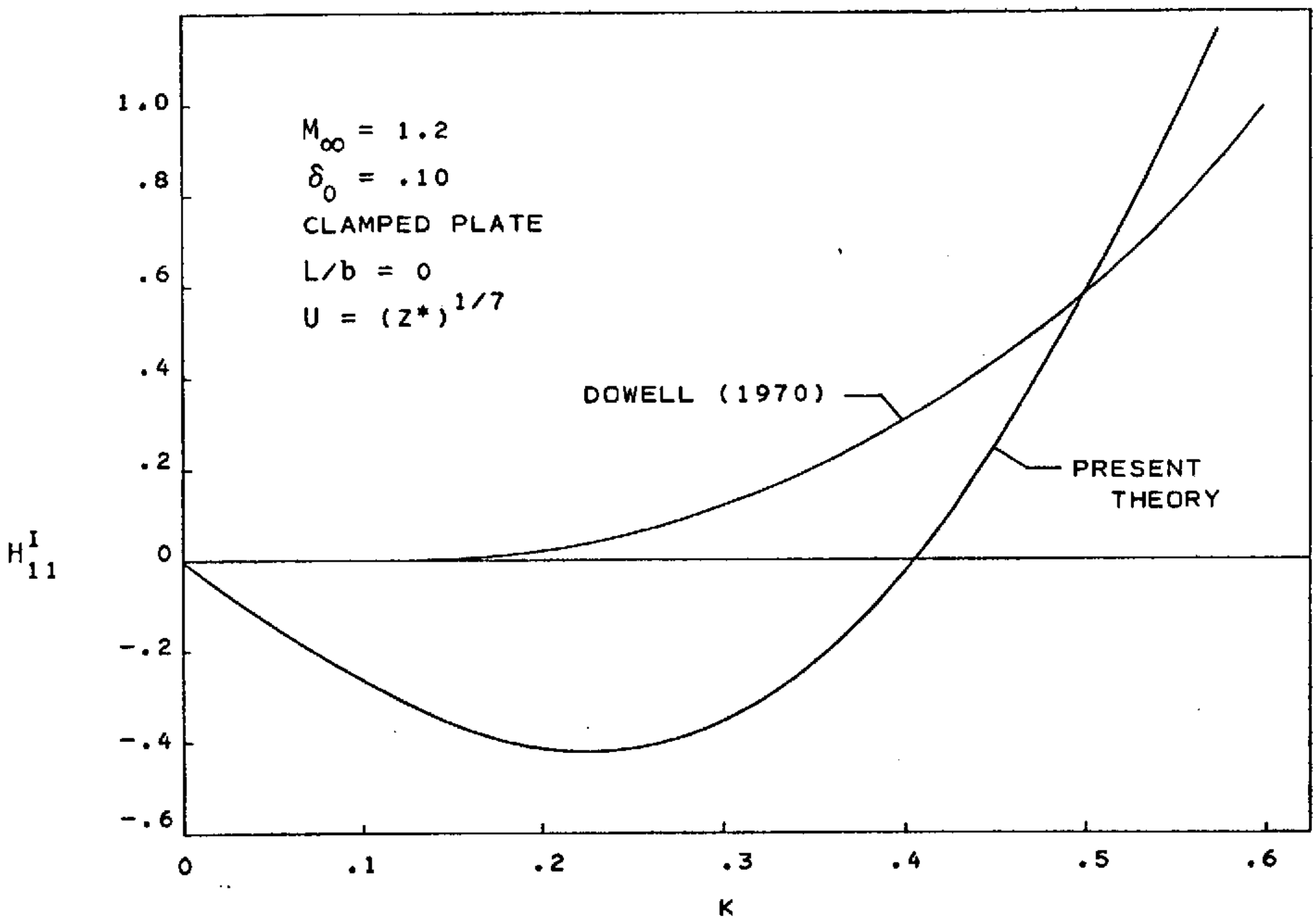

FIGURE 9.4
COMPARISON OF THEORETICAL IMAGINARY COMPONENTS OF MECHANICAL ADMITTANCE VS. REDUCED FREQUENCY FOR δ_0 = .10

drastic changes in the character of $\hat{Q}_{11}$ for Dowell's theory as δ_0 is doubled in value from .05 to .10. Furthermore, these observations tend to contradict Dowell's supposition that applying the surface boundary condition at $\hat{z}_s = 0$ tends to overestimate the stabilizing influence of the boundary layer.

It is interesting to compare the imaginary part of the boundary-layer contributions to the generalized forces, $H^I_{11_{BL}}(k)$, for the two theories. The results for Dowell's theory are obtained from his Figure 6 (1970) [see Figure 9.5] by subtracting the inviscid value (the graph for $\delta_0 = 0$) from the value for a given boundary layer thickness; that is

$$H^I_{11_{BL}}(k;\delta_0) = H^I_{11}(k;\delta_0) - H^I_{11_0}(k) \tag{9.48}$$

In the course of making these comparisons we discovered a small difference between Dowell's curve for $\delta_0 = 0$ and the present results for $\delta_0 = 0$. Recall that the latter results were generated using (9.30) through (9.32) and are presented in Figure 9.2. This discrepancy in $H^I_{11_0}(k)$ can most likely be attributed to a plotting error in preparation of Dowell's Figure 6 rather than to an error in the present inviscid numerical results.

To convince ourselves of this supposition we first attempted to obtain the numbers that were used to generate Dowell's Figure 6. These were not readily available, although we were able to obtain a copy of his original graph. This is reproduced here as Figure 9.5 and is about 1.7 times larger than the figure in his 1970 report. Careful examination of this figure and comparison with the present results in Figure 9.2 for the inviscid case reveals a small error which appears to grow with increasing k. To reassure ourselves that there were no major errors associated with our numerical calculations for the inviscid case we persuaded Mr. P. A. Gaspers of the NASA Ames Research Center's Nonsteady Phenomena Branch to run an independent check on our inviscid results. Gaspers had developed a numerical procedure to calculate generalized forces for simply supported plates for various inviscid aerodynamic theories [see Gaspers (1970)]. Without too much difficulty he was able to obtain results for the clamped plate with which to compare.

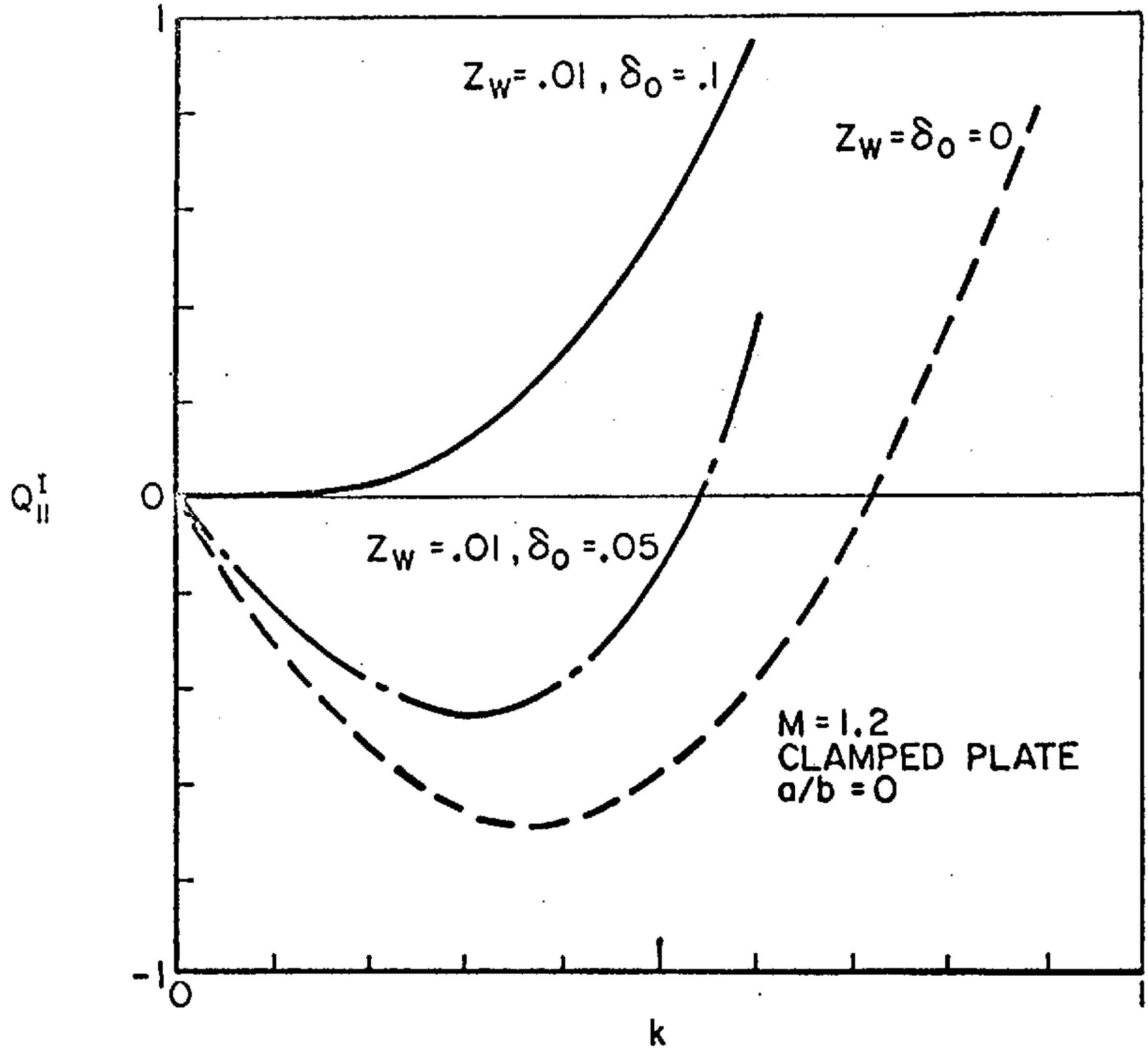

FIGURE 9.5
IMAGINARY COMPONENT OF MECHANICAL ADMITTANCE VS. REDUCED FREQUENCY - FIGURE 6 FROM DOWELL (1970)

His results are obtained using as mode functions the eigenfunctions for the free vibration of a beam clamped at both ends rather than using the mode functions of (9.33). To compare our inviscid procedure with Gaspers' calculations we made some additional calculations using the beam eigenfunctions and found exact agreement for these two independent sets of results for the four significant figures of Gaspers' output. This exercise convinced us that any differences in our inviscid results and Dowell's results were most likely due to a plotting error in preparing his graphs. Dowell (private communication) assures us that his inviscid scheme for indicial aerodynamics gives correct results since it compares favorably with piston theory for $t = 0^+$ and with the Ackeret theory for $t \to M_\infty/(M_\infty-1)$. The error is not significant enough to alter any of our conclusions, so we will not belabor the point any further.

Returning to our discussion of the comparison of the boundary-layer contribution to the generalized forces, we present these results in Figures 9.6 and 9.7. Figure 9.6 compares with Dowell for $\delta_0 = .05$ while Figure 9.7 is for $\delta_0 = .10$. The most interesting feature of these two figures is the behavior of $H^I_{11_{BL}}$ for small values of reduced frequency, k. Comparing the two theories for small values of k we find that Dowell's theory varies approximately linearly with k while the present theory varies more rapidly with k for small k. In fact we can verify that the present theory predicts $H^I_{11_{BL}} \sim k^3$ for small k. This is an interesting result and is indicative of a fundamental difference between the two theories. We discuss this further in Section 9.4.

To complete these comparisons with Dowell's theory we present in Figure 9.8 a plot of the imaginary component of the boundary layer contribution to the mechanical admittance vs. the boundary layer thickness parameter for $k = 0.5$. The present analytical theory, being first-order in δ_0, yields a linear relationship, while Dowell's numerical theory includes the higher order terms in δ_0 and indicates a nonlinear variation of the force with increasing δ_0. Comparing the two graphs near $\delta_0 = 0$ we note that the slopes of the curves are unequal. The slope of the present theory is about 50% larger than the slope

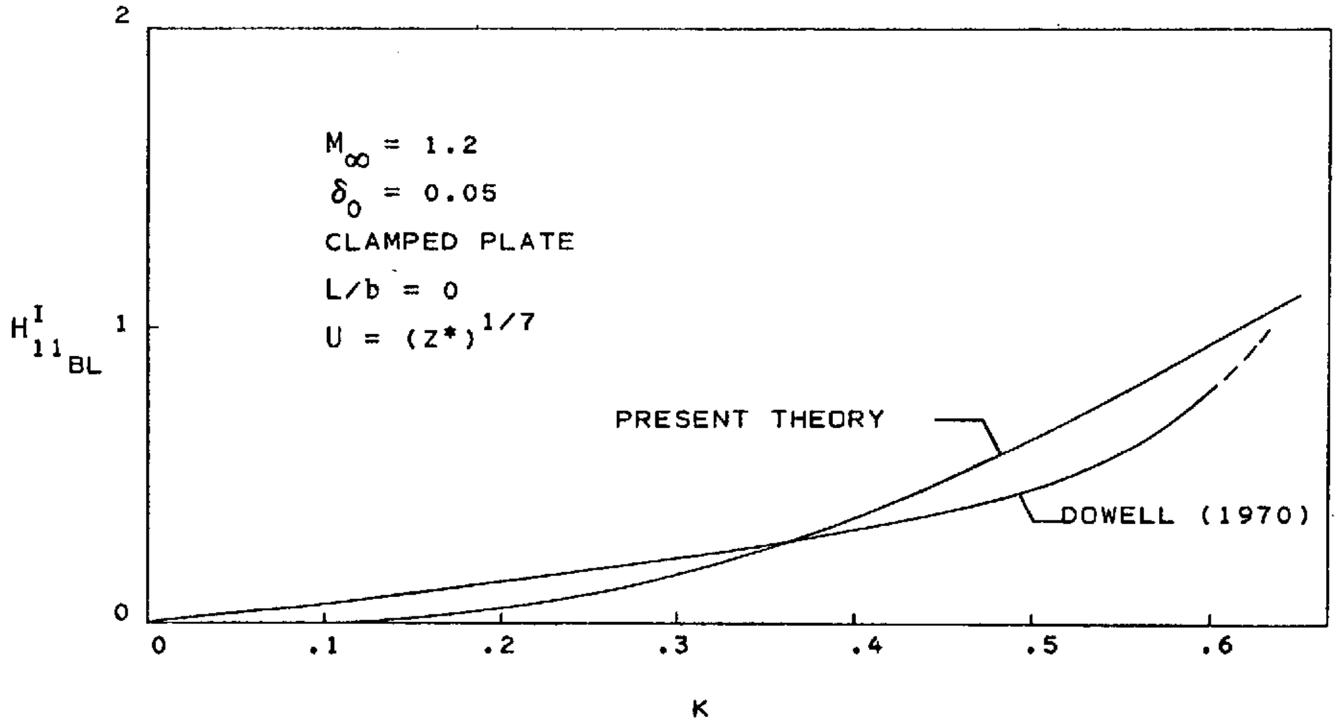

FIGURE 9.6
COMPARISON OF THEORETICAL IMAGINARY COMPONENTS OF THE BOUNDARY-LAYER CONTRIBUTION TO THE MECHANICAL ADMITTANCE VS. REDUCED FREQUENCY FOR δ_0 = .05

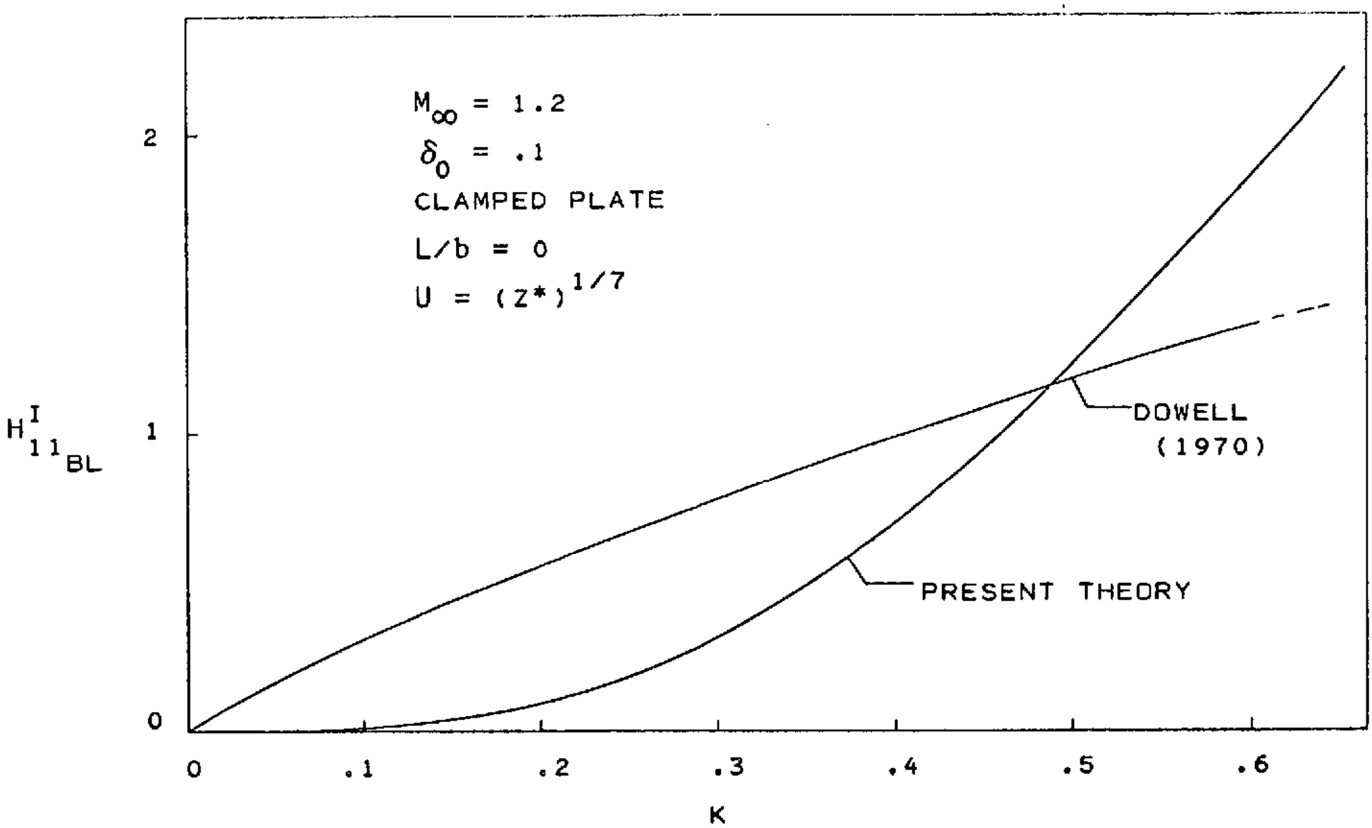

FIGURE 9.7
COMPARISON OF THEORETICAL IMAGINARY COMPONENTS OF THE BOUNDARY-LAYER CONTRIBUTION TO THE MECHANICAL ADMITTANCE VS. REDUCED FREQUENCY FOR δ_0 = .10

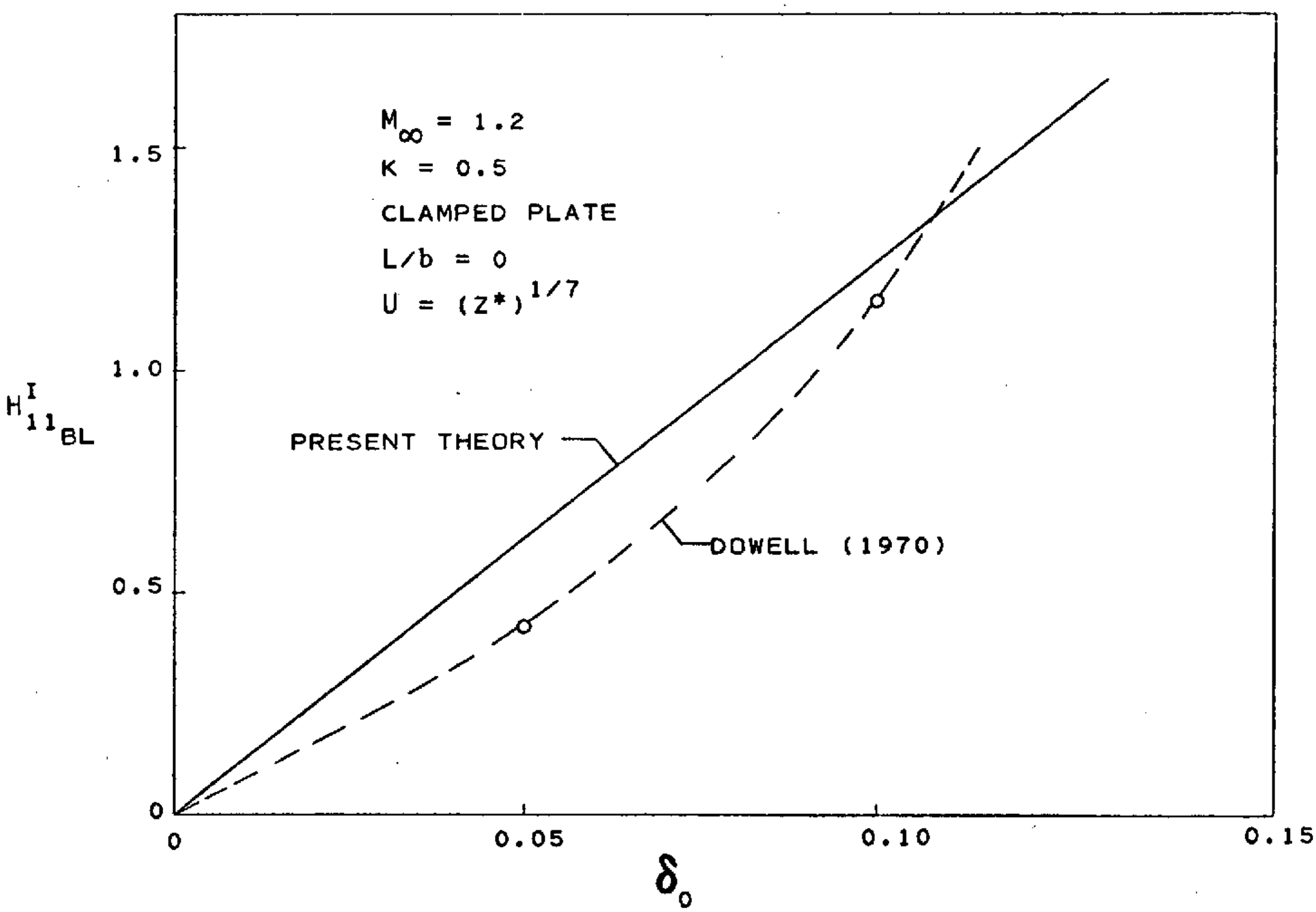

FIGURE 9.8
COMPARISON OF THEORETICAL IMAGINARY COMPONENTS OF THE BOUNDARY-LAYER CONTRIBUTION TO THE MECHANICAL ADMITTANCE VS. BOUNDARY-LAYER THICKNESS FOR K = 0.5

of Dowell's theory at $\delta_0 = 0$. This observation is rather striking, for it implies that the two theories are not equivalent for very thin boundary layers. If the two theories were equivalent for thin boundary layers, we would expect the two curves to agree near $\delta_0 = 0$ and, furthermore, we would expect the error or difference between the two curves to grow with increasing δ_0. Such is not the case, however, as the two curves are not coincident for δ_0 near zero and the error does not continue to grow with increasing δ_0 for δ_0 larger than about .05. We observe, instead, an overlap behavior in which the two curves cross each other at a value of δ_0 equal to about 0.11. This seems to indicate another fundamental difference between the two theories.

9.4 THE LIMITING CASE OF SMALL REDUCED FREQUENCY

In the previous section we observed some interesting behavior of the imaginary component of the boundary-layer contribution to the generalized force for small values of reduced frequency, k. In comparing with Dowell in Figures 9.6 and 9.7 we found that the present theory appears to predict a different variation of $H^I_{11_{BL}}$ with k near zero than Dowell's theory. In this section we examine this behavior in greater detail and attempt to draw some conclusions regarding the applicability of the present theory to this limiting case.

First let us consider the case of inviscid flow at low frequency. For this case we can readily obtain an expression for the pressure or the generalized force in the limit as $k \to 0$. To obtain an expression for the pressure we use (9.17) in conjunction with (9.19), (9.24), and (9.25). Expanding the expression in (9.19) for small values of k we obtain

$$\tilde{p}_0(\alpha;k) = \left[\frac{i\alpha}{B} - \frac{ik}{B}\left(\frac{M_\infty^2}{B^2} - 2\right) + \ldots\right] \tilde{z}_s(\alpha) \qquad (9.49)$$

Inverting the Fourier transform we obtain

$$\hat{p}_0(x;k) = \frac{1}{B}\hat{z}'_s(x) - \frac{ik}{B}\left(\frac{M_\infty^2}{B^2} - 2\right) \hat{z}_s(x) + \ldots \qquad (9.50)$$

Note that the latter result could have been obtained by expanding the exponential and Bessel functions in (9.32) for small values of the arguments, substituting in (9.31), and integrating subject to the boundary condition (9.1). The first term in (9.50) is the familiar Ackeret formula for thin airfoil theory [see Section 5.4 of Ashley and Landahl (1965)], while the second term represents the unsteady perturbation for small reduced frequency which is linear in k according to the potential flow theory.

We can convert the previous result to an expression for the generalized force, $H_{11_0}(k)$, by substituting $\psi_1(x)$ for $\hat{z}_s$ in the above, substituting (9.50) and (9.37) in (9.30), and performing the indicated integration subject to (9.14) to obtain a complex expression of the form (9.34) where

$$H^R_{11_0}(k) = 0 + . . . \tag{9.51}$$

$$H^I_{11_0}(k) = k\, H^I_{11_0}{}'(0) + . . . \tag{9.52}$$

where

$$H^I_{11_0}{}'(0) = -\frac{3}{2B}\left(\frac{M_\infty^2}{B^2} - 2\right)$$

Note that this latter result could also have been obtained by evaluating the integral in (9.28) using (9.17), (9.49), (F-38), and (F-39). In summary we conclude that for the inviscid theory we expect that the imaginary component of the generalized force will be linear in k for small values of k. Compare this with what we have observed about the behavior of the boundary layer perturbations to the generalized force as mentioned in the previous section. We enlarge upon this in the discussion that follows.

Turning now to the boundary-layer contributions we can examine the low frequency regime in more detail by making some additional numerical calculations at small values of k using the expressions developed in Appendix F. In Figures 9.9 and 9.10 we show the results for the real and imaginary components of the boundary-layer contribution to the mechanical admittance, $H^R_{11_{BL}}$ and $H^I_{11_{BL}}$, vs. reduced frequency, k, for k = 0 to .07. The curve in Figure 9.9 appears to be of the form

$$H^R_{11_{BL}}(k) = H^R_{11_{BL}}(0) + \frac{1}{2}k^2 H^R_{11_{BL}}{}''(0) + \ldots \tag{9.53}$$

The curve has been extrapolated to $k = 0$ as it was not possible to compute the value at $k = 0$ without modifying the program. We were able, however, to verify this result analytically. The results in Figure 9.10 are more interesting in that we are able to compare with Dowell (1970) for the imaginary component. Dowell's results appear to be approximately linear in k; that is

$$[H^I_{11_{BL}}(k)]_{DOWELL} \simeq k[H^I_{11_{BL}}{}'(0)]_{DOWELL} \tag{9.54}$$

while the present theory is precisely of the form

$$H^I_{11_{BL}}(k) = \frac{1}{6}k^3 H^I_{11_{BL}}{}'''(0) + \ldots \tag{9.55}$$

This latter result has been verified both numerically and analytically as with (9.53). We do not reproduce the algebraic manipulations that must be performed to obtain the expressions summarized by (9.53) and (9.54). We simply note here that one can obtain these results by specializing the expressions in Appendix F to the case of small reduced frequency. This is accomplished by expanding the expressions for the mechanical admittance in powers of k for small values of k and keeping only the lowest order terms.

We note that the numerical results presented in Figures 9.9 and 9.10 apply only for the 1/7 power law velocity profile, while the analytical results expressed by equations (9.53) and (9.55) appear to be valid for all velocity profiles for which the integral (F-25) [see Appendix F] is convergent. We find that this includes the power law profiles

$$U = (z^*)^{1/n}, \qquad n \geq 5 \tag{9.56}$$

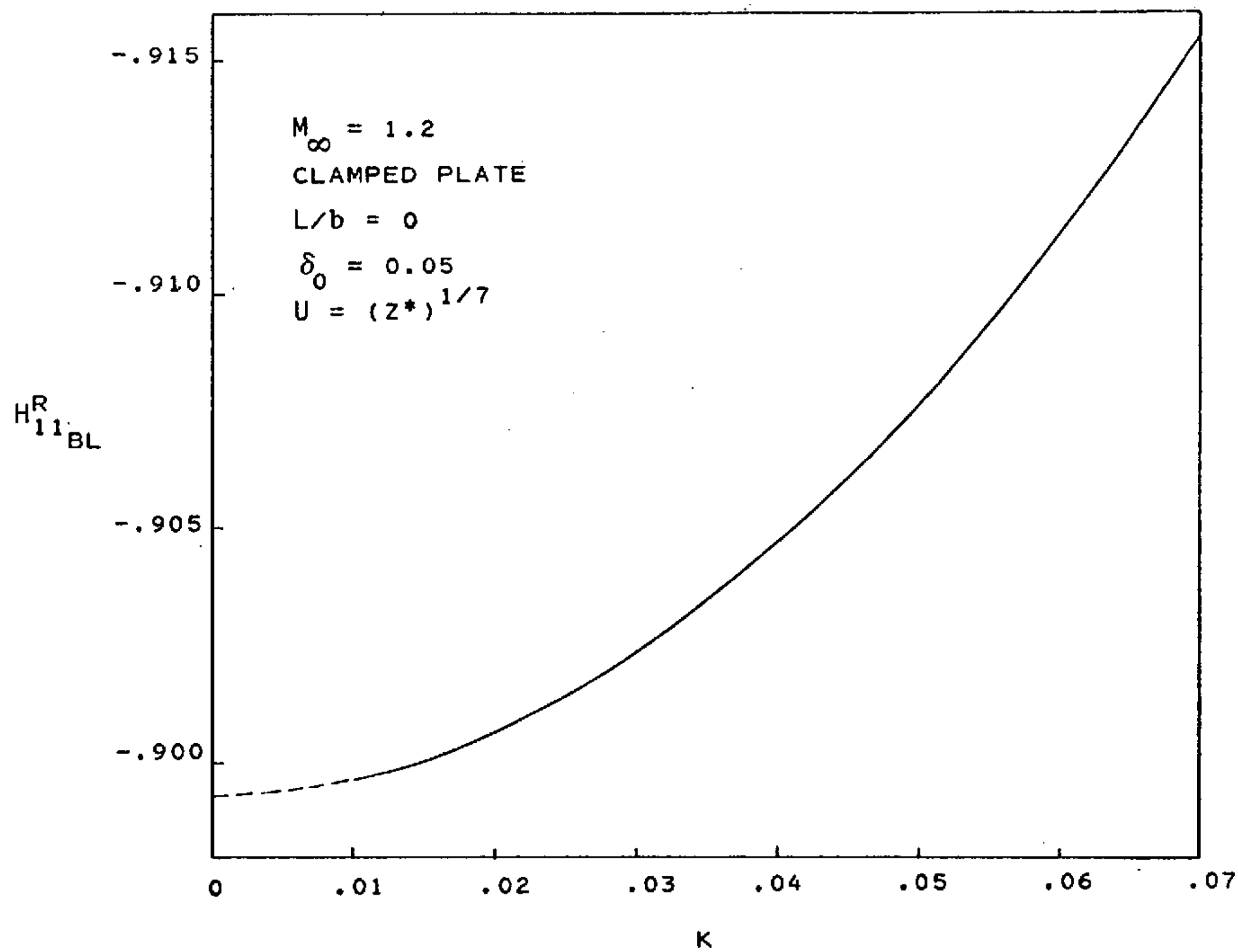

FIGURE 9.9
REAL COMPONENT OF THE BOUNDARY-LAYER CONTRIBUTION
TO THE MECHANICAL ADMITTANCE VS. REDUCED FREQUENCY
FOR THE LOW FREQUENCY LIMIT

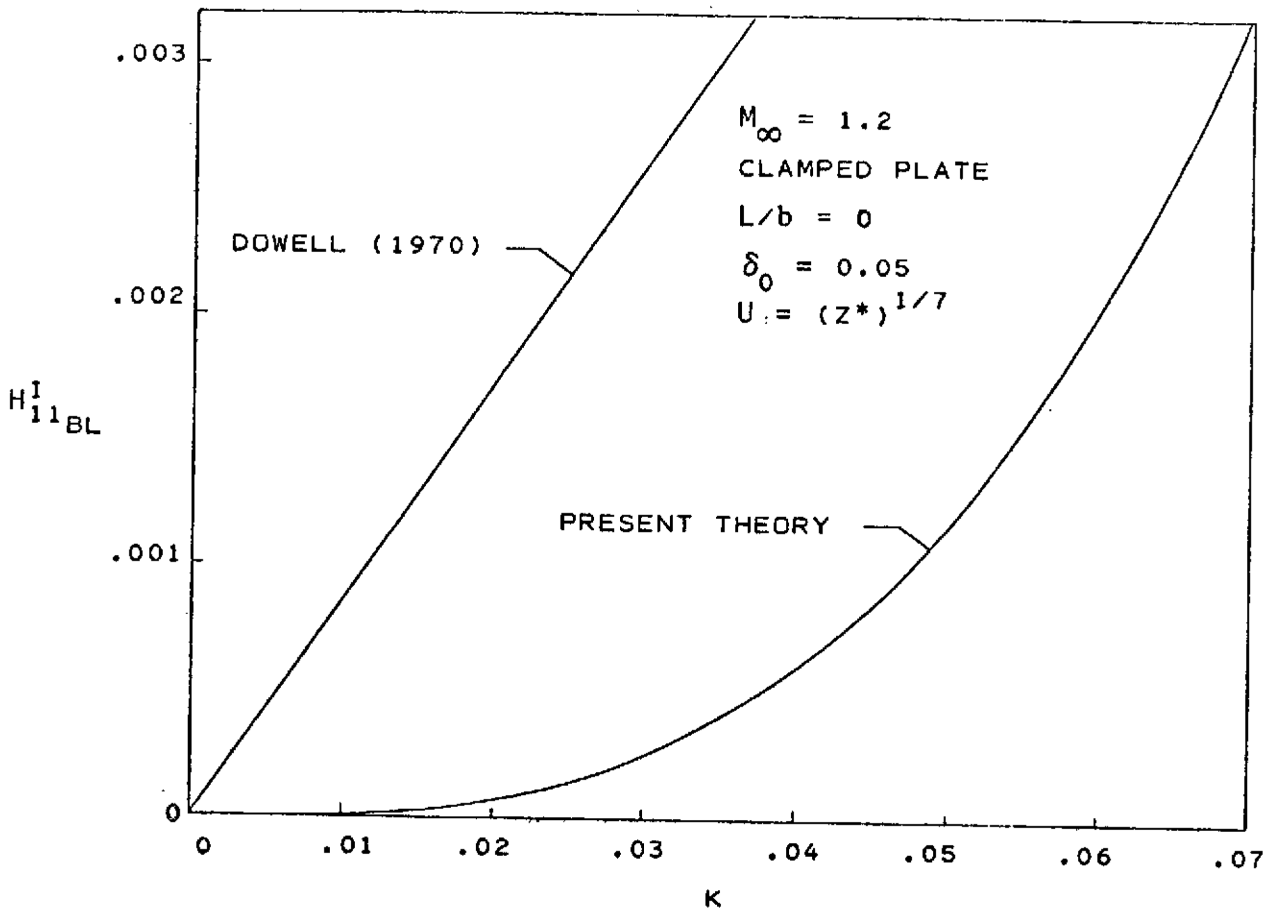

FIGURE 9.10
COMPARISON OF THEORETICAL IMAGINARY COMPONENTS OF THE BOUNDARY-LAYER CONTRIBUTION TO THE MECHANICAL ADMITTANCE VS. REDUCED FREQUENCY FOR THE LOW FREQUENCY LIMIT

The key feature of the power law profiles which ensures convergence of the integral (F-25) is the nature of the derivative

$$z^{*\prime}(U) = nU^{n-1} \tag{9.57}$$

near $U \to 0$. For this special class of profiles the integrand in (F-25) remains finite for $k \to 0$ because $z^{*\prime}(U) \to 0$ faster than the rest of the integrand becomes infinite as $U \to 0$. With this explanation in mind we should not put much confidence in the validity of the present theory for all velocity profiles as $k \to 0$. To illustrate this point consider the fact that for a realistic turbulent velocity profile the behavior near the wall is generally assumed to be linear in z^*; that is,

$$U = U_s \frac{z^*}{z^*_s}, \qquad z^* \le z^*_s \tag{9.58}$$

Where the subscript s refers to the laminar sublayer near the wall. For this type of velocity profile the derivative $z^{*\prime}(U)$ is constant near $U = 0$, and it can be shown that for the case $k \to 0$ the integrand in (F-25) is proportional to U^{-5} as $U \to 0$. We wouldn't be surprised to find that the integral is divergent and that the theory really is suspect for $k \to 0$ for all but a select class of mean velocity profiles.

This finding seems to corroborate our earlier discussion in Sections 3.6 and 6.5 with regard to the validity of the theory for steady flow. Recall condition (6.63) which can be recast in the following form

$$k \gg \delta_0/(U'(0)B) \quad \text{as} \quad k \to 0 \tag{9.59}$$

to indicate the minimum amount of flow unsteadiness required for the present theory to be valid. The condition implies that the theory is not applicable as $k \to 0$ for velocity profiles with finite gradient at $z^* = 0$. The condition is somewhat ambiguous in the limit as $k \to 0$ for the power law profiles with infinite gradient at $z^* = 0$. This may help to explain why we get finite results for this case even though the theory is suspect for $k \to 0$.

The preceding discussion has served to point out the limitations of the present theory for treating the steady flow limit. On account of these limitations we do not attempt to apply the present theory to the case of steady flow past a rigid wavy wall. We have already pointed out in Chapter 4 in our discussion of the effects of including viscosity in the perturbed flow that in the limit as $k \to 0$ the nature of the problem changes drastically and the effects of viscosity on the perturbed flow are no longer confined to a thin region of nonuniformity within the shear layer. On the contrary, the effect of viscosity is felt throughout the shear layer, consequently we find that the inviscid shear flow theory developed in Chapters 3 and 6 is inadequate. For a recent study of the flow over a wavy wall for the Mach number range of interest one should consult the paper by Inger and Williams (1972) in which a theoretical analysis including the effects of viscosity in the perturbed flow is presented along with some experimental results and comparisons of theory and experiment for wall pressure amplitude and phase shift.

9.5 THE LIMITING CASE OF LARGE REDUCED FREQUENCY

Another special case of interest is the regime of high frequency (large reduced frequency). While this case is not of particular interest insofar as panel flutter is concerned (the reduced frequency of panel flutter is generally within the range $0 < k < 1$), it may be of general interest. Hence, we include a brief discussion here, comparing the effects of the present theory with the behavior of the inviscid theory.

To obtain the inviscid behavior of the potential flow theory for high frequency we expand (9.19) for large values of $M_\infty k$, substitute in (9.17), neglect the higher-order terms and invert the Fourier transform to obtain

$$\hat{p}_0(x;k) = \frac{ik}{M_\infty} \hat{z}_s(x) + \ldots \tag{9.60}$$

Thus, we find a linear dependence of the surface pressure on reduced frequency for large values of k.

Now consider the specialization of the boundary-layer perturbation. Expanding (9.21) and (9.22) for large values of k, neglecting higher-order terms, substituting in (9.20) and (9.17), and inverting, we obtain

$$\delta_0 \hat{p}_{BL}(x;k) = -\delta_0 (ik)^2 (1-a)\hat{z}_s(x) + \ldots \tag{9.61}$$

where

$$a = \int_0^1 \rho \, dz^*$$

As in the previous section we can convert this last result to an expression for the generalized force, $H_{11_{BL}}(k)$, by substituting $\psi_1(x)$ for $\hat{z}_s(x)$ in the above, substituting (9.61) and (9.37) in (9.7), and integrating, to obtain an expression of the form (9.34) where

$$H^R_{11_{BL}}(k) = \frac{3}{2}\delta_0 (1-a)k^2 + \ldots \tag{9.62}$$

$$H^I_{11_{BL}}(k) = O(k^{-3}) \tag{9.63}$$

This result has been verified numerically by calculating the boundary layer contributions to the forces by the procedure described in Section 9.2 for "large" values of k. We illustrate the results in Figure 9.11 for $\delta_0 = .05$. The quadratic behavior of $H^R_{11_{BL}}$ with k verifies what we have obtained analytically. The imaginary component appears to be insignificant for sufficiently large values of k.

We remark that for the first-order perturbation of (9.61) to be valid we must require a condition of small perturbations to be satisfied. Applying (6.60) to the present case using the transforms of (9.60) and (9.61) we find that we must have

$$\delta_0 \ll \frac{1}{M_\infty k(1-a)}, \qquad M_\infty k \gg 1 \tag{9.64}$$

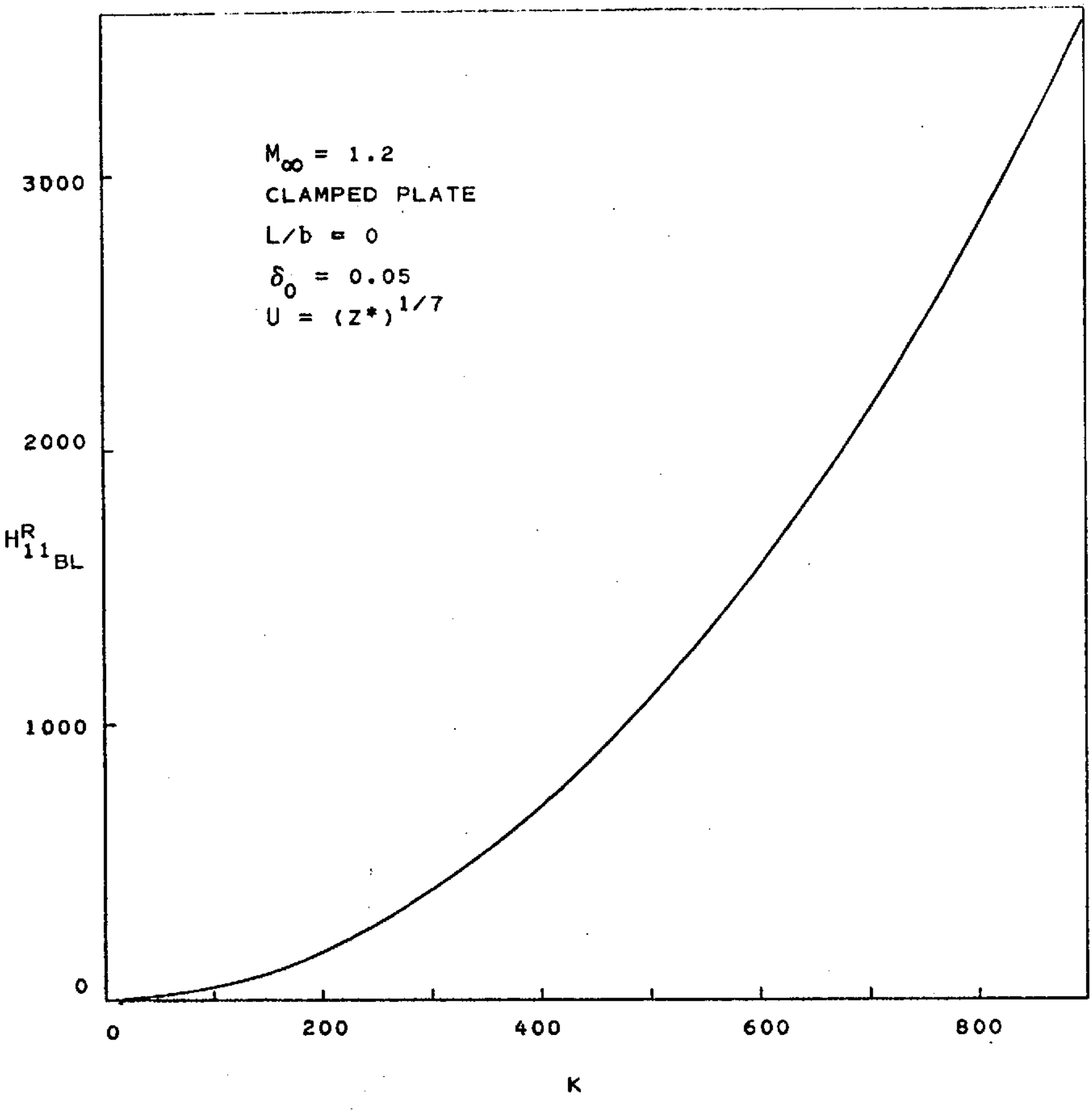

FIGURE 9.11
REAL COMPONENT OF THE BOUNDARY-LAYER CONTRIBUTION TO THE MECHANICAL ADMITTANCE VS. REDUCED FREQUENCY FOR THE HIGH FREQUENCY LIMIT

This puts rather severe restrictions on the practical application of the first-order theory for high frequency. It requires that the boundary layer be extremely thin for large values of the reduced frequency. It is fairly obvious that condition (9.64) is violated for the case considered in Figure 9.11 for most of the range of frequency. With $\delta_0 = .05$, $a = .8$, and $M_\infty \simeq 1$ condition (9.64) requires

$$1 \ll k \ll 100 \tag{9.65}$$

This restricts the theory for this case to values of $k \sim 10$, which is equivalent to a frequency of about 10^3 cyc./sec. for $u_\infty = 10^3$ ft./sec. and $L = 1$ ft. It is possible that the present theory might have some applicability to the problem of the response of panels to turbulent boundary layer excitation or acoustic excitation in which the primary application would be fatigue or noise radiation problems. This conjecture is based upon evidence, both experimental and theoretical, of significant excitation of panels at frequencies of the order of one kilocycle [see, for example, the work of Wilby (1967)]. We leave this problem for future investigation and consider the panel flutter problem in the next section.

9.6 AN APPROXIMATE ANALYSIS FOR THE DETERMINATION OF THE STABILITY BOUNDARIES FOR PANEL FLUTTER

In the present section we develop an approximate technique for analyzing the motion of an oscillating panel and for predicting the critical values of the dynamic pressure, the stability boundary at which the flutter motion becomes unstable and the panel deflections begin to grow exponentially with time. We consider an elementary model of panel flutter for which we make simplifying assumptions. We assume that the panel is initially flat as in Figure 7.1 and that there are no applied in-plane stresses. As indicated previously, we assume that the panel is of infinite span and that the panel is rigidly clamped at the ends $x = 0$ and $x = L$. Finally, we assume that the aerodynamic forces act only on the side of the panel exposed to the moving airstream; that is, we neglect the effects of the cavity on the underside of the panel.

The governing equation for the dimensional plate deflection, $w(x,t)$, is a condition of dynamic equilibrium between the structural, inertial, and aerodynamic forces acting on the panel and is given [see Dowell (1966)] for the simplifying assumptions stated above by

$$D \frac{\partial^4 w}{\partial x^4} - N_x^{(i)} \frac{\partial^2 w}{\partial x^2} + \rho_m h \frac{\partial^2 w}{\partial t^2} + p - p_\infty = 0 \tag{9.66}$$

where D is the plate stiffness for the panel of constant thickness, h, ρ_m is the plate density, $N_x^{(i)}$ is the nonlinear induced in-plane loading, and $p-p_\infty$ is the perturbation aerodynamic pressure on the panel surface. The plate deflection satisfies the boundary conditions at the clamped ends

$$w = \frac{\partial w}{\partial x} = 0, \qquad x = 0, L \tag{9.67}$$

We further confine our analysis to linearized theory for which we neglect the term $N_x^{(i)}$, and we note that the perturbation pressure depends linearly upon w. Nondimensionalizing the variables as in previous chapters; i. e.,

$$\begin{aligned} z_s &= w/L \\ x &= x/L \\ t &= u_\infty t/L \\ p &= (p-p_\infty)/(2q); \; q = \frac{1}{2}\rho_\infty u_\infty^2 \end{aligned} \tag{9.68}$$

and assuming simple harmonic motion,

$$z_s = z_s(x)e^{ikt}, \tag{9.69}$$

we obtain the nondimensional equation of motion

$$z_s^{(iv)}(x) - \frac{\lambda k^2}{\mu} z_s(x) + \lambda p(z_s) = 0 \tag{9.70}$$

where

$$\lambda = 2qL^3/D$$

$$\mu = \frac{\rho_\infty L}{\rho_m h}$$

and boundary conditions

$$z_s = z_s'(x) = 0, \qquad x = 0, 1 \tag{9.71}$$

We propose to solve (9.70), (9.71) by Galerkin's method. We assume the nondimensional panel deflection may be represented as in (9.2) as a sum over N assumed modes

$$z_s(x) = \sum_{m=1}^{N} \epsilon_m \psi_m(x) \tag{9.72}$$

where ϵ_m are the modal amplitudes and ψ_m are the mode functions satisfying (9.71). Substituting (9.72) in (9.70) and noting that

$$p = \sum_{m=1}^{N} p_m \tag{9.73}$$

where p_m is the pressure due to $\epsilon_m \psi_m$, we obtain a single equation of motion for the N modal amplitudes, ϵ_m. To obtain a sufficient number of equations for the number of unknowns we multiply the equation of motion by $\psi_n(x)$ and integrate over x from $x = 0$ to $x = 1$. This gives

$$\frac{\lambda k^2}{\mu} \sum_{m=1}^{N} S_{mn} \epsilon_m - \sum_{m=1}^{N} C_{mn} \epsilon_m - \lambda \sum_{m=1}^{N} \hat{Q}_{mn} = 0 \tag{9.74}$$

$$n = 1, 2, \ldots N$$

where

$$S_{mn} = \int_0^1 \psi_m \psi_n dx \tag{9.75}$$

$$C_{mn} = \int_0^1 \psi_m^{(iv)} \psi_n dx \tag{9.76}$$

$$\hat{Q}_{mn} = \int_0^1 p_m \psi_n dx \tag{9.77}$$

We recognize $\hat{Q}_{mn}$ as the generalized aerodynamic force introduced in Section 9.2 which can also be expressed using (9.7) and (9.9) as

$$\hat{Q}_{mn} = \epsilon_m H_{mn}(k;M_\infty, \delta_0) \tag{9.78}$$

where

$$H_{mn}(k;M_\infty, \delta_0) = \int_0^1 \hat{p}[\psi_m(x);k, M_\infty, \delta_0]\psi_n(x)dx \tag{9.79}$$

is the mechanical admittance.

The system of equations in (9.74) is an eigenvalue problem. To determine the critical values of the pair of parameters (λ, k) we must equate to zero real and imaginary parts of the coefficient determinant of the system of equations. For practical purposes one usually assumes N to be small and determines the flutter eigenvalues by some sort of graphical or numerical process. This could be accomplished for $N = 2$ modes and would require the determination of H_{11}, H_{12}, H_{21}, H_{22} as functions of k for given values of M_∞ and δ_0. Recalling the difficulty of the task just to obtain H_{11}, we wonder if it would be possible to perform a flutter analysis using $N = 1$ mode and obtain meaningful results. From our discussion in Section 9.2 we know that the panel motion is essentially a single-degree-of-freedom-system for inviscid flow at low supersonic Mach number and our results for thin boundary layers in Figure 9.2 seem to support the contention that the behavior remains essentially the same even for $\delta_0 = .10$ in spite of Dowell's results for that case.

In light of this reasoning we propose to perform a single mode approximation to the panel displacement and compare these results with Dowell's two-mode analysis. For the one-mode approximation we have a single equation in the set (9.74)

$$\left(\frac{\lambda k^2}{\mu} S_{11} - C_{11} - \lambda H_{11}\right)\epsilon_1 = 0 \tag{9.80}$$

A nontrivial solution of (9.80) for flutter requires the complex determinant to be zero. Setting the real and imaginary parts equal to zero we obtain two equations for the two flutter eigenvalues

$$H^I_{11}(k_f; M_\infty, \delta_0) = 0 \tag{9.81}$$

$$\lambda_f = \frac{C_{11}}{\left[\dfrac{S_{11}k_f^2}{\mu} - H^R_{11}(k_f; M_\infty, \delta_0)\right]} \tag{9.82}$$

where S_{11} and C_{11} are obtained from (9.75) and (9.76) using (9.37). Integrating, we obtain

$$S_{11} = 3/2 \tag{9.83}$$

$$C_{11} = \frac{1}{2}(2\pi)^4 \tag{9.84}$$

From the preceding it is clear that the flutter eigenvalue λ_f depends upon several parameters; i.e.,

$$\lambda_f = \lambda_f(k_f; M_\infty, \delta_0, \mu) \tag{9.85}$$

To determine λ_f from equations (9.81) through (9.84) we first specify M_∞, and δ_0. We can find k_f graphically from (9.81) as that value of k for which H^I_{11} is zero. For the case $M_\infty = 1.2$ we determine k_f from the curves of Figure 9.2.

δ_0	k_f	$\dfrac{(k_f - k_{f_0})}{k_{f_0}}$ %
0	.745	0
.05	.510	31.5
.10	.405	45.5

$M_\infty = 1.2$

These results lend an interesting physical interpretation to the curves of Figure 9.2. We have already noted that for the single-degree-of-freedom system there is a range of k for which the system has negative aerodynamic damping. According to (9.81) the maximum value of k in this range corresponds to the reduced frequency at flutter. This direct relationship between the flutter frequency and negative aerodynamic damping is unique to the one-mode approximation to the motion. Note that as the boundary layer thickness increases there is a reduction in flutter frequency. From the last column in the table above we note that the percentage reduction in flutter frequency with increasing boundary layer thickness, δ_0, exhibits a "diminishing returns" behavior as δ_0 increases from .05 to .10.

Having determined k_f, we obtain λ_f from (9.82). We must find $H^R_{11}(k_f)$ in order to evaluate this expression, and we obtain this graphically from a plot of H^R_{11} vs. k_f for the given values of M_∞ and δ_0. For example, we use Figure 9.1 for the Mach number of interest. Note that we must also specify the parameter μ prior to calculating λ_f. In the next section we present the results of this one-mode analysis and compare with theory and experiment.

9.7 COMPARISON OF THEORY AND EXPERIMENT FOR FLUTTER PREDICTION

The most recent and thorough experiments to date on the effects of the boundary layer on panel flutter are those of Muhlstein, Gaspers, and Riddle (1968) and Gaspers, Muhlstein, and Petroff (1970). In these experiments flutter dynamic pressure and flutter frequency were obtained for a rectangular unstressed isotropic panel with all edges clamped. For the present comparison we consider the earlier results of Muhlstein et al. (1968) for $L/b = 0.5$, M_∞ in the range 1.05 to 1.40, and δ_0 of 0.032 to 0.111. From these experiments it is shown that the turbulent boundary layer has a large stabilizing influence on the flutter of flat panels and that the effect on flutter dynamic pressure is maximum near $M_\infty=1.2$ and decreases rapidly with increasing Mach number. In comparing with these results we focus on this one Mach number and on the range of boundary layer thicknesses corresponding to the experiments. In Figure 9.12 we show flutter dynamic pressure vs. boundary layer thickness. For the plate we note that the thickness ratio $h/a = .0044$, while the mass ratio, μ, ranged from $\mu = .043$ to $.09$. The theoretical results [with the exception of one case of Dowell (1971)] are for a plate-column $(L/b = 0)$, while the experimental data are for $L/b = 0.5$.

We note that the trend of all the results is an increase in stability with increasing boundary layer thickness; i.e., an increase in the minimum dynamic pressure for flutter. With regard to the quantitative aspects of the comparison, the two-dimensional results are consistently lower than the experimental data and Dowell's (1971) three-dimensional theoretical results. Apparently, most of this difference is due to the two-dimensional nature of the theoretical results. With regard to the three-dimensional results of Dowell (1971) we note that the agreement with experiment is better for the thicker boundary layers. Since Dowell's results do not require the assumption of thin boundary layer, we cannot readily explain this behavior.

Concentrating on the two-dimensional theoretical results in Figure 9.12, we compare the results of the one-mode linear flutter analysis for the present theory with the two-mode nonlinear flutter analyses of Dowell (1971) and Ventres (1972). We should point out that there is some ambiguity introduced by comparing flutter predictions using different flutter analyses. If we had been able to obtain Dowell's results for H_{11}^R vs. k, we could have predicted flutter using his data in a one-mode analysis. According to Dowell's (1971)

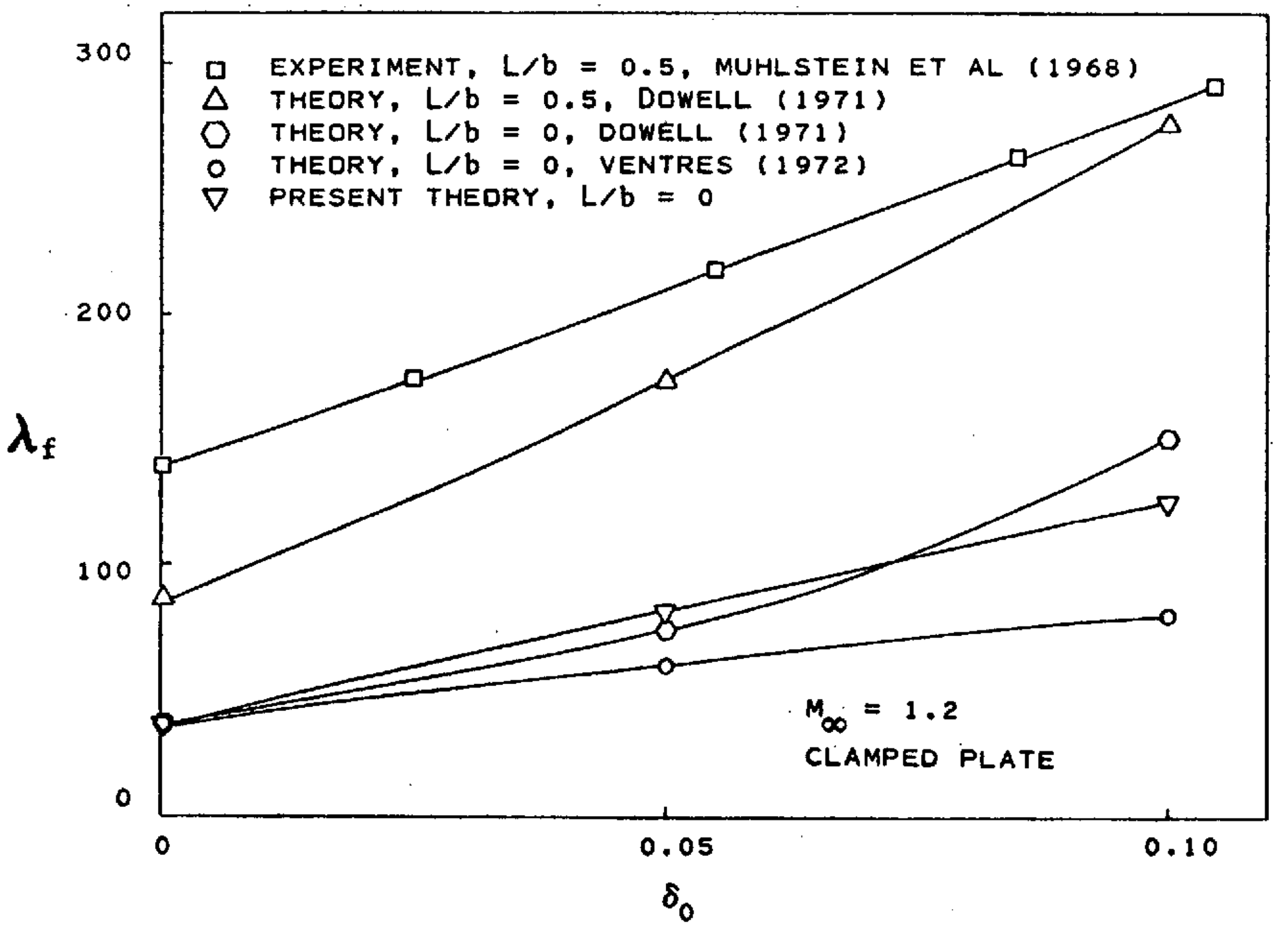

FIGURE 9.12
COMPARISON OF THEORETICAL AND EXPERIMENTAL FLUTTER DYNAMIC PRESSURE VS. BOUNDARY-LAYER THICKNESS

calculations, there is an increase in second mode content relative to first mode content from about 15% for no boundary layer to 40% for $\delta_0 = 0.10$. This indicates that the flutter motion is less of a single-degree-of-freedom type with a boundary layer present, and we might expect to discover a substantial error for the present one-mode analysis for the thicker boundary-layer case. Indeed there are differences in the flutter results for $\delta_0 = .10$. We could have anticipated this earlier when we noted the substantial differences in the theoretical results for H^I_{11} in Figure 9.4.

The theory of Ventres (1972) is similar to the present theory in that the assumption of thin boundary layer is made, and an analytical solution for the pressure in increasing powers of the boundary layer thickness is obtained. Ventres' theory is based on Fourier transformation in x and Laplace transformation in t. His solution differs from the present one in that the Laplace transformation and analytical inversion is employed for the time dependency rather than the more specialized case of simple harmonic motion used in the present theory. Ventres inverts the Fourier transforms numerically, while we have done this analytically; he obtains the z*-integration analytically, while we have done this partly analytically and partly numerically. The results in Figure 9.12 indicate some differences between Ventres' theory and the present theory to first-order in the boundary-layer thickness parameter. In particular, the predicted flutter dynamic pressures for the present theory are higher than for Ventres' theory. It is likely that this is mainly due to the one-mode approximation used in the present analysis, whereas Ventres uses a two-mode analysis. Dowell (private communication) suggests that the effect of performing a two-mode analysis for the present theory would be to reduce the predicted flutter values, thus providing better agreement with Ventres.

In Figure 9.13 we compare the flutter frequency, K_f, for theory and experiment where

$$K_f = k_f(\lambda_f/\mu)^{1/2} \tag{9.86}$$

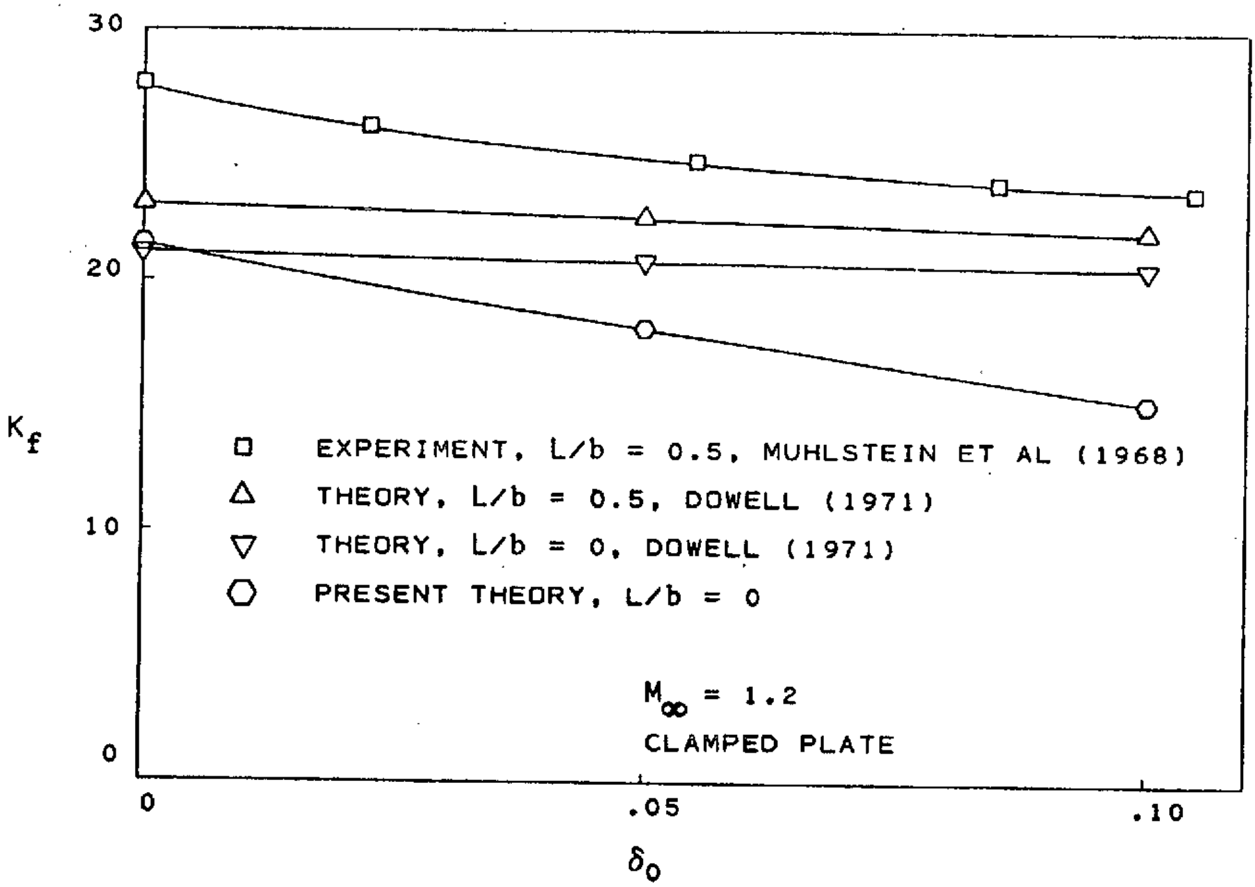

FIGURE 9.13
COMPARISON OF THEORETICAL AND EXPERIMENTAL FLUTTER FREQUENCY VS. BOUNDARY-LAYER THICKNESS

With regard to these results it is interesting to note that Dowell's theory predicts that the flutter frequency is essentially constant over the range of boundary layer thickness, while the experiment and the present theory indicate a decrease in flutter frequency with increasing boundary layer thickness. Since Dowell's results are closer in magnitude to the experimental data, we don't draw any strong conclusions from this observation. With regard to the improved agreement with experiment for Dowell's (1971) three-dimensional results we note that the improvement is not as good for thin boundary layers. Recall that we made the same observation with regard to the flutter dynamic pressure.

X. CONCLUSIONS AND RECOMMENDATIONS

In the previous chapters we have attempted to discuss conclusions along with the theoretical developments. At this point we will try to summarize the important achievements of this study and suggest areas which deserve further investigation. First of all, the major accomplishment of the present study is a systematic development of a theory for the perturbed unsteady boundary-layer flow over an oscillating wavy surface which allows us to consider separately the effects of a mean shear profile for thin boundary layers, the effects of compressibility and three-dimensionality, the effects of viscous stresses, and the effects of the turbulent Reynolds stresses. We have discovered that the inviscid shear flow theory for thin boundary layers is valid for a sufficient amount of flow unsteadiness, and in that case we can neglect the viscous stresses in the perturbed flow. We have been able to show by means of singular perturbation theory that for sufficiently large Reynolds number and reduced frequency the perturbed flow viscous stresses are negligible. Likewise, with regard to the effects of turbulence, we have been able to estimate the magnitude of the perturbation Reynolds stresses and we have found that these terms are important and should really be included in the analysis.

In applying the present theory to the problem of wind-generated water waves we find that an inviscid theory is inadequate for modeling the flow and for predicting the surface pressure. Neither the present inviscid theory nor Miles' theory is very satisfactory in comparison with laboratory measurements. An improved theory including the effects of the turbulent Reynolds stresses is required. This development should include an evaluation of eddy viscosity and eddy-viscoelasticity models proposed by Reynolds and Hussain (1972) and Davis (1972) and should involve careful comparison with field data, as well as laboratory measurements, in order to ascertain the soundness of any proposed analytical treatment. The study of momentum and energy transfer from the wind to the water is an oceanographic problem of considerable interest at the present time, and it is clear that improved theories of wind-wave interaction will be of great benefit for this field of study.

The application of the theory to the calculation of generalized aerodynamic forces and panel flutter prediction has aroused some questions. In the comparison with Dowell there seem to be some significant differences in the predicted mechanical admittance as a function of reduced frequency. In particular, we found differences in the results for the imaginary component of the admittance for the case of a 10%-thick boundary layer and differences at low frequency in the boundary-layer contribution to the admittance. Further study is required to determine whether this behavior represents some novel phenomena or whether it is merely a limitation of the present assumptions. A comparison of predicted behavior for the generalized forces with the first-order theory of Ventres (1972) might be a useful first step. The relatively poor agreement of Dowell's (1971) three-dimensional numerical flutter predictions with the experiments of Muhlstein et al. (1968) for the case of very thin boundary layers is strong motivation for extending the present theory to three-dimensional flow by continuing the analysis outlined in Chapter 7.

Finally, there are several areas of current practical and fundamental interest to which the present methodology might be applied. One possible area is the problem of sound propagation through a shear flow with applications to the possible noise abatement of flows in jet engines and of boundary layer flows around aircraft. The noise problem is currently of great concern in the field of transportation, and any effort which provides fundamental understanding of the mechanism of noise generation and propagation is valuable. Another problem of possible interest is the elusive quest for drag reduction by the use of flexible walls. Perhaps the present approach could be exploited to study viscous effects in the hydrodynamics of aquatic propulsion with the goal of understanding why fish are such efficient swimmers. An area of personal interest is the nature of the fluid-mechanical aspects of flow in the human respiratory and cardio-vascular systems. While the present study is not directly applicable to such problems, there are some fundamentals which could be exploited. For example, the bio-mechanical flows are unsteady, viscous, and they involve flexible boundaries with and without mass exchange. A problem for which the present theoretical approach is directly applicable is the study of the propagation of freestream disturbances in a boundary layer with a view to perhaps understanding the mechanism of transition to turbulence. These problems are challenging, and their study could provide some practical benefits as well as improving our understanding of the physical universe.

REFERENCES

Ashley, H., and Landahl, M. T., (1965), Aerodynamics of Wings and Bodies, Addison-Wesley, Reading, Massachusetts.

Benjamin, T. B., (1959), "Shearing Flow Over a Wavy Boundary," J. Fluid Mech., 6, pp. 161-205.

Blisplinghoff, R. L. and Ashley, H., (1962), Principles of Aeroelasticity, J. Wiley and Sons, New York, Section 6-3(b).

Davis, R., (1970), "On the Turbulent Flow Over a Wavy Boundary," J. Fluid Mech., 42, pp. 721-731.

Davis, R. (1972), "On Prediction of the Turbulent Flow Over a Wavy Boundary," J. Fluid Mech., 52, pp. 287-306.

Dobson, F. W., (1969), "Observations of Normal Pressure on Wind Generated Sea Waves," Ph.D. dissertation, Department of Physics, University of British Columbia, Vancouver, B.C., Canada.

Dowell, E. H., (1966), Nonlinear Oscillations of a Fluttering Plate," AIAA J., 4, pp. 1267-1280.

Dowell, E. H., (1967), "Generalized Aerodynamic Forces on a Flexible Plate Undergoing Transient Motion," Quarterly of Applied Mathematics, 23, 4, pp. 331-338.

Dowell, E. H., (1970), "Generalized Aerodynamic Forces on a Flexible Plate Undergoing Transient Motion in a Shear Flow with an Application to Panel Flutter," AIAA, New York, N.Y., Paper No. 70-76.

Dowell, E. H., (1971), "Generalized Aerodynamic Forces on a Flexible Plate Undergoing Application to Panel Flutter," AIAA J., Vol. 9, No. 5, p. 834.

Fung, Y. C., (1963), "Some Recent Contributions to Panel Flutter Research," AIAA J., Vol. 1, pp. 898-909.

Gaspers, P., Muhlstein, L., and Petroff, D., (1970), "Further Experimental Results on the Influence of the Turbulent Boundary Layer on Panel Flutter," Gaspers, P. A., (1970), "A Critical Evaluation of Panel Flutter Aerodynamics," Analytical Methods in Aircraft Aerodynamics, NASA SP-228, pp. 335-353.

Hinze, J. O., (1959), Turbulence, McGraw Hill, New York.

Hussain, A.K.M.F., and Reynolds, W. C., (1970), "The Mechanics of a Perturbation Wave in Turbulent Shear Flow," Department of Mechanical Engineering, Stanford University, Stanford, Calif., Technical Report FM-6.

Hussain, A.K.M.F., and Reynolds, W. C. (1972), "The Mechanics of an Organized Wave in Turbulent Shear Flow," Part 2, Experimental Results. J. Fluid Mech., 54, pp. 241-261.

Hsu, E. Y., (1965), "A Wind, Water-Wave Research Facility," Department of Civil Engineering, Stanford University, Stanford, Calif., Technical Report No. 57.

Inger, G. R., and Williams, E. P., (1972), "Subsonic and Supersonic Boundary Layer Flow Past a Wavy Wall," AIAA Journal, Vol. 10, No. 5, pp. 636-642.

Karamcheti, K., (1966), Ideal-Fluid Aerodynamics, John Wiley and Sons, Inc., New York, N.Y.

Kendall, J., (1970), "The Turbulent Boundary Layer Over a Wall with Progressive Surface Waves," J. Fluid Mech., 41, pp. 259-281.

Kondo, J., Fujinawa, Y., and Naito, G., (1972), "Wave-Induced Wind Fluctuation Over the Sea," J. Fluid Mech., 51, pp. 751-772.

Landahl, M. T., and Ashley, H., (1968), "Influence of the Boundary Layer," Manual on Aeroelasticity, Vol. II, ed. R. Mazet, Advisory Group for Aerospace Research and Development, North Atlantic Treaty Organization, Technical Editing and Reproduction, Ltd., London, Chapter 9.

Lighthill, M. J., (1954), "The Response of Laminar Skin Friction and Heat Transfer to Fluctuations in the Stream Velocity," Proc. Roy. Soc., A224, 1-23.

Lin, C. C., (1955), The Theory of Hydrodynamic Stability, Cambridge University Press, Cambridge, England.

McClure, J. D., (1962), "On Perturbed Boundary Layer Flows," Massachusetts Institute of Technology, Cambridge, Mass., Fluid Dynamics Research Lab., Report 62-2.

Miles, J. W., (1957), "On the Generation of Surface Waves by Shear Flows," J. Fluid Mech., 3, pp. 185-204.

Miles, J. W., (1959a), "On Panel Flutter in the Presence of a Boundary Layer," J. Aero. Sci., 26, p. 81ff.

Miles, J. W., (1959b), On the Generation of Surface Waves by Shear Flows Part 2," J. Fluid Mech., 6, pp. 568-582.

Miles, J. W., (1960), "On the Generation of Surface Waves by Turbulent Shear Flows," J. Fluid Mech., 7, pp. 469-478.

Miles, J. W., (1962), "On the Generation of Surface Waves by Shear Flows, Part 4," J. Fluid Mech., 13, pp. 433-448.

Miles, J. W., (1967), "On the Generation of Surface Waves by Shear Flows, Part 5," J. Fluid Mech., 30, pp. 163-175.

Moore, F. K., and Ostrach, S., (1957), "Displacement Thickness of the Unsteady Boundary Layer," J. Aero. Sci., 24, pp. 77, 78.

Muhlstein, L., Gaspers, P., and Riddle, D., (1968), "An Experimental Study of the Influence of the Turbulent Boundary Layer on Panel Flutter," NASA, Washington, D.C., Technical Note D-4486.

Pohlhausen, K., (1921), "Zur naherungsweisen Integration der Differential-gleichung der laminaren Reibungsschicht," ZAMM 1, pp. 252-268.

Phillips, O. M., (1966), The Dynamics of the Upper Ocean, Cambridge Univ. Press, London.

Reynolds, W. C., (1968), "A Morphology of the Prediction Methods," Proceedings, Computation of Turbulent Boundary Layers — 1968 AFOSR-IFP-Stanford Conference, Vol. I, Department of Mechanical Engineering Stanford University, Stanford, Calif.

Reynolds, W. C. and Hussain, A.K.M.F., (1972), "The Mechanics of an Organized Wave in Turbulent Shear Flow, Part 3, Theoretical Models and Comparisons with Experiments," J. Fluid Mech., 54, pp. 263-288.

Saeger, J. and Reynolds, W. C., (1971), "Perturbation Pressures Over Traveling Sinusoidal Waves with Fully Developed Turbulent Shear Flow," Department of Mechanical Engineering, Stanford University, Stanford, Calif., Technical Report FM-9.

Schlichting, H., (1968), Boundary-Layer Theory, McGraw-Hill Book Co., San Francisco, Calif., Chapter 5.

Shemdin, O. and Hsu, E. Y., (1967), "Direct Measurement of Aerodynamic Pressure Above a Simple Progressive Gravity Wave," J. Fluid Mech., 30, pp. 403-416.

Stewart, R. H., (1970), "Laboratory Studies of the Velocity Field Over Deep-Water Waves," J. Fluid Mech., 42, pp. 753-754.

Tanaka, I. and Himeno, Y., (1970), "On Velocity Distribution and Local Skin Friction of Two-Dimensional Turbulent Boundary Layer with Pressure Gradient," Osaka University, Osaka, Japan, Technology Reports, 20, pp. 237-248, IAA Accession Number A70-29672, Technical Information Service, 750 3rd Ave., New York, N.Y.

Teipel, I., (1969), "An Integral Method for the Calculation of Incompressible, Oscillating Boundary Layer Flows," Deutsche Luft- und Raumfahrt, Aachen, Germany, FB 69-09, (In German).

Teipel, I., (1970), "Calculation of Unsteady Laminar Boundary Layers by an Integral Method," Z. Flugwiss., 18, Heft 2/3, pp. 58-65.

Van Driest, E. R., (1956), J. Aero. Sci., 23, p. 1007.

Van Dyke, M., (1964), Perturbation Methods in Fluid Mechanics, Academic Press, New York, Chapter 7.

Ventres, C. S., (1972), "Transient Panel Motion in A Shear Flow," unpublished paper, Princeton University, 1970.

von Karman, Th., (1921), "Uber laminare und trubulente Reibung," ZAMM 1, pp. 233-252; NACA TM-1092 (1946).

Wilby, J. F., (1967), "The Response of Simple Panels to Turbulent Boundary Layer Excitation," Air Force Flight Dynamics Laboratory, Wright-Patterson Air Force Base, Dayton, Ohio, Technical Report AFFDL-TR-67-70.

Yates, J. E., (1969), "Unsolicited Proposal for Support of a Study of Three-Dimensional Panel Flutter Including a Turbulent Boundary Layer," Aeronautical Research Associates of Princeton, Princeton, N. J.

Yu, H. Y. and Hsu, E. Y., (1971), "A Refined Measurement of Aerodynamic Pressures over Progressive Water Waves," Department of Civil Engineering, Stanford University, Stanford, Calif., Technical Report No. 146.

Zeydel, E. F. E., (1967), "Study of the Pressure Distribution on Oscillating Panels in Low Supersonic Flow with Turbulent Boundary Layer," NASA, Washington, D.C., Contractor Report No. 691.

APPENDIX A

DERIVATION OF THE MOMENTUM-INTEGRAL EQUATION FOR UNSTEADY FLOW

The governing equations of momentum and mass conservation for the two-dimensional incompressible unsteady boundary layer are

$$u_t + uu_x + wu_z = u_{e_t} + u_e u_{e_x} + \tau_z/\rho \tag{A-1}$$

$$u_x + w_z = 0 \tag{A-2}$$

In order to obtain the momentum-integral equation we multiply the continuity equation (A-2) by $(u_e - u)$ and add it to the momentum equation (A-2). Thus we find

$$\frac{\partial}{\partial t}(u_e - u) + \frac{\partial}{\partial t}(u_e u - u^2) + (u_e - u)u_{e_x} + \frac{\partial}{\partial z}(u_e w - uw) = -\tau_z/\rho \tag{A-3}$$

Integrating equation (3) with respect to z from 0 to $\delta_{b.l.}$, assuming $\delta_{b.l.}$ is constant, yields

$$\frac{\partial}{\partial t}\int_o^{\delta_{b.l.}}(u_e - u)dz + \frac{\partial}{\partial x}\int_o^{\delta_{b.l.}} u(u_e - u)dz + u_{e_x}\int_o^{\delta_{b.l.}}(u_e - u)dz - w_o(u_e - u_o) = \tau_o/\rho \tag{A-4}$$

where τ_o is the shear stress and u_o and w_o are the velocity components at $z = 0$. It has been assumed that $w(u_e - u)$ and τ tend to 0 as $z \to \delta_{b.l.}$. Upon introducing the two boundary layer thicknesses

$$\delta^* = \int_o^{\delta_{b.l.}} (1 - u/u_e)dz \quad \text{(displacement thickness)} \tag{A-5}$$

$$\theta = \int_o^{\delta_{b.l.}} u/u_e(1 - u/u_e)dz \quad \text{(momentum thickness)} \tag{A-6}$$

we obtain the momentum-integral equation for unsteady flow

$$\frac{\partial}{\partial t}(u_e\delta^*) + \frac{\partial}{\partial x}(u_e^2\theta) + u_e\delta\, u_{e_x} - w_o(u_e - u_o) = \tau_o/\rho \tag{A-7}$$

APPENDIX B

THE SURFACE PRESSURE IN LINEARIZED UNSTEADY POTENTIAL FLOW

Consider the two-dimensional incompressible irrotational flow over an oscillating surface of small amplitude which can be described in nondimensional variables as

$$z = \epsilon\hat{z}_s(x)e^{ikt}, \qquad 0 \le x \le 1 \tag{B-1}$$

Assume that the nondimensional velocity potential can be represented as follows:

$$\Phi(x, z, t) = x + \epsilon\hat{\varphi}(x, z)e^{ikt} \tag{B-2}$$

where x is the potential for uniform flow in the x-direction and where $\hat{\varphi}$ is the amplitude function for the perturbation potential. The governing equation for $\hat{\varphi}$ is Laplace's equation,

$$\nabla^2\hat{\varphi} = 0 \tag{B-3}$$

and the linearized boundary conditions for $\hat{\varphi}$ are flow tangency at the surface and vanishing velocity perturbations at infinity; thus,

$$\hat{w}(x, 0) = \hat{\varphi}_z(x, 0) = (ik + d/dx)\hat{z}_s(x) \tag{B-4a}$$

$$\hat{\varphi}_x, \hat{\varphi}_z = 0 \quad \text{as} \quad z \to \infty \tag{B-4b}$$

The unsteady surface pressure is of the form

$$p_o = \epsilon\hat{p}_o(x)e^{ikt} \tag{B-5}$$

where

$$p_o = -(ik + \partial/\partial x)\hat{\varphi}(x, 0)$$

The problem for $\hat{\varphi}$ can be recast in terms of the Fourier transform defined as follows:

$$\tilde{\varphi}(\alpha; z^*) = \int_{-\infty}^{\infty} \hat{\varphi}(x, z)e^{-i\alpha x}dx \tag{B-6}$$

Thus

$$\tilde{\varphi}_{zz} - \alpha^2\tilde{\varphi} = 0 \tag{B-7}$$

$$\tilde{\varphi}_z(\alpha;0) = i(k+\alpha)\tilde{z}_s(\alpha) \tag{B-8a}$$

$$\tilde{\varphi}, \tilde{\varphi}_z = 0 \quad \text{as} \quad z \to \infty \tag{B-8b}$$

A solution to the above problem is given by

$$\tilde{\varphi} = -\, i(k+\alpha)e^{-|\alpha| z}\tilde{z}_s(\alpha)/|\alpha| \tag{B-9}$$

The transform of the surface pressure amplitude is

$$\tilde{p}_o = i(k+\alpha)\tilde{\varphi}(\alpha;0) \tag{B-10}$$

Introduction of (B-9) gives

$$\tilde{p}_o = -\,(k+\alpha)^2\tilde{z}_s(\alpha)/|\alpha| \tag{B-11}$$

To obtain the amplitude function $\hat{p}_o(x)$ one must formally invert the Fourier transform in (B-11). It is more convenient to use the potential for a distribution of sources situated on the x-axis which simulates the flow and satisfies the differential equation (B-3) and boundary conditions (B-4). For the case of a finite-chord panel on the x-axis between $x = 0$ and $x = 1$ we distribute sources of intensity $q(x)$ per unit length. The perturbation potential amplitude at (x, z) of an individual source located at $(x_1, 0)$ is

$$d\hat{\varphi}(x,z) = 1/2\pi\, q(x)dx \log r \tag{B-12}$$

where r is the distance between the source and the field point. Superimposing the effect of all the sources we obtain the perturbation potential

$$\hat{\varphi}(x,z) = 1/2\pi \int_0^1 q(x_1)\log[(x-x_1)^2 + z^2]^{1/2} dx_1 \tag{B-13}$$

We determine the source distribution $q(x)$ in the following manner. First we obtain the velocity component $\hat{w}$ from (B-13) by differentiating $\hat{\varphi}$

$$\hat{w} = \hat{\varphi}_z = 1/2\pi \int_0^1 q(x_1)\frac{z dx_1}{[(x-x_1)^2 + z^2]} \tag{B-14}$$

We use the boundary condition (B-4a) by requiring that

$$\lim_{z\to 0}\left[1/2\pi\int_0^1 q(x_1)\frac{z}{[(x-x_1)^2+z^2]}dx_1\right] = \hat{w}(x,0) = (ik + d/dx)\hat{z}_s(x) \qquad \text{(B-15)}$$

We find after careful evaluation of the left-hand side of (B-15) (see Section 17.6 and Appendix E.3 of Karamcheti (1966))

$$q(x) = 2\hat{w}(x,0^+) = 2(ik + d/dx)\hat{z}_s(x) \qquad \text{(B-16)}$$

Substituting (B-16) in (B-13), evaluating the potential at $z = 0$, and substituting the result in (B-5) we obtain the surface pressure amplitude

$$\hat{p}_o = -1/\pi(ik + d/dx)\int_0^1 (ik + d/dx_1)\hat{z}_s(x_1)\log|x - x_1|dx_1 \qquad \text{(B-17)}$$

Alternate forms of the same result are

$$\hat{p}_o(x) = -1/\pi(ik + d/dx)^2\int_0^1 \log|x - x_1|\hat{z}_s(x_1)dx_1 \qquad \text{(B-18)}$$

$$\hat{p}_o(x) = -1/\pi\int_0^1 \log|x - x_1|(ik + d/dx_1)^2\hat{z}_s(x_1)dx_1 \qquad \text{(B-19)}$$

APPENDIX C

INVERSION OF THE FOURIER TRANSFORMS OF THE UNSTEADY BOUNDARY-LAYER CONTRIBUTION TO THE SURFACE PRESSURE IN INCOMPRESSIBLE FLOW

The Fourier transform of the unsteady boundary-layer effect is given by

$$\tilde{p}_{BL} = \tilde{p}_1(\alpha;k) + \tilde{p}_2(\alpha;k) \tag{C-1}$$

where

$$\tilde{p}_1 = -\int_0^1 (k + \alpha U)^2 dz^* \tilde{z}_s(\alpha)$$

$$\tilde{p}_2 = (k + \alpha)^4 \tilde{F}(\alpha, k) \tilde{z}_s(\alpha)$$

and where

$$\tilde{F}(\alpha, k) = \int_0^1 (k + \alpha U)^{-2} dz^*$$

The inversion of $\tilde{p}_1$ is accomplished by first integrating with respect to z^* which gives

$$\tilde{p}_1 = -(k^2 + 2kb\alpha + c\alpha^2)\tilde{z}_s(\alpha) \tag{C-2}$$

where

$$b = \int_0^1 U(z^*) dz^*$$

$$c = \int_0^1 U^2(z^*) dz^*$$

Taking the inverse Fourier transform of $\tilde{p}_1$ we find

$$\hat{p}_1(x;k) = 1/2\pi \int_{-\infty}^{\infty} [(ik)^2 + 2(ik)b(i\alpha) + c(i\alpha)^2]\tilde{z}_s e^{ix\alpha} d\alpha \tag{C-3}$$

This is equivalent to

$$\hat{p}_1(x;k) = (ik)^2 \hat{z}_s(x) + 2ikb\hat{z}_s'(x) + a\hat{z}_s''(x) \tag{C-4}$$

where we have used the fact that $(i\alpha)^n z_s(\alpha)$ is the transform of the n-th derivative with respect to x of $\hat{z}_s(x)$.

The inversion of $\tilde{p}_2$ is determined most economically by performing the z^*-integration after the Fourier inversion has been carried out. Taking the inverse transform of $\tilde{p}_2$ and interchanging the order of integration we find

$$\hat{p}_2(x;k) = \int_0^1 U^{-2} 1/2\pi \int_{-\infty}^{\infty} (\alpha + k/U)^{-2} (k + \alpha)^4 \tilde{z}_s(\alpha) e^{ix\alpha} d\alpha dz^* \tag{C-5}$$

Hence

$$\hat{p}_2(x;k) = (ik + d/dx)^4 \int_0^1 U^{-2} 1/2\pi \int_{-\infty}^{\infty} (\alpha + k/U)^{-2} \tilde{z}_s(\alpha) e^{ix\alpha} d\alpha dz^* \tag{C-6}$$

The Fourier inversion indicated in the inner integrals in either (C-5) or (C-6) may be accomplished by use of the convolution theorem for Fourier transforms,

$$1/2\pi \int_{-\infty}^{\infty} \tilde{f}(\alpha)\tilde{g}(\alpha) e^{ix\alpha} d\alpha = \int_{-\infty}^{\infty} f(x - x_1) g(x_1) dx_1 \tag{C-7}$$

Application of this result to (C-5) and (C-6) yields

$$\hat{p}_2(x;k) = \int_0^1 U^{-2} \int_{-\infty}^{\infty} f(x - x_1, U;k)(ik + d/dx_1)^4 \hat{z}_s(x_1) dx_1 dz^* \tag{C-8}$$

or

$$\hat{p}_2(x;k) = (ik + d/dx)^4 \int_0^1 U^{-2} \int_{-\infty}^{\infty} f(x - x_1, U;k) \hat{z}_s(x_1) dx_1 dz^* \tag{C-9}$$

where

$$f(x, U;k) = 1/2\pi \int_{-\infty}^{\infty} (\alpha + k/U)^{-2} e^{ix\alpha} d\alpha \qquad \text{(C-10)}$$

Interchange of the order of integration produces the equivalent forms

$$\hat{p}_2(x) = \int_{-\infty}^{\infty} K(x - x_1;k)(ik + d/dx_1)^4 \hat{z}_s(x_1)dx_1 \qquad \text{(C-11)}$$

or

$$\hat{p}_2(x) = (ik + d/dx)^4 \int_{-\infty}^{\infty} K(x - x_1;k)\hat{z}_s(x_1)dx_1 \qquad \text{(C-12)}$$

where the kernel function is given by the following integral:

$$K(x;k) = \int_{o}^{1} U^{-2} f(x, U;k)dz^* \qquad \text{(C-13)}$$

The function $f(x, U;k)$ may be obtained by inverting the Fourier transform as indicated in (C-10). In order for the integral to converge, k must have a negative imaginary part that may be taken to be infinitesimally small. With this provision we can evaluate the transform in (C-10) which can be expressed in a form suitable for evaluation by means of contour integration

$$f(x, \gamma_o) = 1/2\pi \int_{-\infty}^{\infty} (\alpha - \gamma_o)^{-2} e^{ix\alpha} d\alpha \qquad \text{(C-14)}$$

where

$$\gamma_o = - k/U$$

We shall employ contour integration in the complex plane defined by $\gamma = \alpha + i\beta$. Consider a function F of the complex variable γ,

$$F(\gamma) = \frac{1}{2\pi} (\gamma - \gamma_o)^{-2} e^{ix\gamma} \qquad \text{(C-15)}$$

which has a double-pole singularity at $\gamma = \gamma_o$, a point assumed to be located in the upper left-hand quadrant of the complex plane. Consider the following contours in the γ-plane:

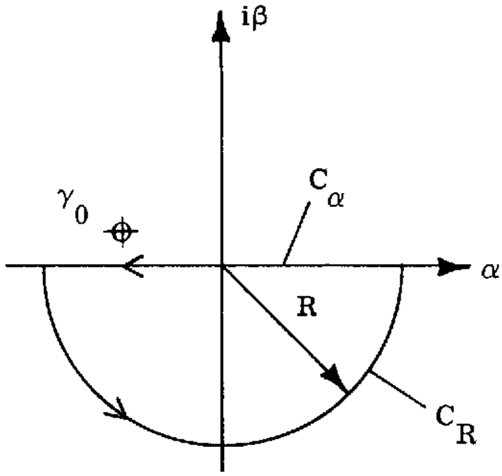

Contour for $x < 0$

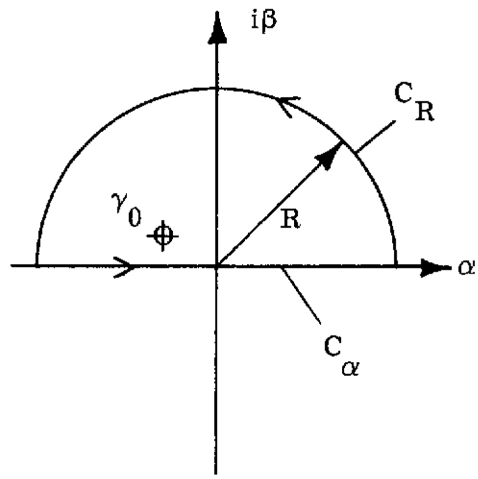

Contour for $x > 0$

The residue theorem provides a means of calculating an integral around a closed contour, namely,

$$\oint_C F(\gamma) d\gamma = 2\pi i \Sigma \text{ Residues of } F(\gamma) \tag{C-16}$$

provided $F(\gamma)$ is analytic everywhere on and inside the contour except for a finite number of singularities inside the contour. We can apply the theorem to the contours shown here. For either contour the theorem gives

$$\int_{C_\alpha} F(\alpha) d\alpha + \int_{C_R} F(\gamma) d\gamma = 2\pi i \Sigma \text{ Res } F(\gamma) \tag{C-17}$$

Consider first the case where $x < 0$. For this case $F(\gamma)$ has no singularities within the contour so that the right-hand side of (C-17) is zero. In the limit as $R \to \infty$ the integral on C_R is zero and the integral on the α-axis is the negative of $f(x, \gamma_o)$. Hence,

$$f(x, \gamma_o) = 0, \qquad x < 0 \tag{C-18}$$

Consider next the case where $x > 0$. In this case $F(\gamma)$ has a double pole singularity within the contour. In the limit as $R \to \infty$ the integral on C_R is zero, and we have

$$f(x,\gamma_o) = 2\pi i \text{ Res } F(\gamma)\Big|_{\gamma=\gamma_o} \tag{C-19}$$

For the double-pole singularity the residue is found to be

$$\text{Res } F(\gamma)\Big|_{\gamma=\gamma_o} = \frac{d}{d\gamma}\left[(\gamma - \gamma_o)^2 F(\gamma)\right]\Big|_{\gamma=\gamma_o} \tag{C-20}$$

Thus,

$$f(x,\gamma_o) = -\,x e^{i\gamma_o x}, \qquad x > 0 \tag{C-21}$$

The kernel function defined in (C-13) with (C-18) and (C-21) is

$$K(x;k) = \begin{cases} 0, & x < 0 \\ -\,x\displaystyle\int_0^1 U^{-2} e^{-ikx/U} dz^*, & x > 0 \end{cases} \tag{C-22}$$

Since the kernel is zero for negative values of its argument the integral in (B-11) which gives the pressure can be written as

$$\hat{p}_2(x;k) = \int_{-\infty}^{x} K(x - x_1;k)(ik + d/dx_1)^4 \hat{z}_s(x_1)dx_1 \tag{C-23}$$

for a generalized disturbance, and as

$$\hat{p}_2(x;k) = \int_{0}^{x} K(x - x_1;k)(ik + d/dx_1)^4 \hat{z}_s(x_1)dx_1 \tag{C-24}$$

for a finite-chord panel on the x-axis between $x = 0$ and $x = 1$.

APPENDIX D

INVERSION OF THE FOURIER TRANSFORMS OF THE UNSTEADY BOUNDARY-LAYER CONTRIBUTION TO THE SURFACE PRESSURE IN COMPRESSIBLE FLOW

The Fourier transform of the unsteady boundary-layer effect is given by

$$\tilde{p}_{BL} = \tilde{p}_1 + \tilde{p}_2 \tag{D-1}$$

where

$$\tilde{p}_1 = -\int_0^1 \rho(k + \alpha U)^2 dz^* \tilde{z}_s$$

$$\tilde{p}_2 = \frac{(k + \alpha)^4 \left(-\alpha^2 \int_0^1 \rho^{-1}(k + \alpha U)^{-2} dz^* + M_\infty^2\right)\tilde{z}_s}{(M_\infty^2 - 1)(\alpha - \gamma_1)(\alpha - \gamma_2)}$$

and where

$$\gamma_1 = -kM_\infty/(M_\infty - 1)$$

$$\gamma_2 = -kM_\infty/(M_\infty + 1)$$

The inversion of (D-1) gives

$$\hat{p}_{BL} = 1/2\pi \int_{-\infty}^{\infty} (\tilde{p}_1 + \tilde{p}_2) e^{ix\alpha} d\alpha \tag{D-2}$$

We treat the first term by performing the z*-integration before inverting. Thus

$$\hat{p}_1(x;k) = 1/2\pi \int_{-\infty}^{\infty} [(ik)^2 a + 2(ik)b(i\alpha) + c(i\alpha)^2]\tilde{z}_s e^{ix\alpha} d\alpha \tag{D-3}$$

where

$$a = \int_0^1 \rho dz^*$$

$$b = \int_0^1 \rho U dz^*$$

$$c = \int_0^1 \rho U^2 dz^*$$

Note that a, b, c are functions of M_∞ since ρ depends upon M_∞. Now inverting each term in the above expression we obtain

$$p_1(x;k, M_\infty) = (ik)^2 a\hat{z}_s(x) + 2ikb\hat{z}_s'(x) + c\hat{z}_s''(x) \tag{D-4}$$

This is quite similar to the expression for incompressible flow, (see Appendix C) except that the coefficients a, b and c depend upon the freestream Mach number, M_∞.

We treat the second term by noting that the inverse of the product of two Fourier transforms is their convolution. This gives

$$\hat{p}_2(x;k, M_\infty) = (ik + d/dx)^4 \int_{-\infty}^{\infty} K(x - x_1;k, M_\infty)\hat{z}_s(x_1)dx_1 \tag{D-5}$$

or equivalently,

$$\hat{p}_2(x;k, M_\infty) = \int_{-\infty}^{\infty} K(x - x_1;k, M_\infty)(ik + d/dx_1)^4 \hat{z}_s(x_1)dx_1 \tag{D-6}$$

where

$$K(x;k, M_\infty) = K_1(x;k, M_\infty) + K_2(x;k, M_\infty)$$

where the Kernel functions K_1 and K_2 are the inverse Fourier transforms

$$K_1(x;k, M_\infty) = -1/(2\pi B^2) \int_{-\infty}^{\infty} \frac{\alpha^2 \int_0^1 \rho^{-1}(k + \alpha U)^{-2} dz^* e^{ix\alpha}}{(\alpha - \gamma_1)(\alpha - \gamma_2)} d\alpha \tag{D-7}$$

$$K_2(x;k,M_\infty) = M_\infty^2/(2\pi B^2)\int_{-\infty}^{\infty}\frac{e^{ix\alpha}}{(\alpha-\gamma_1)(\alpha-\gamma_2)}d\alpha \tag{D-8}$$

where

$$B^2 = M_\infty^2 - 1$$

By interchanging the order of integration in (D-7) we can express K_1 as follows:

$$K_1(x;k,M_\infty) = \int_0^1 \rho^{-1}U^{-2}F_1(x,U;k,M_\infty)dz^* \tag{D-9}$$

$$F_1(x,U;k,M_\infty) = -1/(2\pi B^2)\int_{-\infty}^{\infty}\frac{\alpha^2 e^{ix\alpha}}{(\alpha-\gamma_o)^2(\alpha-\gamma_1)(\alpha-\gamma_2)}d\alpha \tag{D-10}$$

and where

$$\gamma_o = -k/U$$

We can evaluate the expressions for K_2 and F_1 by contour integration in the complex γ-plane, $\gamma = \alpha + i\beta$. Since we assume that k is complex with a negative imaginary part (see Appendix C) the integrands in (D-8) and (D-10) have isolated singularities at $\gamma = \gamma_o$, γ_1, and γ_2. Note that the location of γ_1 and γ_2 is dependent upon the freestream Mach number, M_∞. In particular, γ_1 is located in the lower half-plane depending upon whether the freestream is subsonic or supersonic. For this reason we consider these two cases separately. We will use the same two contours as in the incompressible case (see figures in Appendix C) depending upon the sign of x. For $x < 0$ we use the semi-circular contour located in the lower half-plane. Recall that for these contours the contribution of the semi-circular portion of the contour, C_R, is zero for integrals of the form

$$\lim_{R\to\infty}\int_{C_R} f_i(\gamma)d\gamma$$

where

$$f_2 = \frac{M_\infty^2}{2\pi B^2} (\gamma - \gamma_1)^{-1}(\gamma - \gamma_2)^{-1} e^{ix\gamma} \quad \text{for evaluating } K_2$$

$$f_1 = - \frac{\gamma^2}{2\pi B^2} (\gamma - \gamma_o)^{-2}(\gamma - \gamma_1)^{-1}(\gamma - \gamma_2)^{-1} e^{ix\gamma} \qquad \text{(D-11)}$$

for evaluating F_1

For subsonic flow ($M_\infty < 1$) γ_o and γ_2 are located in the upper left quadrant while γ_1 is located in the lower right quadrant. By application of the residue theorem (see Appendix C) we obtain

$$K_2 = \begin{cases} -2\pi i \, \text{Residue}[f_2(\gamma)] \Big|_{\gamma=\gamma_1}, & x < 0 \\ 2\pi i \, \text{Residue}[f_2(\gamma)] \Big|_{\gamma=\gamma_2}, & x > 0 \end{cases} \qquad \text{(D-12)}$$

Evaluating the residues using (D-11) and using the definitions of γ_1 and γ_2 we have

$$K_2(x;k,M_\infty) = \begin{cases} iM_\infty/(2k)e^{-ikx/U_1}, & x < 0 \\ iM_\infty/(2k)e^{-ikx/U_2}, & x > 0 \end{cases} \qquad \text{(D-13)}$$

where

$$U_1 = (M_\infty - 1)/M_\infty$$

$$U_2 = (M_\infty + 1)/M_\infty$$

The residue theorem also yields

$$F_1 = \begin{cases} -2\pi i \, \text{Residue}[f_1(\gamma_1)] \Big|_{\gamma=\gamma_1}, & x < 0 \\ 2\pi i \Sigma \, \text{Residues}[f_1(\gamma)] \Big|_{\gamma=\gamma_o, \gamma_2}, & x > 0 \end{cases} \qquad \text{(D-14)}$$

Note that in this case there is a double-pole singularity at $\gamma = \gamma_o$ in addition to the two simple poles at $\gamma = \gamma_1$ and γ_2. Evaluating the residues in (D-14) and simplifying the result using partial fractions we obtain

$$F_1(x, U;k, M_\infty) = \begin{cases} -\, i/(2kM_\infty)U^2(U - U_1)^{-2}e^{-ikx/U_1}, & x < 0 \\ i/(2kM_\infty)\Big\{-\, U^2(U - U_2)^{-2}e^{-ikx/U_2} + \\ \quad + [U_2U(U - U_2)^{-2} - U_1U(U - U_1)^{-2} + \\ \quad + (ikx - U)((U - U_1)^{-1} - (U - U_2)^{-1})]e^{-ikx/U}\Big\}, \\ x > 0 \end{cases} \tag{D-15}$$

For supersonic flow $(M_\infty > 1)$ we find that all three singularities are located in the upper left quadrant of the complex plane. Since there are no singularities within the contour for $x < 0$, both K_2 and F_1 are zero for $x < 0$; hence we can replace the upper limit of the integrals in (D-5) and (D-6) with x. For $x > 0$ we have

$$K_2 = 2\pi i \Sigma\, \text{Residues}[f_2(\gamma)]\Big|_{\gamma=\gamma_1, \gamma_2} \tag{D-16}$$

$$F_1 = 2\pi i \Sigma\, \text{Residues}[f_1(\gamma)]\Big|_{\gamma=\gamma_o, \gamma_1, \gamma_2} \tag{D-17}$$

By evaluating the residues using (D-15) we obtain for $x > 0$

$$K_2(x;k, M_\infty) = iM_\infty/2k(e^{-ikx/U_2} - e^{-ikx/U}) \tag{D-18}$$

$$\begin{aligned} F_1(x, U;k, M_\infty) = i/(2kM_\infty)\Big\{&U^2(U - U_1)^{-2}e^{-ikx/U_1} \\ &- U^2(U - U_2)^{-2}e^{-ikx/U_2} + [U_2U(U - U_2)^{-2} - U_1U(U - U_1)^{-2} \\ &+ (ikx - U)((U - U_1)^{-1} - (U - U_2)^{-1})]e^{-ikx/U}\Big\} \end{aligned} \tag{D-19}$$

It is interesting to note that the kernel function in (D-6) for the supersonic case exhibits no upstream influence in the sense that the function is zero for negative values of the argument $x - x_1$. In the case of subsonic flow the kernel function is nonzero for both positive and negative values of the argument $x - x_1$.

Note the existence of apparent singularities in F_1 at $U = U_1, U_2$. (See (D-15), (D-16).) These can affect the determination of K_1 using (D-9) if the singularities occur for z^* between 0 and 1. This is equivalent to the range of U between 0 and 1. We note that for subsonic flow the singularities occur outside the range of integration, while for supersonic flow only the singularity at U_1 is within the range of integration. If we expand F_1 in (D-19) in a power series in powers of $(U - U_1)$ and take the limit as $(U - U_1)$ approaches zero we find that the two lowest order terms of $0(U - U_1)^{-2}$ and $0(U - U_1)^{-1}$ are identically zero, leaving terms of $0(1)$ and higher. The singularity at U_1 is only apparent and does not affect the evaluation of K_1.

Note that we recover the incompressible limit in the subsonic case as $M_\infty \to 0$. In the limit of small M_∞ we have $U_1 = -1/M_\infty$ and $U_2 = 1/M_\infty$. Substituting these in (D-13) and (D-15) and taking the limit as M_∞ approaches zero we find $K_2 = 0$ and

$$F_1(x, U;k, 0) = \begin{cases} 0, & x < 0 \\ -xe^{-ikx/U}, & x > 0 \end{cases} \tag{D-20}$$

This gives

$$K(x;k, 0) = -x\int_0^1 U^{-2} e^{-ikx/U} dz^* \tag{D-21}$$

For the transonic case we find that by taking the limit as $M_\infty \to 1$ in either (D-13) and (D-15) or (D-18) and (D-19) we obtain

$$K_2(x;k, M_\infty = 1) = \begin{cases} 0, & x < 0 \\ \frac{i}{2k} e^{-ikx/2}, & x > 0 \end{cases} \tag{D-22}$$

$$F_1(x, U;k, M_\infty = 1) = \begin{cases} 0, & x < 0 \\ \frac{i}{2k} \left\{ U^2 (U - 2)^{-2} e^{-ikx/2} + [(ikx - U)(U - 2)^{-1} \right. \\ \left. \quad - 2U(U - 2)^{-2}] e^{-ikx/U} \right\}, & x > 0 \end{cases} \tag{D-23}$$

APPENDIX E

EVALUATION OF THE INTEGRALS $H_1(c)$ AND $K_1(c)$ FOR A LOGARITHMIC MEAN SHEAR VELOCITY PROFILE

We want to evaluate

$$H_1(c) = c^2 - 2b_1 c + c_1 \tag{E-1}$$

where

$$b_1 = \int_0^1 U(z^*)\,dz^* \tag{E-2}$$

and where

$$c_1 = \int_0^1 U^2(z^*)dz^* \tag{E-3}$$

and

$$K_1(c) = -z^{*\prime}(0)/c - z^{*\prime}(1)/(1-c) + I_s + I_r \tag{E-4}$$

where

$$I_s = z_c^{*\prime\prime}\,\{\log[(1-c)/c] - i\pi\} \tag{E-5}$$

and where

$$I_r = \int_0^1 \frac{(z^{*\prime\prime} - z_c^{*\prime\prime})dz^*}{(U-c)} \tag{E-6}$$

for

$$U(z^*) = U_1 \log(z^*/z_0^*) \tag{E-7}$$

or, equivalently,

$$z^* = z_0^*\, e^{U/U_1} \tag{E-8}$$

Substituting (E-7) in (E-2) we have

$$b_1 = U_1 \int_0^1 \log(z^*/z_0^*) dz^* \tag{E-9}$$

Changing variables using $t = z^*/z_0^*$ we find (E-10)

$$b_1 = U_1 z_0^* \int_0^{z_0^{*-1}} \log t \, dt \tag{E-11}$$

This integrates to

$$b_1 = U_1 z_0^* (t \log t - t) \Big|_0^{z_0^{*-1}} \tag{E-12}$$

Evaluating the result at the two limits and noting that

$$\lim_{t \to 0} (t \log t) = 0 \tag{E-13}$$

we find

$$b_1 = -U_1 [\log z_0^* + 1] \tag{E-14}$$

We may simplify this expression by eliminating one of the parameters. Evaluating the profile at the edge of the boundary layer where $U(1) = 1$ we find that

$$\log z_0^* = -1/U_1 \tag{E-15}$$

Substituting this result in (E-14) we have

$$b_1 = 1 - U_1 \tag{E-16}$$

Similarly, by substituting (E-7) in (E-3) we have

$$c_1 = U_1^2 \int_0^1 [\log(z^*/z_0^*)]^2 dz^* \tag{E-17}$$

Changing variables using (E-10) and integrating we obtain

$$c_1 = U_1^2 z_0^* [t(\log t)^2 - 2t \log t + 2t] \Big|_0^{z_0^{*-1}} \tag{E-18}$$

Evaluating (E-18) at the two limits using (E-13) and using L'Hospital's rule to evaluate

$$\begin{aligned}
\lim_{t\to 0}[t(\log t)^2] &= \lim_{u\to\infty} \frac{[\log(u^{-1})]^2}{u} \\
&= \lim_{u\to\infty} \frac{2\log(u^{-1})\cdot u(-u^{-2})}{1} \\
&= -2 \lim_{t\to 0} t \log t \\
&= 0,
\end{aligned} \tag{E-19}$$

we find using (E-15) that

$$c_1 = 1 - 2U_1 + 2U_1^2 \tag{E-20}$$

We note that (E-7) is not accurate right down to $z^* = 0$ where it gives $U = -\infty$, but the contribution to b_1 and c_1 for negative values of U is negligible for z_0^* sufficiently small.

To evaluate K_1 we take the derivatives using (E-8) and find

$$z^{*\prime} = z_0^* e^{U/U_1}/U_1 = z^*/U_1 \tag{E-21}$$

and

$$z^{*\prime\prime} = z_0^* e^{U/U_1}/U_1^2 = z^*/U_1^2 \tag{E-22}$$

Evaluating (E-21) at $U = 0, 1$ we find

$$z^{*\prime}(0) = z_0^*/U_1 \tag{E-23}$$

and

$$z^{*\prime}(1) = (z_0^*/U_1)e^{1/U_1} \tag{E-24}$$

Evaluating (E-22) at $U = c$ we find

$$z_c^{*''} = z^{*''}(c) = z_0^* e^{c/U_1}/U_1^2 \tag{E-25}$$

Substituting (E-22) and (E-25) in (E-6) we have

$$I_r = z_0^*/U_1^2 \int_0^1 \frac{(e^{U/U_1} - e^{c/U_1})dU}{(U-c)} \tag{E-26}$$

Making a change of variables

$$w = (U-c)/U_1 \tag{E-27}$$

We find upon simplification using (E-25)

$$I_r = z_c^{*''} \int_{-c/U_1}^{(1-c)/U_1} (e^w - 1)dw/w \tag{E-28}$$

The integrand in (E-28) is finite at $w = 0$ by L'Hospital's rule

$$\lim_{w \to 0} (e^w - 1)/w = \lim_{w \to 0} e^w/1 = 1, \tag{E-29}$$

and the integral in (E-28) may be evaluated using the power series representation for the exponential. We find after integrating the series term by term

$$I_r = z_c^{*''}\{f[(1-c)/U_1] - f[-c/U_1]\} \tag{E-30}$$

where

$$f[w] = \sum_{n=1}^{\infty} \frac{w^n}{n \cdot n!} \tag{E-31}$$

Substituting equations (E-5), (E-23), (E-24), (E-25), and (E-30) in (E-4) we obtain

$$K_1(c) = K_1^R(c) + i K_1^I(c) \tag{E-32}$$

where

$$K_1^R(c) = -z_0^*/(U_1 c) - z_0^* e^{1/U_1}/[U_1(1-c)]$$

$$+ z_0^* e^{c/U_1}/U_1^2 \{\log[(1-c)/c] + f[(1-c)/U_1] - f[-c/U_1]\} \qquad \text{(E-33)}$$

$$K_1^I(c) = -\pi z_0^* e^{c/U_1}/U_1^2 \qquad \text{(E-34)}$$

APPENDIX F

EVALUATION OF THE UNSTEADY BOUNDARY-LAYER CONTRIBUTION TO THE GENERALIZED AERODYNAMIC FORCE FOR SUPERSONIC FLOW OVER A CLAMPED PLATE USING A POWER-LAW VELOCITY PROFILE

The unsteady boundary-layer contribution to the generalized aerodynamic force given in terms of the mechanical admittance for simple harmonic motion is

$$H_{mn_{BL}} = \delta_0 \frac{1}{2\pi} \int_{-\infty}^{\infty} \widetilde{K}_{BL}(\alpha;k,M_\infty)G_{mn}(\alpha)d\alpha \tag{F-1}$$

where

$$\widetilde{K}_{BL}(\alpha;k,M_\infty) = \widetilde{K}_1 + \widetilde{K}_2 \tag{F-2}$$

$$\widetilde{K}_1 = -\int_0^1 \rho(k+\alpha U)^2 dz^* \tag{F-3}$$

$$\widetilde{K}_2 = \frac{(k+\alpha)^4 \left[-\alpha^2 \int_0^1 \rho^{-1}(k+\alpha U)^{-2} dz^* + M_\infty^2\right]}{B^2(\alpha-\gamma_1)(\alpha-\gamma_2)} \tag{F-4}$$

and where

$$B^2 = M_\infty^2 - 1 \tag{F-5}$$

$$\gamma_1 = -kM_\infty/(M_\infty - 1) \tag{F-6}$$

$$\gamma_2 = -kM_\infty/(M_\infty + 1) \tag{F-7}$$

$$\rho = [1 + (\gamma-1)/2\, M_\infty^2(1-U)^2]^{-1} \tag{F-8}$$

where

$$G_{mn}(\alpha) = \int_0^1 \psi_m(x)e^{-i\alpha x}dx \int_0^1 \psi_n(\alpha)e^{i\alpha x}dx \tag{F-9}$$

and where

$$\psi_m(x) = \cos[(m-1)\pi x]-\cos[(m+1)\pi x] \tag{F-10}$$

is the mode shape for a clamped plate-column satisfying the end conditions

$$\psi_m(x) = \psi'_m(x) = 0, \quad x = 0,1 \tag{F-11}$$

Substituting (F-10) in (F-9) and evaluating the resulting integrals we obtain

$$G_{mn} = \frac{16mn\pi^2\alpha^2[1+(-1)^m e^{-i\alpha}+(-1)^n e^{i\alpha}+(-1)^{m+n}]}{[\alpha^2-(m-1)^2\pi^2][\alpha^2-(m+1)^2\pi^2][\alpha^2-(n-1)^2\pi^2][\alpha-(n+1)^2\pi^2]} \tag{F-12}$$

Substituting (F-2) through (F-4) in (F-1) we obtain

$$H_{mn_{BL}} = \delta_0[I_{mn}+J_{mn}+K_{mn}] \tag{F-13}$$

where

$$I_{mn} = -\frac{1}{2\pi}\int_{-\infty}^{\infty}\int_0^1 \rho(k^2+2\alpha kU+\alpha^2U^2)G_{mn}dz^*d\alpha \tag{F-14}$$

$$J_{mn} = M_\infty^2/(2\pi B^2)\int_{-\infty}^{\infty}\frac{(k+\alpha)^4G_{mn}(\alpha)d\alpha}{(\alpha-\gamma_1)(\alpha-\gamma_2)} \tag{F-15}$$

$$K_{mn} = -1/(2\pi B^2)\int_{-\infty}^{\infty}\int_0^1 \frac{\alpha^2(k+\alpha)^4\rho^{-1}U^{-2}G_{mn}dz^*d\alpha}{(\alpha-\gamma_1)(\alpha-\gamma_2)(\alpha-\gamma_0)^2} \tag{F-16}$$

and where

$$\gamma_0 = -k/U(z^*) \tag{F-17}$$

We can express (F-14) compactly as

$$I_{mn} = -[aA_{mn}k^2 + 2bB_{mn}k + cC_{mn}] \tag{F-18}$$

where

$$a = \int_0^1 \rho dz^* = \int_0^1 \rho z^{*\prime}(U)dU \tag{F-19}$$

$$b = \int_0^1 \rho U dz^* = \int_0^1 \rho U z^{*\prime}(U)dU \tag{F-20}$$

$$c = \int_0^1 \rho U^2 dz^* = \int_0^1 \rho U^2 z^{*\prime}(U)dU \tag{F-21}$$

and where

$$A_{mn} = 1/(2\pi)\int_{-\infty}^{\infty} G_{mn}d\alpha \tag{F-22}$$

$$B_{mn} = 1/(2\pi)\int_{-\infty}^{\infty} \alpha G_{mn}d\alpha \tag{F-23}$$

$$C_{mn} = 1/(2\pi)\int_{-\infty}^{\infty} \alpha^2 G_{mn}d\alpha \tag{F-24}$$

Interchanging the order of integration in (F-16) we have

$$K_{mn} = \int_0^1 \rho^{-1}U^{-2}L_{mn}dz^* = \int_0^1 \rho^{-1}U^{-2}z^{*\prime}(U)L_{mn}dU \tag{F-25}$$

where

$$L_{mn} = \frac{-1}{2\pi B^2} \int_{-\infty}^{\infty} \frac{\alpha^2 G_{mn} \, d\alpha}{(\alpha-\gamma_1)(\alpha-\gamma_2)(\alpha-\gamma_0)^2} \tag{F-26}$$

One can evaluate the integrals (F-15), (F-22) through (F-24), and (F-26) using the expression in (F-12) for G_{mn}. We will illustrate the procedure for the case $m = n = 1$. In that case (F-12) may be simplified to

$$G_{11} = \frac{2(2\pi)^4(1-\cos\alpha)}{\alpha^2(\alpha-2\pi)^2(\alpha+2\pi)^2} \tag{F-27}$$

where we have used the identity

$$\cos\alpha = 1/2(e^{i\alpha} + e^{-i\alpha}) \tag{F-28}$$

Note that G_{11} has apparent singularities at $\alpha = 0, \pm 2\pi$. Taking the limit of the expression in (F-27) and applying L' Hospital' s rule successively we find that the limits G_{11} as $\alpha \to 0, \pm 2\pi$ are finite. The fact that G_{11} is analytic allows us to use contour integration to evaluate the desired integrals; however care must be taken to include the contributions to the integral from the apparent singularities. For each of the integrals we choose the contour Γ_1 in the complex γ-plane as shown in the sketch below

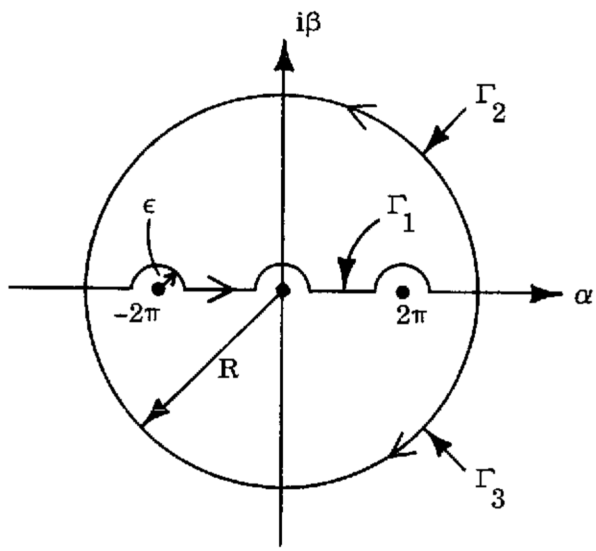

An equivalent contour for Γ_1 would be the line $\beta = \epsilon$ where ϵ is the infinitesimal radius of the small semi-circles above. In the limit as $\epsilon \to 0$ this contour is equivalent to the one in the sketch.

We evaluate A_{11} by substituting (F-27) and (F-28) in (F-22) to obtain

$$A_{11} = 2(2\pi)^3 [I_1 - I_2 - I_3] \tag{F-29}$$

where

$$I_1 = \int_{-\infty}^{\infty} \frac{d\alpha}{\alpha^2(\alpha-2\pi)^2(\alpha+2\pi)^2} \tag{F-30}$$

$$I_2 = 1/2 \int_{-\infty}^{\infty} \frac{e^{i\alpha} d\alpha}{\alpha^2(\alpha-2\pi)^2(\alpha+2\pi)^2} \tag{F-31}$$

$$I_3 = 1/2 \int_{-\infty}^{\infty} \frac{e^{-i\alpha} d\alpha}{\alpha^2(\alpha-2\pi)^2(\alpha+2\pi)^2} \tag{F-32}$$

We evaluate these integrals using the appropriate contour in the sketch above. Thus to evaluate (F-30) we apply the residue theorem to obtain

$$\int_{\Gamma_1} f(\gamma)d\gamma + \int_{\Gamma_2} f(\gamma)d\gamma = 0 \tag{F-33}$$

where

$$f(\gamma) = \frac{1}{\gamma^2(\gamma-2\pi)^2(\gamma+2\pi)^2} \tag{F-34}$$

In the limit as $\epsilon \to 0$ and $R \to \infty$ the first integral is I_1 and the second integral is zero since the magnitude of the integral is $O(R^{-5})$ as R becomes large. Thus

$$I_1 = 0 \tag{F-35}$$

Similarly, applying the residue theroem to evaluate (F-31) we have

$$1/2 \int_{\Gamma_1} f(\gamma)e^{i\gamma}d\gamma + 1/2 \int_{\Gamma_2} f(\gamma)e^{i\gamma}d\gamma = 0$$

Again we take the limits, note that the first integral is I_2 and the second integral is zero since its magnitude is $O(R^{-5}e^{-R})$ as R becomes large. Thus,

$$I_2 = 0 \tag{F-36}$$

Applying the same technique to evaluate (F-32) we have

$$1/2 \int_{\Gamma_1} f(\gamma)e^{-i\gamma}d\gamma + 1/2 \int_{\Gamma_2} f(\gamma)e^{-i\gamma}d\gamma = 2\pi i \sum_{\gamma=0,2\pi,-2\pi} \mathrm{Res}[\tfrac{1}{2}f(\gamma)e^{-i\gamma}] \tag{F-37}$$

Note that we have used the large lower semi-circular contour in this case to take advantage of the fact that the contribution of the second integral is zero in the limit as $R \to \infty$. Upon taking the limits the left-hand side of (F-37) becomes equal to I_3. Evaluating the residues in (F-37), substituting this along with (F-35) and (F-36) into (F-29), we obtain

$$A_{11} = 3/2 \tag{F-38}$$

By the same technique we find that

$$B_{11} = 0 \tag{F-39}$$

$$C_{11} = 2\pi^2 \tag{F-40}$$

Note that we could have surmised the result in (F-39) by simply noting that the integrand is an odd function of α [see (F-23), (F-27)] and hence is equal to zero over the doubly-infinite range of integration.

Similarly we evaluate J_{11} using (F-15), (F-27), (F-28), and the technique of separating the integral into 3 integrals as in (F-29). In this case the integrand has singularities at γ_1 and γ_2 located in the upper-half plane for infinitesimal negative values of the imaginary part of k. Evaluating the integrals using the residue theorem and taking the limit as $I_m(k) \to 0$ we obtain after a little manipulation

$$J_{11} = M_\infty^2 \alpha_0^4 / B^2 \, [j_{11}^R + i \, j_{11}^I] \tag{F-41}$$

where

$$j_{11}^R = \frac{1}{(\gamma_1-\gamma_2)} \left[\frac{(\gamma_1+k)^4 \sin\gamma_1}{\gamma_1^2(\gamma_1-\alpha_0)^2(\gamma_1+\alpha_0)^2} - \frac{(\gamma_2+k)^4 \sin\gamma_2}{\gamma_2^2(\gamma_2-\alpha_0)^2(\gamma_2+\alpha_0)^2} \right]$$

$$+ \frac{(k+\alpha_0)^4}{4(\gamma_1-\alpha_0)(\gamma_2-\alpha_0)\alpha_0^4} + \frac{(k-\alpha_0)^4}{4(\gamma_1+\alpha_0)^2(\gamma_2+\alpha_0)^2} + \frac{k^4}{\gamma_1\gamma_2\alpha_0^4}$$

$$j_{11}^I = \frac{1}{(\gamma_1-\gamma_2)} \left[\frac{(\gamma_1+k)^4(1-\cos\gamma_1)}{\gamma_1^2(\gamma_1-\alpha_0)^2(\gamma_1+\alpha_0)^2} - \frac{(\gamma_2+k)^4(1-\cos\gamma_2)}{\gamma_2^2(\gamma_2-\alpha_0)^2(\gamma_2+\alpha_0)^2} \right]$$

where $\alpha_0 = 2\pi$. Similarly, we evaluate L_{11} using (F-26) through (F-28) and by applying the same technique using the residue theorem and noting the appearance of an additional double-pole singularity at γ_0, we obtain

$$L_{11} = -\alpha_0^4/B^2 [\ell_{11}^R + i \, \ell_{11}^I] \tag{F-42}$$

where

$$\ell_{11}^R = \frac{1}{(\gamma_1-\gamma_2)} \left[\frac{(\gamma_1+k)^4 \sin\gamma_1}{(\gamma_1-\gamma_0)^2(\gamma_1-\alpha_0)^2(\gamma_1+\alpha_0)^2} - \frac{(\gamma_2+k)^4 \sin\gamma_2}{(\gamma_2-\gamma_0)^2(\gamma_2-\alpha_0)^2(\gamma_2+\alpha_0)^2} \right]$$

$$+ \sin\gamma_0 \left\{ \frac{4(\gamma_0+k)^3}{(\gamma_0-\gamma_1)(\gamma_0-\gamma_2)(\gamma_0-\alpha_0)^2(\gamma_0+\alpha_0)^2} \right.$$

(continued)

$$-(\gamma_0+k)^4\left[\frac{1}{(\gamma_0-\gamma_1)^2(\gamma_0-\gamma_2)(\gamma_0-\alpha_0)^2(\gamma_0+\alpha_0)^2}\right.$$

$$+\frac{1}{(\gamma_0-\gamma_1)(\gamma_0-\gamma_2)^2(\gamma_0-\alpha_0)^2(\gamma_0+\alpha_0)^2}+\frac{2}{(\gamma_0-\gamma_1)(\gamma_0-\gamma_2)(\gamma_0-\alpha_0)^3(\gamma_0+\alpha_0)^2}$$

$$\left.\left.+\frac{2}{(\gamma_0-\gamma_1)(\gamma_0-\gamma_2)(\gamma_0-\alpha_0)^2(\gamma_0+\alpha_0)^3}\right]\right\}+\frac{(k+\gamma_0)^4\cos\gamma_0}{(\gamma_0-\gamma_1)(\gamma_0-\gamma_2)(\gamma_0-\alpha_0)^2(\gamma_0+\alpha_0)^2}$$

$$+\frac{1}{4\alpha_0^2}\left[\frac{(k+\alpha_0)^4}{(\gamma_1-\alpha_0)(\gamma_2-\alpha_0)(\gamma_0-\alpha_0)^2}+\frac{(k-\alpha_0)^4}{(\gamma_1+\alpha_0)(\gamma_2+\alpha_0)(\gamma_0+\alpha_0)^2}\right]$$

$$\ell_{11}^{I}=\frac{1}{(\gamma_1-\gamma_2)}\left[\frac{(\gamma_1+k)^4(1-\cos\gamma_1)}{(\gamma_1-\gamma_0)^2(\gamma_1-\alpha_0)^2(\gamma_1+\alpha_0)^2}-\frac{(\gamma_2+k)^4(1-\cos\gamma_2)}{(\gamma_2-\gamma_0)^2(\gamma_2-\alpha_0)^2(\gamma_2+\alpha_0)^2}\right]$$

$$+(1-\cos\gamma_0)\left\{\frac{4(\gamma_0+k)^3}{(\gamma_0-\gamma_1)(\gamma_0-\gamma_2)(\gamma_0-\alpha_0)^2(\gamma_0+\alpha_0)^2}\right.$$

$$-(\gamma_0+k)^4\left[\frac{1}{(\gamma_0-\gamma_1)^2(\gamma_0-\gamma_2)(\gamma_0-\alpha_0)^2(\gamma_0+\alpha_0)^2}\right.$$

$$+\frac{1}{(\gamma_0-\gamma_1)(\gamma_0-\gamma_2)^2(\gamma_0-\alpha_0)^2(\gamma_0+\alpha_0)^2}+\frac{2}{(\gamma_0-\gamma_1)(\gamma_0-\gamma_2)(\gamma_0-\alpha_0)^3(\gamma_0+\alpha_0)^2}$$

$$\left.\left.+\frac{2}{(\gamma_0-\gamma_1)(\gamma_0-\gamma_2)(\gamma_0-\alpha_0)^2(\gamma_0+\alpha_0)^3}\right]+\frac{(k+\gamma_0)^4\sin\gamma_0}{(\gamma_0-\gamma_1)(\gamma_0-\gamma_2)(\gamma_0-\alpha_0)^2(\gamma_0+\alpha_0)^2}\right\}$$

Note that the expressions in (F-41) and (F-42) have apparent singularities for values of k such that

$$\gamma_{1,2}\rightarrow 0,\ \pm\alpha_0 \qquad \text{(F-43)}$$

and for values of U such that

$$\gamma_1 \to \gamma_0 \tag{F-44}$$

Fortunately the singularies are "apparent" in the sense that a careful evaluation of the expressions for the limits given in (F-43) and (F-44) shows that the functions are analytic at those points.

In summary we note that the essential ingredients for the calculation of the admittance, $H_{11_{BL}}(k)$, are contained in equations (F-13), (F-18) through (F-21), (F-38) through (F-40), (F-41), (F-25), and (F-42). In order to complete the calculation one must assume a particular mean flow velocity profile, $U(z^*)$. For the 1/n power-law profile for turbulent flow,

$$U = (z^*)^{1/n}, \tag{F-45}$$

we find that it is convenient to evaluate the integrals $a, b, c,$ and K_{11} [(F-19) through (F-21), (F-25)] using U rather than z^* as the variable of integration. From (F-45) we find

$$z^{*\prime} = nU^{n-1} \tag{F-46}$$

Substituting (F-46) and (F-8) in (F-19) and (F-21) we obtain

$$a = n\,I_{n-1}(A, B) \tag{F-47}$$

and

$$c = n\,I_{n+1}(A, B) \tag{F-48}$$

where

$$I_q(A, B) = \int_0^1 \frac{U^q dU}{A-BU^2} \tag{F-49}$$

and where

$$A = 1 + \frac{(\gamma-1)}{2} M_\infty^2$$

$$B = \frac{(\gamma-1)}{2} M_\infty^2$$

The integral defined by (F-49) is successfully treated by integrating by parts an appropriate number of times. This is equivalent to using the recursion formula

$$\int U^q f^{-1} dU = \frac{-U^{q-1}}{B(n-1)} + \frac{A}{B} \int U^{q-2} f^{-1} dU \tag{F-50}$$

where

$$f(U) = A - BU^2$$

For turbulent flow the parameter $n = 7$ is an appropriate number to use over a wide range of Reynolds number. Successive application of the rule (F-50) to (F-47) and (F-48) for $n = 7$ yields

$$I_8(A, B) = -1/(7B) + (A/B) I_6(A, B) \tag{F-51}$$

$$\begin{aligned} I_6(A, B) = & -1/B[1/5 + 1/3(A/B) + (A/B)^2] \\ & + 1/2(A/B)^3/(AB)^{1/2} \log\left[\frac{A + (AB)^{1/2}}{A - (AB)^{1/2}}\right] \end{aligned} \tag{F-52}$$

The remaining integral, K_{11}, is found by substituting (F-46) and (F-8) in (F-25). This yields

$$K_{11} = n[AF_{n-1}(k) - BF_{n+1}(k)] \tag{F-53}$$

where

$$F_q(k) = \int_0^1 U^q L_{11}(U;k) \frac{dU}{U^2} \tag{F-54}$$

and where $L_{11}(U;k)$ is given in (F-42). The explicit dependence upon U is found using (F-17). It is convenient to make a change of variables

$$U = 1/t, \qquad dU/U^2 = -dt \tag{F-55}$$

in evaluating (F-54) owing to the fact that the integrand is indeterminate for $U \to 0$. This gives

$$F_q(k) = \int_1^{\infty} t^{-q} L_{11}(t;k)dt \qquad \text{(F-56)}$$

This change merely transfers the difficulty to $t \to \infty$, however the form (F-56) is more suitable for numerical integration. It would be possible to evaluate (F-56) analytically using partial fraction expansions to simplify the function $L_{11}(t)$; however, the algebraic manipulation required to determine the unknown coefficients is horrendous. The alternative is to evaluate $F_q(k; M_\infty, \gamma)$ numerically, specifying the parameters q, k, M_∞, and γ [γ being the ratio of specific heats in (F-8)] for each computation. The only possible difficulty in such an undertaking is the treatment of the apparent singularities of $L_{11}(t)$. In any numerical evaluation care must be taken to exclude the contribution to the integral within ϵ of the singularities, where ϵ is chosen so as to provide a desired accuracy.